INVESTIGATION AND IMPLEMENTATION OF DICODE PULSE POSITION MODULATION OVER INDOOR VISIBLE LIGHT COMMUNICATION SYSTEM

ADEL MOHAMED BUHAFA

A thesis submitted to the University of Huddersfield in partial fulfilment of the requirements for the degree of Doctor of Philosophy

The University of Huddersfield
Submission date. March 2015

Abstract

A visible light communication (VLC) system with green technology is available and enables users to use white LEDs for illumination as well as for high data rate transmission over wireless optical links. In addition, LEDs have advantages of low power consumption, high speed with power efficiency and low cost. Therefore, a great deal of research is considered for indoor VLC, as it offers huge bandwidth whilst using a significant modulation technique.

This thesis is concerned with the investigation and implementation of the dicode pulse position modulation (DiPPM) scheme over a VLC link using white LED sources. Novel work is carried out for applying DiPPM over a VLC channel theoretically and experimentally including a comparison with digital PPM (DPPM) in order to examine the system performance. Moreover, a proposal of variable DiPPM (VDiPPM) is presented in this thesis for dimming control.

The indoor VLC channel characteristics have been investigated for two propagation prototypes. Two models have been proposed and developed with DiPPM and DPPM being applied over the VLC channel. A computer simulation for the proposed models for both DiPPM and DPPM systems is performed in order to analyse the receiver sensitivity with the effect of intersymbol interference (ISI). Both systems are operating at 100 Mbps and 1 Gbps for a BER of 10-9. An improvement in sensitivity being achieved by the DiPPM compared to the DPPM VLC system. The system performance has been carried out by Mathcad software. The predicted DiPPM receiver sensitivity outperforms DPPM receiver at by -5.55 dBm and -8.24 dBm, at 1 Gbps data rate, and by -5.53 dBm and -8.22 dBm, at 100 Mbps, without and with guard intervals, respectively. In both cases the optical receiver sensitivity is increased when the ISI is ignored. These results based on the received optical power required by each modulation scheme.

Further work has been done in mathematical evaluation carried out to calculate the optical receiver sensitivity to verify the comparison between the two systems. The original numerical results show that DiPPM VLC system provides a better sensitivity than a DPPM VLC system at a selected BER of 10-9 when referred to the same preamplifier at wavelength of 650 nm and based on the equivalent input noise current generated by the optical front end receiver. The results show that the predicted sensitivity for DPPM is greater than that of DPPM by about 1 dBm when both systems operating at 100 Mbps and 1 Gbps. Also, it is show that the receiver sensitivity is increased when the ISI is limited.

Experimentally, a complete indoor VLC system has been designed and implemented using Quartus II 11.1 software for generating VHDL codes and using FPGA development board (Cyclone IV GX) as main interface real-time transmission unit in this system. The white LEDs chip based transmitter and optical receiver have been constructed and tested. The measurements are performed by using LED white light as an optical transmitter faced to photodiode optical receiver on desk. Due to the LED bandwidth limitation the achieved operating data rate, using high speed LED driver, is 5.5 Mbps at BER of 10-7. The original results for the measurements determined that the average photodiode current produced by using DiPPM and DPPM optical receivers are 8.50 μA and 10.22 μA, respectively. And this in turn indicates that the DiPPM receiver can give a better sensitivity of -17.24 dBm while compared to the DPPM receiver which gives is -16.44 dBm.

The original practical results proved the simulation and theoretical results where higher performance is achieved when a DiPPM scheme is used compared to DPPM scheme over an indoor VLC system.

Table of Contents

List of Figures

List of Tables

Dedications and Acknowledgements

I would like to thank first and foremost my supervisor Dr. M.J.N Sibley who supported me by providing me with guidance, context and encouragement over the duration of my research.

I would also like to thank my co-supervisor Dr. P.J. Mather for his advice and assistance with VHDL coding.

Special thanks must also go to, Mr Martin Webster, Mr Dennis Town and Mr Chris Sentance for their support and help.

Quite naturally I also wish to thank both my Mother and Father who instilled in me the belief to pursue my education. I am grateful for the guidance, love and confidence they invested in me.

Lastly but not least, I would like to thank my Wife without whom this work would not have been possible.

1 INTRODUCTION

In In recent and future communication systems, such as 4G and 5G mobile wireless, the requirements of using wireless local area networks (LANs), with high capacity backbone and short range communication links, for accessing portable computers and telecommunication devices, have grown rapidly in offices, medical facilities manufacturing plants, business establishments shopping areas and houses (Li, Gani, Salleh, & Zakaria, 2009). Mobile users need to access a high speed network similar to that which supports wired services. A possible future proposed wireless link is shown in Fig.1.1. Designing LANs with high data rates needs a large bandwidth. Radio systems can give a reasonably high data rate, but can only support limited bandwidths due to spectrum limitation and interference. Optical fibre cable offers an attractive alternative to these requirements, but with some inherent problems in setting up and in its expansion. Alternatively, optical wireless systems have been widely investigated and seem to be ideal for future wireless communications (J. Kahn et al., 1992; J. M. Kahn & Barry, 1997). Practically, optical wireless systems (indoor or outdoor) offer all the advantages of optical fibre links with fast installation and low cost and have more advantages than radio systems as a medium for indoor wireless communications. It takes into consideration the capacity requirements of a wireless network and its applications, such as video and high data transmission. Compared with radio frequency, there is no interference within the electromagnetic spectrum and no interference with similar systems operating next door because the optical power is limited to each room. It offers a potentially huge bandwidth and is capable of supporting the high data rates demanded by future multi-media applications. The following is a list of advantages of optical wireless systems over radio systems (A. Moreira, Valadas, & de Oliveira Duarte, 1996):

1. Use of cheap optoelectronic devices.
2. Unregulated bandwidth, theoretically 200 THz in the range of wavelength of 700-1550 nm
3. No inter-channel interference due to frequency re-use in the same room.
4. No multipath fading: intensity modulation and direct detection.
5. High security from eavesdropping and interferences.
6. Smaller cell size and higher capacity.

However, there are some disadvantages associated with indoor optical wireless systems, direct (line- of- sight (LOS)) link and non-direct (diffuse) link, such as:

1. Mobility.

2. Link blocking for LOS.
3. Interference due to ambient light.
4. Inter-Symbol Interference (ISI) due to multi-path dispersion(J. M. Kahn & Barry, 1997).

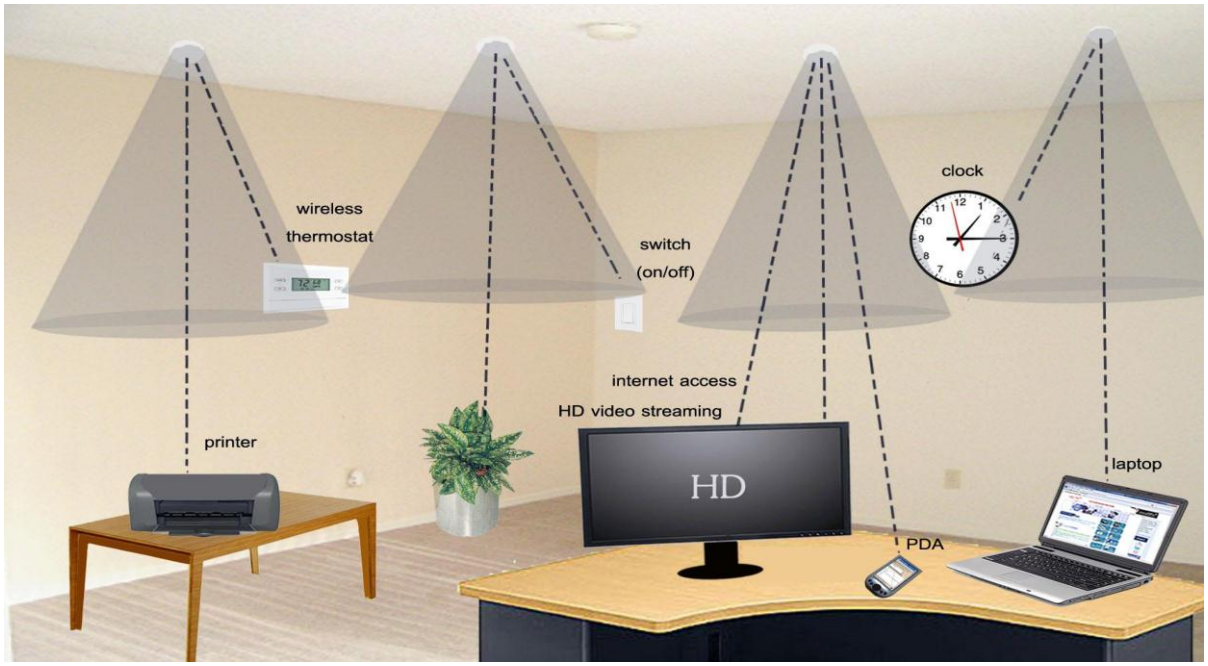

Figure 1-1-Possible future of VLC Networks (Sangwongngam, 2015)

Mobility of optical wireless communications could be improved by utilizing a wide beam angle optical transmitter. A diffuse link is preferable in comparison to LOS link, because there is no specific arrangement requirement, no link blocking and it is more robust to shadowing. However, problems associated with such a diffuse configuration are high path loss, due to multipath signal fading and dispersion, the reason for this is the reception of signals via different paths by the receiver. For the multipath fading the receiver photodiode is huge relative to light wavelength where the detector diameter is on the order of thousands of the received wavelength, As a result the detector can have many variation in the received intensity. In practice these fades are effectively averaged out over the surface of the detector producing an inherent degree of spatial diversity against multipath fading. The major impairment is the multipath dispersion due to the multiple delay which causes intersymbol interference (ISI) that ultimately limits the bandwidth. Thus, a diffuse link needs more transmitted power than LOS link(Carruthers & Kahn, 1997; Ghassemlooy & Hayes, 2003a).

1.1 Optical Wireless Communication Systems

After the demonstration of laser light in 1962 by T. Mainman, optical transmission as a communication system became feasible. In March 1963, the first TV transmission over

laser was demonstrated by a group of researchers in North America(Goodwin, 1970). Later, in 1970, a small semiconductor laser for high-speed modulation of optical transmission equipment was produced. Furthermore, in 1979, Gfeller and Bapst proposed an indoor optical wireless communication system (OWC). The diffuse system used optical radiation to establish a communication link located in the same room(Gfeller & Bapst, 1979). In the decade from 1970 to 1980 most research concentrated on optical transmission over fibre cable, because the fibre transmission loss was very low. The fibre cable became widely used due to large bandwidth and high data rate. But still there is a demand for compatible wireless link, rather than radio link which can offer the same benefits of the fibre cable.

Since 1990, infrared optical wireless systems have been investigated and shown to have all the advantages of optical fibre.

Many researchers and industrial sectors are applying a continuous development for the future applications of OWC. A higher data rate of up to 50 Mbps for a full duplex infrared link has been achieved by a number of companies, BT Labs, Hitachi, IBM, Fujitsu, Hewlett-Packard and others (Kotzin & van den Heuvel, 1986; Poulin, Pauluzzi, & Walker, 1992).

In London, 1996, an optical wireless system operating at a data rate of 1 Gbps has been reported using two dimensional arrays of surface laser transmitter, where a tracked architecture is adopted and allows the use of small, high sensitivity receiver with high gain for low power transmitter. The architecture offers a prospect of demonstrating a practical mobile ATM (Asynchronous Transfer Mode) (Wisely, 1996).

From 2003, academic research and industrial development concentrated on studying the indoor OWC channel modelling, low power high performance modulation schemes as well as low cost high speed optical wireless transceivers (D. C. O'Brien et al., 2003; Carruthers & Carroll, 2005; Liu, 2008; H. S. Lee, 2009).

Many applications for short range communications have been successful due to the presence of the IrDA (Infrared Data Association, a group of device used for transmitting data via infrared light waves)transceivers, such as in hospitals, laptops, mobile phones, PC's and other application which are supported by academic research and many companies.

In general, OWC are classified according to where the system is applied into two types: indoor and outdoor applications. In these applications, infrared light offers a large bandwidth and fast transmission systems due to very high frequency used for the optical carrier (A. Moreira et al., 1996). Unfortunately, these modules have human restrictions due to eye and skin optical power regulation. Researchers and industrial companies have changed their aims to develop an alternative to overcome these disadvantages.

Recently, many studies have investigated Visible Light Communication (VLC) as a future technology which can replace infrared systems without human restrictions. VLC is a short range OWC using white light LEDs for illumination and communication simultaneously. In addition, and compared to IR link, VLC can handle much higher radiation power that can support VLC to provide high quality transmission services.

As the LED cost decreases, a wide range of LEDs applications is increased in different colours including white source for general illumination. The LED field application is also expanding for all automotive lights. Due to the solid state reliability and compactness of the LED, output power and device efficiency have increased(Humphreys, 2008).

Moreover, the first LED headlights and the cars with white LED have become available. The solid-state technology offers a possibility for using LEDs with high data rate for communication transmission including illumination establishment. In Japan, the visible light communications consortium (VLCC) has been established for several years and is now rapidly globally growing. This encouraged the IEEE to outline a compatible standard for short range VLC technology in 2008(VLCC, 2008).

The focus on VLC is the future demand for short range with the high bandwidth communication systems and a presence of a new idea to modulate the wide band over the range of the visible light brought to this area using a LI-FI (Light Fidelity) technology. This is based on a very fast LED switching and visible light wave modulation. The LI-FI technology is a VLC technology which has been proposed by a team of researchers at the University of Edinburgh in 2011, where a stream of video is transmitted through a standard LED lamp. In this case the LED is based as an alternative technology to the Wi-Fi (Rani, Chauhan, & Tripathi, 2012).

In 2013, at Fundan University, a 1 watt LED was modulated and accessed the internet at a speed of 3.7 Gbps off line and 150 Mbps real time(Technology., 2013). In the same year, a team of researchers from many UK Universities proposed a new micro-LED light bulb and achieved a data rate of up to 3.5 Gbps via white light (by converging red, blue and green LEDs). The team showed that a data rate of over 10 Gb/s was possible(EPSRC's, 2013).

Using LED’s can save energy; in reality about 33% of the total electrical energy consumed is used for general lighting. Replacing all lighting sources with LEDs could reduce the total global power consumption by 50%. In the United States, if LEDs were used for 20 years, 760GW of power could be saved and in Japan, the Ministry of International Trade estimated that if half of all lamps are replaced by LEDs this will save electricity generated from six mid-sized power plants. Furthermore LEDs are classified as green technology (Kavehrad, 2010; Komine & Nakagawa, 2004).

1.2 Intensity Modulation and Direct Detection (IM/DD)

In optical wireless communication systems, the most feasible method of communication is Intensity Modulation with Direct Detection (IM/DD) for optical carrier. Intensity modulation (direct modulation) is performed by varying the drive current of a light emitting diode (LED) or laser diode (LD). At the receiver, direct detection is completed by using photo-diodes to generate an electric current proportional to the incident optical power (Ghassemlooy & Rajbhandari, 2007). The eye and skin safety regulation sets a limitation on the transmitted optical power, thus the average optical power is restricted. In order to collect as much optical power as possible, a large area photo-detector should be used. However, the high capacitance of large-area photo-detectors limits the bandwidth of the receiver. Typically, the bandwidth is specified by the response time which is the combination of the diode capacitance and the overall series resistance of the driver circuit. Consequently work has been going on to develop a modulation with high bandwidth (Carruthers & Kahn, 1997; A. Moreira et al., 1996).

There are different modulation schemes, which are suitable for IM/DD, each with its own advantages and drawbacks. The common modulation schemes used for IM/DD are On-Off Keying (OOK) and Pulse Position Modulation (PPM) in different formats such as; digital Pulse Position Modulation (digital PPM), differential Pulse Position Modulation (differential PPM) and multiple Pulse Position Modulation (multiple PPM). Practically, the average optical power radiated by an optical transmitter is restricted, thus the performance of various modulation schemes is compared in order to achieve the required received power at a given data rate. Of all the different modulation schemes, OOK is the simplest technique for IM/DD implementation (Barry, Kahn, Krause, Lee, & Messerschmitt, 1993). Unfortunately the mean power of OOK is relatively high and this impacts on eye safety issues. Alternative modulations for low power transmission are PPM schemes that can operate with high peak powers but low mean powers. PPM with its modifications has been widely considered for optical communication systems (Carruthers & Kahn, 1997; Ian Garrett, 1983). One such technique is digital PPM that has been commonly proposed for optical wireless communication systems and has been accepted for the IEEE 802.11 infrared physical layer standard. It offers high receiver sensitivity but at a cost of increased bandwidth leading to difficult implementation (I Garrett, 1983).

Lately, in 2003, a new coding technique; dicode pulse position modulation (DiPPM), has been proposed as an alternative modulation scheme of PPM. DiPPM system offers good sensitivity and operates at only twice the speed of the original PCM, thus it is very simple to implement in comparison to other PPM modulations (M. J. Sibley, 2003b, 2004).

One application of DiPPM on direct optical wireless communication system was proposed in 2005. The author demonstrated that the high sensitivity and the low line rate provided by the DiPPM technique make it an extremely attractive modulation scheme for indoor optical wireless applications. (Menon & Cryan, 2005).

Later, in 2009, a DiPPM coding scheme has been developed and implemented over dispersive optical channel, the received signal is dispersed in time due to multipath propagation which results in increased delay spread and causes intersymbol interference and reduced the amplitude of the received pulses that limits the maximum transmitted data rate. The result showed that the performance of a DiPPM scheme has advantages compared to PPM (Romanos Charitopoulos, 2009). Following in 2010, pulse position modulation schemes; such as multiple pulse position modulation (MPPM), DPPM and DiPPM, have been incorporated for comparison over intersatellite links in free space. The researcher showed the system obtained high performance when MPPM is used and DiPPM offers a better performance than PPM, all coding schemes were operated at data rate of 1 Gbps(Ghosna, 2010).

Different from IR all modulation techniques are applied only for improvement of data transmission of communication systems, while over VLC the requirements such as high data rate with sufficient illumination on the desk are required to satisfy end user. Therefore, dimming is an important feature of VLC systems where control of the LED brightness can be achieved.

1.3 Aims and Objectives

The purpose of this project is to investigate and it is aimed to analyse the performance of a DiPPM modulation technique applied over indoor VLC link utilizing white LEDs and comparing the relative value of DiPPM with a similarly performance of digital PPM system.

The specified objectives of the thesis are:

- ***To Investigate and analyse the DiPPM and DPPM coding schemes***

Investigation of the DiPPM over VLC link will be studied. Mathematical models for both DiPPM and DPPM systems are to be developed. The simulations through the use of the mathematical models will be done by using Mathcad software and includes the effects of the input noise, ISI and the channel dispersion due to light propagation. The analyse of the DiPPM system performance has to be compared to the DPPM system, the equivalent PCM error probability includes erasure and false-alarm errors will be evaluated and the receiver sensitivity has to be obtained.

☐ ***To investigate the dimming control over indoor VLC system***

The dimming control of various modulation coding schemes will be investigated according the modulations properties included OOK and PPM. Dimming control for VLC system has to be considered when using DiPPM coding scheme is used. Thus a variable DiPPM (VDiPPM) is to be proposed according to the DiPPM structure technique and will be verified for the indoor VLC link.

☐ ***To confirm theoretical calculation with simulation results***

The VLC system performance has to be compared with the simulation model results when utilizing both coding schemes, DiPPM and DPPM. The comparison will be verified whether the DiPPM VLC system outperformed the DPPM VLC system. The spectral noise density has to be obtained when refereed to the input and the received sensitivity will be evaluated.

☐ ***To design and implement a complete indoor VLC system and practically confirm with the simulation mode and theoretical evaluation***

The main goal of this thesis is to study the performance of DiPPM through visible light communication using white LED and comparing to the relative values of DPPM. As no experimental construction of indoor VLC system has to be assembled based on the hardware components; LED transmitter, optical receiver and FPGA interface unit. The two modulation coding schemes will be programmed in VHDL and downloaded to FPGA as the main interface board for the communication link in real time mode. The optical received pulses are to be detected for certain BER and the average received optical power has to be measured. The optical receiver performance sensitivity is to be obtained. The experimental results will be proved if DiPPM confirms the theoretical predictions with real time measurements.

1.4 Original Contributions

As a result of the study, the following original contributions are made:

1. Investigation of the DiPPM and DPPM coding schemes for indoor VLC is carried out. Mathematical analysis is developed for this model. Chapter 5
2. Computer simulation using Matlab and Altera DSP builder software for DiPPM coding over optical wireless channel is implemented and the outcome is simulated (Adel M. Buhafa, Al-Nedawe, Sibley, & Mather, 2013)
3. DiPPM performance for fully diffuse VLC system is evaluated and error probability is obtained in order to examine the optical receiver sensitivity. Mathcad software

is implemented for this simulation and evaluation. An improvement in sensitivity is achieved for DiPPM VLC system compared to an equivalent DPPM system (Adel M Buhafa, Al-Nedawe, Sibley, & Mather, 2014).

4. Proposed of two models of VLC channel are using DiPPM and DPPM as modulation techniques. The models have been simulated and the results have been evaluated in order to analyse the optical receiver sensitivity.
5. MathCAD programs are used in order to obtain optical receiver sensitivity and evaluate the performance for both DiPPM VLC system and DPPM VLC system.
6. Experimental tests have been performed in order to examine DiPPM VLC system performance in a real-time transmission link. Also, DPPM VLC system has been inspected in a similar environment.

1.5 Thesis Outline

The organization of this thesis is planned as follows:

Chapter1, Introduction, introduces a brief history of visible light communication systems in areas of applying such modulation schemes and justifies the benefit of using VLC as a future technology utilizing white LED for high data rate.

Chapter 2, Literature Review; presents the background and the motivation of this work, describing the studies which have been proposed and demonstrated in the last and recent years. The review included changing the aim of researches and has concentrated on VLC technology with LED as a light source rather than Infrared technology.

Chapter 3, Coding Techniques; describes the two modulation coding schemes used in this thesis and the necessary theory to evaluate the system performance in terms of error types, error probability, output voltage and channel noise.

Chapter 4, Fundamentals of OWC; gives an over view on OWC and how the propagations of light is classified. The OWC channel is described and the characteristic of LED as a source of light is explained.

Chapter 5, Indoor VLC Channel Models; describes indoor optical wireless channel, followed by verification of the mathematical model used to simulate a DiPPM over indoor VLC.

Chapter 6, Variable DiPPM for Dimming Control; demonstrates the necessity of controlling the dimming while an LED is used for lighting as well as for data transmission. A variable DiPPM (VDiPPM) technique is proposed.

Chapter 7, VLC Simulation; MathCAD software is implemented to illustrate the received pulse shape at the detection instant. The simulations and results are analysed and discussed in order to determine outcome of the performance of the VLC system.

Chapter 8, Evaluation of VLC receiver Sensitivity; Verify the results of chapter 7 through steps of calculations for both DiPPM and DPPM systems and the performance is evaluated.

Chapter 9, Design Construction of Indoor VLC System; Presents an implementation of a complete indoor VLC link based on a white LED as transmitter and FPGA as main interface unit. The system performance for both DiPPM and DPPM coding schemes are measured and confirmed with the simulation results as well as the numerical calculations.

Chapter 10, Conclusions; presents the conclusions of the work projected in this thesis, demonstrating and highlighting the original contribution of DiPPM VLC system and outlines a possible further work related to this work.

2 LITERATURE REVIEW

The utilisation of diffuse link for indoor optical wireless was proposed in 1979, by Gfeller et al. The first scheme was on-off keying (OOK) which is the simplest scheme for implementation (Gfeller & Bapst, 1979). OOK is unable to offer the power efficiency that is required for many high data rate optical wireless applications because the regulation of eye safety standards leads to a restriction in power. OOK also suffers from ISI due to multipath dispersion for data rates above 100 Mbps.

By the early 1980s digital PPM had been proposed for optical fibre links. A year later Garrett proposed optical fibre digital systems that used direct-detection and coherent-detection PIN-FET optical receivers for received pulses with Gaussian shapes. The results showed that a PPM system with PIN-FET offers an advantage to PPM schemes over optical fibre with improvement of sensitivity up to 20 dB greater than that of PCM (I Garrett, 1983).

Calvert et al 1988, completed, for the first time, a theoretical and experimental analysis based on the Garrett model. It was found that use of digital PPM can increase receiver sensitivity by 4 dB over PCM systems(Calvert, Sibley, & Unwin, 1988).

In the 1990s, digital PPM has been adopted for IEEE 802.11 standardization for Local Area Networks in indoor optical wireless communication systems. This supported can investigations about the use of PPM schemes for high speed indoor wireless data rate, the results showed that 100 Mbps data can be detected using OOK in presence of ISI (Audeh & Kahn, 1994).

Alternative ways to provide more power efficiency include the use of pulse position modulation (PPM). PPM was originally developed to offer high power efficiency for long distance, point-to-point optical fibre communication systems(J. M. Kahn & Barry, 1997).

Digital PPM is an attractive technique which offers improvement in receiver sensitivity. It can offer better sensitivity 5-11 dB than OOK at the expense of a large bandwidth. Thus the final line rate can be prohibitively high, up to 23 times that of the original PCM. Unfortunately, this makes overall system implementation difficult. Compared with OOK, PPM does increase system complexity since both slot and symbol synchronisations are required in the receiver in order to demodulate the signal (Cryan, Unwin, Garrett, Sibley, & Calvert, 1990; M. J. Sibley, 2003b).

In 1990, Cryan et al., and in 1991, Massarella and Sibley, found that when PPM is used over high dispersive optical channel and replaced the complex pre-detection filter, proposed by Garrett, by a matched filter alone or by a simple sub-optimal filter, the

receiver sensitivity of PPM system was only degraded by 1.3 dB and 1 dB, respectively (Cryan et al., 1990; Massarella & Sibley, 1991).

Later Massarella and Sibley, using a coherent heterodyne test rig with sub-optimum filter, showed that the receiver sensitivity of the PPM system improved by 16.6 dB compared with OOK system. However, PPM technique requires more bandwidth as the maximum symbol length increases. Over all PPM and OOK, are still suffer from ISI for when a high data rate is used (M. J. Sibley & Massarella, 1993).

Currently, most of the modulation schemes applied over the infrared OWC are changed over for VLC because the channel characteristics for Infrared and VLC are similar and have the same propagation behaviour both indoor and outdoor.

Data transmission via VLC is done by changing the light intensity which is so small that it is un-noticeable by human eye. Choosing a right modulation scheme can improve the performance of LEDs and make them a suitable candidate for high speed data transmission.

Recently, many studies have concentrated on the characteristics of the indoor VLC propagation channel based on IR channel characteristics. For both LOS and multipath reflections the impulse response channel has been investigated. Furthermore implementation of many modulation schemes have been investigated and proposed in order to increase the VLC system performance, SNR improvement, and reduce the error due to ISI and environments (Barry et al., 1993; Jungnickel, Pohl, Nonnig, & Von Helmolt, 2002).

In (Gfeller & Bapst, 1979), the LOS and multiple reflections of indoor free space optical impulse response is evaluated and found multiple reflections significantly affect ISI. Following this in 2002, V. Jungnickel et al modelled an indoor infrared channel for both LOS and diffuse link as well as proposed the effect of the FOV at the receiver on the received power and data rate. The measurements and computer simulation concluded that using a moderate directivity it can help increase the transmission data rate beyond 100 Mb/s(Jungnickel et al., 2002).

As the area of LEDs becomes more interesting, many researchers proposed VLC systems using white LEDs (Y. Tanaka, T. Komine, S. Haruyama and M. Nakagawa). Based on that, an analysis of VLC channel was proposed and showed that an LED can be used to setup a communication link under lighting as well. The authors found that the data rate is limited by intersymbol interference (ISI) mostly when the way between LED and receiver is blocked or a narrow FOV receiver is used. Moreover, the results show that the proposed VLC system is suitable for transmission of data over indoor wireless links similar to the infrared system (Komine & Nakagawa, 2004).

In 2005, LED transmission of data from a traffic light to a car was demonstrated followed by a scheme for parallel communication in 2007 (Iwasaki, Wada, Endo, Fujii, & Tanimoto, 2007; Wada, Yendo, Fujii, & Tanimoto, 2005).

Based on the results (2002, V. Jungnickel et al), in 2007, VLC for multipath reflections was investigated and showed that modulation bandwidth of commercially LEDs can be extended to 20MHz. Also the performance of the VLC system was compared for OOK, Binary Phase Shift Keying (BPSK) and Discrete Multitone (DTM). A data rate was achieved for 200 Mbps when using DTM and the system implemented with fast interface unit FPGA and DSP builder (Grubor, Jamett, Walewski, Randel, & Langer, 2007).

In 2008 the simulation of a proposed VLC system showed that a system with dual optical receivers can achieve a data rate of 100 Mbps for a 20 m distance away from the LED. This receiver was used outdoor and had the capability to reject the ambient light influences and its variance during the day time (I. E. Lee, Sim, & Kung, 2008).

In order to provide enough lighting throughout a room, as well as high data rate transmission, many white LEDs are used. Komine et al proposed a VLC system with adaptive equalization to overcome the effects of ISI due to multipath reflections. The conclusion was that up to 1 Gbps can be achieved and this makes the proposed system have a capability for future high data rate indoor optical wireless networks (Komine, Lee, Haruyama, & Nakagawa, 2009).

Besides investigating the VLC channel characteristics, practical designs and demonstrations have taken place. In 2010 a VLC system over LOS link was modelled and more optical power at the receiver can be collected compared with the non-LOS link. The design of the system included white LED arrays as the optical transmitter and PD as optical receiver followed by preamplifier and post-equalizer stages. The system operated at data rate of 115 kbps, the BER and the optical received power were measured in order to evaluate the system performance. (Cui, Chen, Xu, & Roberts, 2010).

A study in 2011 investigated the characteristics of VLC in present of multipath dispersion using white LED. It described the light undergoing multiple bounces and for direct line of sight in order to propose the received optical power compared to infrared signal. The study was extended utilizing a number of modulation schemes such as: variable PPM (VPPM) and variable OOK (VOOK) that was required for dimming control to achieve the same BER (K. Lee & Park, 2011).

Agreeing to the wide investigation about visible light communications (VLC), IEEE provided the first global standard for VLC in 2011, IEEE 802.15.7 (IEEE, 2011).

In a study in 2012, overlapping PPM and PWM were combined to setup a communication link over VLC channel using LED and FPGA as drives to transmit a sequence of data.

The results showed that improvements of data rate and a better system quality have been achieved experimentally by OPPM-PWM for 80Mbps compared to OOK. (Yang, Li, & Jiang, 2012).

Experimental and simulation of indoor VLC link have been investigated using short pulse and frequency sweep techniques. In 2012, Zhang et al, characterized the impulse response and frequency response of VLC for LOS as well as non-LOS links. The measurements were carried out inside a typical room, the results of the measurements and of the simulations were examined and showed that a good similarity even when the light undergoing K reflection. Also the effect of the receiver orientation and FOV on the channel bandwidth was tested and showed they have similar effect. (Zhang, Cui, Yao, Zhang, & Xu, 2012).

In 2012, a VLC system based on a 3 watt white LED as transmitter and PD as a receiver has been designed for an indoor wireless optical system. The measurements showed that illuminating the receiver surface was done at different distances from the transmitter in order to evaluate a better system performance. The results denoted were at 1.5 m and a data rate of up to 111.6 Kbps at a given BER (J.-y. WANG et al., 2012).

Recently, 2013, indoor VLC has been investigated with PPM scheme for multipath channel with additive Gaussian noise. In this model a fixed gain optical repeater is involved and examined with the impulse response of the VLC and BER performance is evaluated. The results obtained that SNR gain for BER of 10^{-3} and for un-blocked link with repeater is 2.78 dB and when the shadowed is presented the SNR is reached 7.75 dB (R. C. KIZILIRMAK, 2013).

M Saadi et al investigated VLC in case of opportunities, challenges and channel models. They concluded VLC is a secure technology and satisfies the requirements of users at home or for any small LAN. They also described VLC channel models and found that it has many challenges such as; ambient noise, ISI and SNR development(Saadi, Wattisuttikulkij, Zhao, & Sangwongngam, 2013).

Lately, in 2014, the VLC system BER performance was investigated using OOK and combined PPM with pulse shape modulation schemes. The paper shows that an improvement in BER performance is achieved at the higher data rates and higher band widths in order to increase the number of the pulses (Ali, Zhang, & Zong, 2014).

Tabl1 2-1 shows the modulation schemes that mostly used for optical communication systems, each with their advantages and disadvantages.

Table 2-1 Modulation Schemes for Optical Communications (D.-s. S. J. M. Kahn, 199; Shalaby, 1993)

Modulation Scheme	*Scheme Properties*
DiPPM	*Data rate only 4times PCM rate fixed bandwidth compared to digital PPM.* *No symbol synchronisation.*
digital PPM	*High power efficiency.* *Poor bandwidth efficiency and more complex to implement than OOK.*
differential PPM	*Required less average power than PPM*
multiple PPM	*High power efficiency, with small bandwidth*
overlapping PPM	*High power efficiency with small bandwidth.*
digital-pulse-interval modulation (DPIM)	*Higher transmission capacity compared with digital PPM, Less complexes to implement.*
dual header pulse-interval modulation (DH-PIM)	*Offers higher bit rate and requires less transmission bandwidth compared with PPM and DPIM.*
OOK	*The simplest and uses 1 & 0.* *Low power efficiency for many applications.*

2.1 Dimming Control for VLC

For future wireless communication, VLC is in demand where a wide bandwidth and high data rate are required. VLC through LED has two main objectives, dimming control and data link support, where both are achieved and accepted in using a suitable modulation technique. Moreover, VLC optical intensity over communication link is constrained and remains constant to satisfy the illumination end user requirements(Sugiyama, Haruyama, & Nakagawa, 2007; J.-B. Wang, Hu, Wang, Huang, & Wang, 2013).

Researchers consider these two issues in order to investigate using LED for VLC systems. Consequently, for dimming control, pulse amplitude modulation (PAM) and pulse width modulation (PWM) are widely proposed. An optical average power can be regulated when a fixed peak power is transmitted by a VLC system. The average power is proportional to LED illumination. Many modulation techniques such as; PPM, OOK and Multiple PPM (MPPM), have been proposed in order to support data transmissions and achieving high bandwidth with power efficiencies. Typically, when PPM and OOK modulation technique are used for high data for VLC reductions in brightness level and system performance

are arises. Nevertheless, PPM is still the attractive modulation scheme due to simplicity in structures and ease of implementation. To overcome the weakness of PPM and improve VLC system performance, many developments have been done, for example; Overlapped-PPM (OPPM), Multiple PPM (MPPM), Variable PPM (VPPM), Variable OOK (VOOK) and Expurgated PPM (EPPM) (Din, 2014; Noshad & Brandt-Pearce, 2014).

In, 2007, at the same time, both dimmer and wireless communication have been achieved using two methods. One adopted PPM for data transmission and PWM for brightness control; it shows a range of 0% to 87.5% of brightness that can be controlled. In the second method in addition of PPM the brightness control is achieved when modulation depth is changed with no variation in data rate for the brightness range of 0% to 100% (Sugiyama et al., 2007).

In the beginning of 2011, a method of joint brightness control while LED emits data was proposed with MPPM. The brightness is controlled by varying the number of slots per symbol containing information, whereas the data rate is changed according the brightness(Siddique & Tahir, 2011).

A further PPM enhancement is a Variable PPM (VPPM) proposed by IEEE 802.15.7 standard(IEEE, 2011). VOOK and RZ-OOK were also compared to VPPM. VPPM is a variant similar to 2-PPM. The results showed that VOOK and VPPM required the same power, but the first offers better spectral efficiency. In case of VOOK and RZ-OOK, the latter required a power of 3 dB less than VPPM or VOOK at 50% brightness (K. Lee & Park, 2011a).

VPPM is based on the changing of the pulse width related to dimming level, in the same time a binary PPM is sent for data information. A flexible dimming control is achieved compared to PPM, where a lower spectral efficiency is adopted. Beside that and for increasing the data rate when using VPPM overlapping cannot be used (Noshad & Brandt-Pearce, 2014; Yang et al., 2012).

Later, a combination of OPPM and PWM modulation schemes have been developed and a high data rate of LED for indoor VLC is reached by using GBF algorithm at BER of 10^{-5} but with additional complexity. In the same time the LED light becomes more brightness when using OPPM-PWM compared to OOK modulation, and on average it rises from 50% t0 68.75% as the results showed (Yang et al., 2012).

Recently, in 2014, a transmission scheme using Expurgated PPM (EPPM) over indoor VLC has been proposed for dimming control as well as for improving VLC system performance and support white LED at high data rate. The results show using EPPM with interleaving decreases the effects of ISI in order to reduce error probability and improve VLC system performance in comparing when using PPM modulation scheme(Noshad & Brandt-Pearce, 2014).

Tabl1 2-2 shows the modulation schemes that mostly used for dimming control over VLC systems, each with their advantages and disadvantages.

Table 2-2 Modulation Schemes for Dimming Control

Modulation Scheme	*Scheme Properties*
digital PPM (DPPM)	*High power efficiency. Un-flexible dimming control due to variance of time slot.*
pulse width modulation (PWM)	*Low efficiency at VLC high data rate and difficult to control PAPR. It is combined with DPPM for data transmission and brightness control, respectively.*
Continuous Current Reduction (CCR)	*Low efficiency at VLC high data rate and complicated.*
Variable PPM (VPPM)	*A flexible dimming control is offered. Low spectral efficiency compared to DPPM.*
Expurgated PPM (EPPM)	*Improves VLC system performance compared to PPM*

2.2 DiPPM over Optical Fibre System

In 2003, Dicode pulse position modulation (DiPPM) was theoretically presented by M.J.N. Sibley, as a novel coding scheme for optical fibre communications. DiPPM is an attractive modulation format of digital PPM. DiPPM technique offers many advantages than other modulation formats such as; significant sensitivity than PCM and comparable to digital PPM, can run at lower data rate (twice the original PCM), very simple in implementation and has less power consumption (M. J. Sibley, 2003b).

The performance of DiPPM was analysed and compared to that of digital PPM and PCM. The results showed that, with varying fibre bandwidths, the DiPPM gave receiver sensitivity greater than DPPM while operating at a speed only four times that of original data; the predicted sensitivities were -44.27 dBm over 1 Gbps and -50.44 dBm over 155.52 Mbps. This is comparable to digital PPM and better than the equivalent PCM of about 12 dB and 16 dB respectively. It also showed that for low fibre bandwidths, of one times the bit-rate, DiPPM outperforms digital PPM with sensitivity significantly greater by

3.02 dB. This makes DiPPM a practical alternative scheme to digital PPM (M. J. Sibley, 2003b).

In the same year, Sibley analysed the performance of DiPPM system with the use of a PINFET receiver and a noise-whitened matched filter over a slightly/highly dispersive optical channel. The author demonstrated that the DiPPM system offered a sensitivity of 7.76 dB better than that of its equivalent PCM, and 2.38 dB than a digital PPM with a large fibre bandwidth at 155.52 Mbps. The system can offer, with considering the effects of ISI, a sensitivity of -53.33 dBm at a bandwidth of 1.5 times the PCM bit-rate. With this particular implementation the system was operated at a final line rate of four times that of the PCM(M. J. Sibley, 2003a).

Next, in 2004, Sibley examined the performance of the DiPPM system, over dispersive optical channels, by using a third-order Butterworth filter in zero-guard interval, as an alternative method of using digital PPM with noise-whitened matched filter and proportional-derivative-delay (PDD) network. The author concluded that the DiPPM system with a Butterworth filter can greatly simplify the design of the receiver and can operate over a channel with a lower bandwidth at 1.2 times the original PCM. In this case the predicted sensitivity was -37.48 dBm for normalised channel bandwidth f_n=100 at 1 Gbps and -32.24 dBm at f_n=1.2. Also the effects of intersymbol interference (ISI) were considered and the filter bandwidth became critical, especially with f_n=1.2, due to the large amount of ISI (M. J. Sibley, 2004).

Subsequently, the same author in 2005, investigated the performance of DiPPM using maximum likelihood sequence detection (MLSD), the results showed that a DiPPM system with MLSD can operate on a bandwidth of 0.29 times PCM data, also indicated that sensitivity can be increased by 12.2 dB(M. Sibley, 2005).

Following, in 2006, R.A. Cryan and M.J.N. Sibley presented DiPPM technique in a different form. They considered minimising the effects of ISI on DiPPM by using central decision detection. They simplified the design of the DiPPM receiver, by using raised cosine filtering and a simple Butterworth pre-detection filter. The results showed that for both models a good performance can be achieved and both offered at the higher fibre bandwidth significant improvements in sensitivity and considerable improvements at lower bandwidth (Cryan & Sibley, 2006).

In 2009, a complete optical system was constructed using DiPPM coder and decoder. The results showed that mathematical and simulation model agreed with real time results that were obtained in the experimental tests. The experimental was done for fibre optical and free optical space in short distance(Romanos Charitopoulos, 2009).

In addition, an experimental verification of DiPPM had been considered, with measurements of practical signal in terms of using mathematical model and computer

simulation. A complete coding simulation demonstrated that the theoretical and practical power spectrum density (PSD) of an optical DiPPM, signals could be present. The conclusive was that DiPPM can be a very attractive scheme that can achieve a good performance in practical applications of optical communication systems (RA Charitopoulos & Sibley, 2007; RA Charitopoulos & Sibley, 2010, 2011).

2.3 DiPPM over Optical Wireless System

All of these studies have proposed DiPPM as feasible alternative modulation format to conventional digital PPM, for the reason that it offers high receiver sensitivity at a considerably lower line rate. This makes the DiPPM modulation scheme ideal for both optical fibre and optical wireless communications. Therefore, practically, DiPPM may increase the mobility and the flexibility for users.

For the first time, in 2005, DiPPM has been proposed for use in indoor optical wireless communication systems via LOS link, by M. Menon and R.A. Cryan. The performance of the DiPPM was analysed in terms of system sensitivity. The calculation of the receiver sensitivity demonstrated that DiPPM system offered an improvement of 10.3 dB compared to equivalent PCM and 0.3 dB over -50.7 dBm that achieved by digital PPM system. These results show that DiPPM is an attractive modulation format for direct indoor optical wireless transmissions(Menon & Cryan, 2005).

An implementation of a complete DiPPM system has been developed in order to evaluate system performance. The results showed that DiPPM offered more advantages for optical free space communication system because the clock can be recovered from the DiPPM sequence including slot synchronisation. This ensures a possibility of transmitting data bits over optical wireless communication link, and this was done for a short distance using visible Laser diode(Romanos Charitopoulos, 2009).

In 2010, G. Fadi, showed that pulse position modulation schemes; such as multiple pulse position modulation (MPPM), DPPM and DiPPM, are used in comparison over intersatellite links in free space. In order to determine the receiver sensitivity for certain error rate, the comparison results show that MPPM offer high sensitivity than DPPM and DiPPM, whereas DiPPM is better than DPPM in use over free space inter-satellite link at a data rate of 1 Gbps (Ghosna, 2010).

Recent studies investigated DiPPM in order to evaluate system power spectral density and its synchronisation. They showed that DiPPM format is highly suitable for development over optical channels. Thus, DiPPM may be ideal for optical wireless portable devices (RA Charitopoulos & Sibley, 2007; RA Charitopoulos & Sibley, 2010, 2011).

In this thesis DiPPM system has been investigated and analysed over indoor VLC link using white light LED for data transmission. This includes theoretical investigation for designing the model of a VLC channel. DiPPM and DPPM systems, including coding and decoding schemes, have been applied over the VLC link and considered in comparison in order to evaluate the system performance and determine the sensitivity of optical receiver. Further practical work carried out for real time experimental, for both DiPPM and DPPM systems using FPGA interface board, in order to implement a complete VLC system for transmitting and receiving and as proof for the model results. The measurements include photodiode current, received optical power and sensitivity calculation according to the chosen data rate. As the line rate of the DiPPM is fixed and is half of the PCM data rate, a 3 bit PCM code is used in this case to have a data rate for DPPM close to the DiPPM date rate that leads to make the comparison with high precision. A dimming control is investigated for DiPPM and other schemes in this case by trying maintain of control of LED brightness without affecting data rate transmission.

3 CODING TECHNIQUE

In this chapter both the original digital pulse position modulation (DPPM) and dicode pulse position modulation (DiPPM) coding techniques are described in detail where the last is used as an alternative technique of DPPM for many applications. Both coding schemes are based on transmission and receiving modes on the position of received pulses to regenerate the PCM bits information. The differences are how many pulses can be transmitted in one slot within a certain time for fixed frame or variable frames. For any communication systems the communication channels suffered from several types of errors which effected the transmission of information bits and the system performance. Both DPPM and DiPPM coding schemes have the same type of errors.

3.1 Dicode Pulse Position Modulation (DiPPM)

DiPPM is a very attractive simple coding scheme for coding and implementation. There are four slots used to transmit one bit of PCM. In the dicode technique, the data transitions from logic zero to logic one are coded by positive (+V) and transitions from logic one to logic zero are coded by negative (–V) and if there is no change in the PCM signal a zero pulse is present. However, in DiPPM, as shown in Fig.3.1, two signals SET and RESET are converted into two pulse positions in data frames. If no data transition is present, there is no pulse, while if transitions occur from zero to one or one to zero there are SET(S) and RESET(R) pulses, respectively. If the PCM data is constant, no signal is transmitted (M. J. Sibley, 2003b).

Moreover to reduce the effects of ISI two guard intervals can be added to the time slot. It is also clear a single slot in PCM can be coded into a single slot in DiPPM (S or R), which means the power requirement is reduced. DiPPM slot duration T_s is expressed as

$$T_s = \frac{T_b}{2 + gu} \tag{1}$$

where $T_b = 1/B$ denotes the PCM bit time, B is the original data rate and gu is the guard intervals.

In a zero-guard DiPPM system, only two slots are used to transmit one bit of PCM, the line rate becomes two times that of original PCM with a significant reduction in speed compared to digital PPM. In addition a lower bandwidth is required in comparison to digital PPM (M. J. Sibley, 2003b).

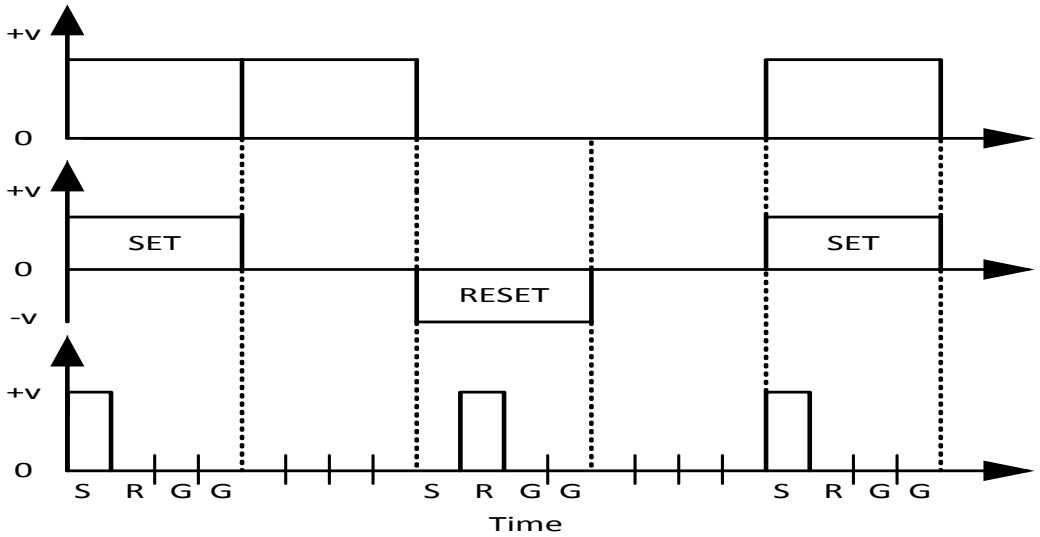

Figure 3-1 Conversion of PCM data (top trace) into dicode (middle trace)

DiPPM uses a four symbols alphabet: S, R, 2N for 00 and 11 transitions, as shown in Table.3.1. In the case of a transmitted S pulse, only symbols R or N can follow it as both have the same probability of 1/2. If the original PCM is line coded so that the run of like symbol is limited to *n*, the maximum DiPPM run could be R, *n*N and S. According to this condition, the probability of the next pulse (R symbol) is 1, because its presence is guaranteed at the end of a run of *n* lots of N symbol. A similar situation can apply if an R pulse is originally transmitted (Cryan & Unwin, 1993; M. J. Sibley, 2003b).

Table 3-1 DiPPM Symbol Alphabet

PCM	Probability	DiPPM	Symbol
00	1/4	No pulse	N
01	1/4	SET	S
10	1/4	RESET	R
11	1/4	No pulse	N

3.2 Digital Pulse Position Modulation (DPPM)

In the digital PPM technique *N* bits PCM is encoded by the presence of one pulse in one of *M* time slots and $M = 2^N$. In other words each frame has $\log_2 M$ data bits mapped into one of *M* possible symbols. The single pulse is repeated every T seconds and has constant power for each time slot, followed by *M*-1 empty slot. The length of each frame equals the length of the time frame of PCM. The coding scheme is based on the position of each pulse within the symbol. The encoded pulse place related to the decimal value of

each data bit is shown in Fig.3.2. A number of guard intervals may be added to a PPM frame to eliminate inter-frame interference (IFI) and improve system performance (Cryan et al., 1990; Ian Garrett, 1983). The digital PPM slot duration is expressed as

$$T_s = \frac{N.T_b}{2^N} \tag{2}$$

where $T_b = 1/B$ denotes the PCM bit time, B is the original data rate and *N* is the Number of PCM bits.

The received pulses are decoded and the PCM information is recovered in the presence of both slot and symbol synchronisation. A threshold signal detector is used to obtain the arrival time of PPM pulses at the crossing point. Due to signal interference the arrival time can also be influenced (M. J. Sibley & Massarella, 1993).

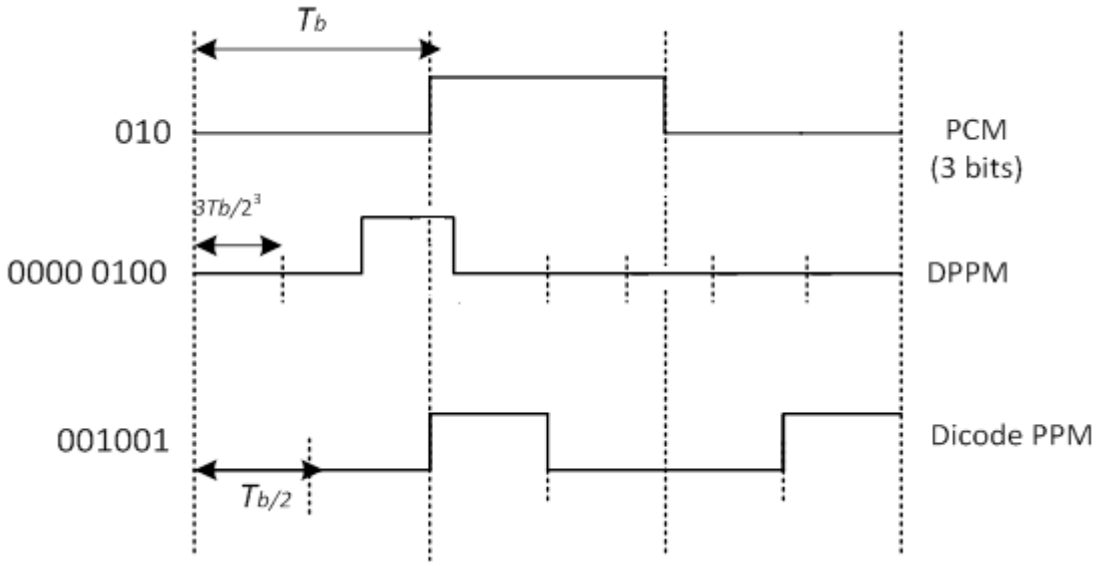

Figure 3-2 Conversion of PCM data (top trace) into DPPM (middle trace) and DiPPM (bottom trace)

3.3 Pulse Detection Errors

In a digital (PCM) communication system, massages are transmitted by only two symbols, one symbol represented by a pulse (bit 1) with duration *T* seconds and the other is represented by the absence of the pulse (bit 0) with same duration *T* seconds. Usually, the detection of the waveform is not a problem, because the waveform is already known. The most important thing is to determine whether the pulse is present or not present. Therefore, the detector at the receiver is required to be a decision making device with a threshold level to test the received signal over T_s seconds, and decide if the received pulse is present or absent. Hence, the detector must be implemented with the least probability of error in making a decision for an optimal result. On the other hand, if

the detection decision is wrong due to the inter-symbol interference and distortion in the received signal, then there are errors in a detected pulse (RA Charitopoulos & Sibley, 2007; M. J. Sibley, 2003a).

As with digital PPM, DiPPM system suffers from three types of errors, wrong slot, erasure and false alarm. The three errors are described in the following sections

3.3.1 Wrong-Slot Errors

These types of errors occur when the noise present are on the rising edge of a detected pulse, the pulse appears in adjacent time slots, before or after the current slot. These errors can be minimised when the pulse is detected in the centre of the time slot T_s, and then the errors will appear at the time when the pulse edge is shifted by $T_s/2$ (I Garrett, 1983; M. J. Sibley, 2003b; M. J. Sibley & Massarella, 1993).Thus the error probability of wrong slot P_s can be expressed as

$$P_s = 0.5\, erfc\left(\frac{Q_s}{\sqrt{2}}\right) \tag{3}$$

where

$$Q_s = \frac{T_s}{2}.\left(\frac{\text{slope}(t_d)}{\sqrt{\langle {n_0}^2\rangle}}\right) \tag{4}$$

and $\text{slope}\,(t_d)$ denotes the slope of the received pulse at the threshold crossing instant t_d and $\langle {n_0}^2\rangle$ is the mean square noise of the receiver.

In DPPM operation, due to noise, the received pulse may appear after or before the correct slot. Hence, the wrong-slot error can be evaluated by the following error probability equation as

$$P_{wsDPPM} = erfc(\frac{Q_s}{\sqrt{2}}) \tag{5}$$

Based on the equivalent PCM error probability is given by

$$P_{ewsDPPM} = \frac{2^M}{2(2^M-1)} P_{wsDPPM} \tag{6}$$

In DiPPM operation, the wrong slot error can cause four possible cases of errors. In case 1, the pulse in slot S can cause the edge to appear in the preceding guard, so it will not cause any detection error because the decoder will not recognise the false threshold crossing. Moreover, the pulse is still present in the S slot and so it will be detected correctly. In case 2 and 3, the errors arise due to S to R wrong slot (P_{ewsSR}) and R to S wrong slot (P_{ewsRS}), where the S pulse appears in a preceding R slot and the R pulse appears in a preceding S slot, respectively. Thus the detection error causes an

immediate PCM error. Both error types have the same number of errors and same equivalent error probability.

In case 4, when the pulse is in slot R, the edge can appear into the following guard slot (P_{ewsRG}), this error has the similar effect and same equivalent error probability as in case 2 and 3.

As the DiPPM scheme uses four symbol alphabet, as shown in Table 3.1, if the number of following N signals is x, then the transmitted and received sequences would be as assumed as in Table-3.2. Accordingly, the number of PCM errors is $x+1$ and the maximum number of following like symbols is n over the line coding. Under this condition, the probability of an R pulse in case 1 and an S pulse in case 2 will be one. Hence, the equivalent PCM error probability for each of two cases (M. J. Sibley, 2003; M. J. Sibley & Massarella. 1993) is given by

$$P_{ewsSR} = P_{ewsRS} = P_{ewsRG} = \sum_{x=0}^{n-1} \left(\frac{1}{2}\right)^{x+3} P_s(x+1) + \left(\frac{1}{2}\right)^{x+2} P_s(\mathrm{n}+1) \tag{7}$$

Therefore, the total equivalent PCM error probability due to wrong slot errors can be accumulated as following:

$$P_{ewsDiPPM} = P_{ewsSR} + P_{ewsRS} \tag{8}$$

$$P_{ewsDiPPM} = 3.\sum_{x=0}^{n-1} \left(\frac{1}{2}\right)^{x+3} P_s(x+1) + \left(\frac{1}{2}\right)^{x+2} P_s(\mathrm{n}+1) \tag{9}$$

Table 3-2 Wrong-slot Error (Transmitted and Received Sequences)

Transmitted	S	xN	R
Received	R	xN	R
Probability	$\frac{1}{4}P_s$	$\left(\frac{1}{2}\right)^x$	$\frac{1}{2}$

3.3.2 Erasure Errors

An erasure error occurs when the noise level is larger than the pulse signal and reduces the peak signal voltage below the threshold level, thus giving an incorrect detection (I Garrett, 1983; M. J. Sibley, 2003b; M. J. Sibley & Massarella, 1993).Thus, the probability of this error is given by

$$P_{er} = 0.5\, erfc\left(\frac{Q_{er}}{\sqrt{2}}\right) \tag{10}$$

where

$$Q_{er} = \frac{v_{pk} - v_d}{\sqrt{\langle {n_0}^2 \rangle}} \tag{11}$$

and

v_o= is the voltage level of the slot.

v_d=$v_o(t_d)$ is the receiver output at the threshold crossing timet_d.

v_{pk}=$v_o(t_{pk})$ is the peak signal voltage at the output of the receiver.

For a DPPM system, the equivalent PCM error probability, due to erasure error for the received pulse, is given by

$$P_{erDPPM} = \frac{2^M}{2(2^M - 1)} P_{er} \tag{12}$$

For a DiPPM system, erasure of a SET or RESET pulse creates the same number of PCM errors, thus the equivalent PCM error probability (M. J. Sibley & Massarella, 1993) can expressed as:

$$P_{erDiPPM} = 2.\left(\sum_{x=0}^{n-1} \left(\frac{1}{2}\right)^{x+3} P_{er}(x+1) + \left(\frac{1}{2}\right)^{x+2} P_{er}(\mathrm{n}+1) \right) \tag{13}$$

3.3.3 False-alarm Errors

The false-alarm error occurs when the noise causes a threshold-crossing event in an unoccupied data slot (I Garrett, 1983; M. J. Sibley, 2003b; M. J. Sibley & Massarella, 1993).So the probability of this event is given by

$$P_t = 0.5\, erfc\left(\frac{Q_t}{\sqrt{2}}\right) \tag{14}$$

where

$$Q_t = \frac{v_d}{\sqrt{\langle {n_0}^2 \rangle}} \tag{15}$$

The number of uncorrelated samples per time slot can be estimated in terms of T_s/τ_R where τ_R is the time when the noise autocorrelation function, at the receiver filter output, becomes small. Hence, the probability of the false alarm error becomes

$$P_f = (T_s/\tau_R)0.5\, erfc(\frac{Q_t}{\sqrt{2}}) \tag{16}$$

For a DPPM system, the equivalent PCM error probability due to false-alarm error is given by

$$P_{efDPPM} = \frac{2^M}{4} P_f \tag{17}$$

For DiPPM system, when the pulse is in slot S, a false alarm can occur in the following R slot. Therefore no PCM errors are generated because the decoder stops when a pulse is

received. On the other hand, an error will be generated if a false alarm occurs in the following string of N (NO PULSE) signals. Accordingly, the severity of the error depends on the location where the false alarm occurs, as shown in Table 3.3.

Table 3-3 False-alarm Error (Transmitted and Received Sequences

Transmitted	S	N	N	N	N	N	R
Received	S	N	N	R	N	N	R

When a run of *x*N symbols are expected the false alarm error will occur on the k^{th}N symbol, thus the PCM error becomes (*x*+1-k) and *x* must be greater than zero. In this case, as the pulse S is transmitted the false alarm error in the R slot has no effect. The effect of a false alarm in slot S is similar to that in slot R, and so the equivalent PCM error probability (M. J. Sibley, 2003b) is given by

$$P_{efNR} = P_{efNS} = \sum_{x=0}^{n-1}\sum_{k=0}^{x}\left(\frac{1}{2}\right)^{x+3} P_f(x+1-k) + \sum_{k=0}^{n}\left(\frac{1}{2}\right)^{x+2} P_f(\mathrm{n}+1-\mathrm{k}) \tag{18}$$

Hence, the equivalent PCM error probability which generated by false alarm error is therefore

$$P_{efDiPPM} = 2.\left(\sum_{x=0}^{n-1}\sum_{k=0}^{x}\left(\frac{1}{2}\right)^{x+3} P_f(x+1-k) + \sum_{k=0}^{n}\left(\frac{1}{2}\right)^{x+2} P_f(\mathrm{n}+1-\mathrm{k})\right) \tag{19}$$

Finally, for both DPPM and DiPPM systems the total equivalent PCM error probability can be determine by adding together the three errors of each (I Garrett, 1983; M. J. Sibley, 2003b; M. J. Sibley & Massarella, 1993).

3.3.4 Signal and Noise

The evaluation of the error probabilities for such communication systems are based on the received pulse voltage $v_o(t)$ and the mean square receiver output noise $\langle n(t)_o^2 \rangle$, and this in turn depends upon the type of preamplifier employed, the associated noise power spectral density and the type of equalisation filter used. For a received pulse energy *b*, the received pulse shape $h_p(t)$, which is the convolution of the transmitted signal and the channel impulse response of the communication link, has the following property (Audeh & Kahn, 1994; Cryan & Unwin, 1993)

$$\int_{-\infty}^{\infty} h_p(t)dt = 1 \tag{20}$$

The received pulse voltage at the output of the optimum desired filter of transfer function $H(\omega)$ and at the input of the detector is expressed as (M. J. Sibley, 2003a) (M. J. Sibley, 2003b; M. J. Sibley & Massarella, 1993),

$$v_o(t) = \frac{bR}{2\pi}\int_{-\infty}^{\infty} H_p(\omega).H(\omega)e^{-j\omega t}d\omega \tag{21}$$

where, R is the mid-band transimpedance of the receiver preamplifier.

At the detector the decision making can be possible and easy if the signal passes through a filter that maximises the signal component at a predicted instant and which suppress the amplitude of the noise at the same time. Assuming the pulse is present; the output will appear to have a significant peak at this instant. On the other hand if the pulse is absent, no such peak will appear. Thus it is possible to decide whether the pulse is present or absent with a reduced probability of error. Since the purpose of the receiving filter is to increase the signal component and decrease the noise component, this is equivalent to getting the maximum ratio of the signal amplitude to the noise amplitude at same instant at the output. The received signal consists of $h_p(t)$ signal pulse and channel noise $n_o(t)$, which is a random signal and hence cannot be described exactly. Thus its mean square value $\langle n(t)_o^2 \rangle$ must be considered. If a matched filter is used at the receiver, the receiver noise at its output can be expressed as (Audeh & Kahn, 1994; M. J. Sibley, 2003a, 2003b).

$$\langle n(t)_o^2 \rangle = \frac{S_o}{2\pi}\int_{-\infty}^{\infty} \left| H_p(\omega)\, H(\omega)\right|^2 d\omega \tag{22}$$

where, $H_p(\omega)$ is Fourier transform of the matched filter at the receiver, $H(\omega)$ is the transfer function of the desired optimum filter, and S_o is the double-sided equivalent input noise current spectral density of the preamplifier.

3.4 Characteristics of Modulation Techniques

One of the main features for the transmission system is the modulation technique, to increase the system performance and reduce the error probability as well as support the transmitter to operate at a high data rate with low power consumption. In other wards the modulation is a method used to convert the required signal to another shape that can be sent throughout communication systems with less interference. OWC based on IM/DD modulation has two stages; data carrier frequency and emitted optical light modulation. The very low frequency band close to DC components should not be used; where the shot noise ambient light can interfere and affects the receiver performance. High system performance should have a built-in high quality modulation technique (J. Kahn et al., 1992; A. Moreira et al., 1996).

There are several digital modulation techniques being proposed. For designing a communication system with high performance, the selection of a modulation technique has a great significance in a specific application. In general, the selection of a modulation technique is influenced by channel characteristics; performance desired from the overall communication systems, application of transmitted data, simplicity of implementation of modulation scheme and cost factors (Gagliardi & Karp, 1976).
In practice, the design of any optical communication system depends on the following most important parameters:

3.4.1 Transmission Reliability

The bit-error-rate (BER) should be within the acceptable limit at the receiver end to ensure the receiver is compatible with the transmission symbols. This needs a modulation technique that has the ability to control BER and reliability to avoid intersymbol interference. In OWC multipath distortion, pulse spread and variation of the signal power leads to severe ISI and degrades system performance (Ghassemlooy & Hayes, 2003b; Hirt, Hassner, & Heise, 2001; J. M. Kahn & Barry, 1997). The modulation technique should have independent facilities that support it to work away from the link behaviour in order to improve the system performance.

3.4.2 Power Efficiency

This factor is the most important parameter to be considered in designing a particular modulation scheme. Current optical techniques are already achieving high power efficiency and a reduction in power consumption. In addition, and for future demand, more power reduction with higher system performance is required. OWC has wide bandwidth including infrared and visible light according to the spectrum of the light. Infrared power is limited under the conditions set for eye and skin safety although for visible light higher power is permitted, but for obtaining long battery life the power consumption has to be minimised. The power of the transmitter is selected to achieve a given BER at a given transmission rate (Gagliardi & Karp, 1976; Lueftner et al., 2003; M. Sibley, 2005).

3.4.3 Bandwidth Efficiency

In an OWC system, theoretically, unlimited bandwidth can be accessible, practically, due to the presence of multipath propagation, in a diffuse link, this causes high ISI and leads to limited channel bandwidth and will impair system performance. The bandwidth of the

OWC system is also controlled by the receiver bandwidth. This makes the bandwidth efficiency of a particular modulation scheme one of the most important considerations. Therefore, a modulation scheme is required with high bandwidth efficiency. In this case the receiver should be compatible to the transmitted bit rate (Lueftner et al., 2003).

3.4.4 Simplicity and Cost

In addition to the previous requirements for suitable modulation technique, the simplicity in designing and implementing of a modern coding scheme are required. The complexity and the power consumption make this scheme not particularly useful because of the cost. Most of the designers of new coding circuit take into account the circuit efficiency in case of power consumption and bandwidth to achieve the future demand of high bandwidth transmission system with low cost (Ghassemlooy & Hayes, 2003b; Hirt et al., 2001; J. M. Kahn & Barry, 1997).

3.4.5 Receiver Sensitivity

A necessary parameter in evaluating the system performance of an optical transmission system is the receiver sensitivity, which is defined as the minimum average optical power for a given Bit Error Rate (BER). A good receiver means a receiver with high sensitivity, it is important to study the different parameters that have significant effects on overall receiver sensitivity. In other words for any communications system, the better the receiver sensitivity the better the system performance (Personick, 1973; Proakis, 2001).

The higher the data rate the poorer the receiver sensitivity will be because at the receiver more power is required to support the higher data rate. Optical power is limited by eye and skin regulations, thus high sensitivity is required. To achieve the best optical sensitivity, it is important to maximize the signal before data decision. In optical systems, and for a given delay spread, increasing the data rate leads to shorter pulses, increasing the effect of ISI and degrading the system performance. The degradation of system performance due to unwanted high ISI will reach a point where the BER is irreducible at any rate of transmission power. Practically, improved receiver sensitivity offers more freedom to system designer to make trade-offs between system performance and economics. Increasing a data rate with significant receiver sensitivity is achieved by using suitable modulation techniques (Personick, 1973; Proakis, 2001; M. J. Sibley, 1994).

3.5 Optical Power for DiPPM and digital PPM

Two of optical wireless communication modulation schemes are proposed in the present study, in terms of optimising the system performance in comparison of the relative values of DiPPM and a similarly performing digital PPM system.

For DiPPM the slot duration T_s is

$$T_s = \frac{T_b}{2 + gu} \tag{23}$$

For digital PPM the slot duration is

$$T_s = \frac{N.T_b}{2^N + gu} \tag{24}$$

Where $T_b = 1/B$ denotes the PCM bit time,B is the original data rate and gu is the guard intervals and *N* is the number of PCM bits (M. J. Sibley, 2003b).
The required optical power for the DiPPM system is

$$P_{DiPPM} = bhv\frac{n+1}{8.n}B \tag{25}$$

And required optical power for the digital PPM system for (M. J. Sibley, 2003a)

$$P_{DiPPM} = bhv\frac{B}{M} \tag{26}$$

where, v is the photon frequency, b is the number of photons per pulse, n is the DiPPM run length and *h* is the Planck's constant.
Receiver sensitivity indicates how minor the transmitted signal can be successfully received by the receiver, the lower the power level that the receiver can successfully process the better the receiver sensitivity. The receiver sensitivity is calculated in decibel on a logarithmic scale.

4 FUNDAMENTALS OF OWC

In simple terms, OWC combines two way data transmission between two points through optical radiation over unguided channel. The propagation link prototypes in VLC are basically classified relating to two principles, the degree of direction of the radiation pattern (directed, non-directed or hybrid) and how the link is set up in LOS or non-LOS. The LOS link always includes narrow field of view (FOV) transceivers that are directed for successful communication link, and depend on a direct path between transmitter and the receiver (Navina Kumar, Lourenco, Spiez, & Aguiar, 2008).

In practice, LOS links offer high power efficiency as the path loss is minimised and the transmitted signal is concentrated into a narrow beam. In addition LOS does not suffer from multipath distortion, so a higher data rate can be achieved through this link. Also, LOS link is independent on the reflective properties of the room and the distance between the transceivers can always assured for a given optical power. On the other hand, if the LOS link is interrupted and blocked the transfer of the data information would be miscarried. A tracked system is suitable for this case; a small FOV is permitted

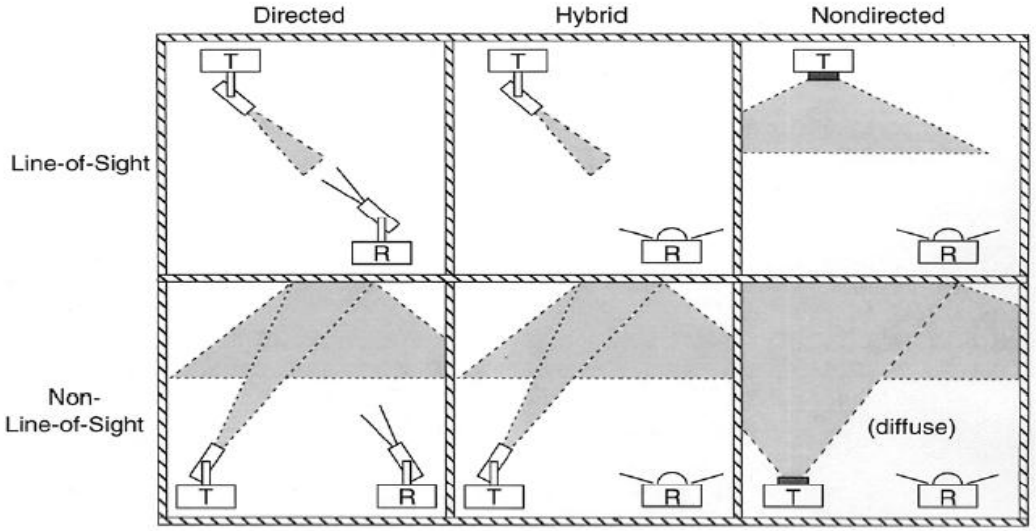

Figure 4-1 Indoor OWC Configurations Prototypes(J. M. Kahn & Barry, 1997)

at the receiver to reduce multipath reflection and dispersion. It offers high coverage with high power efficiency (J. M. Kahn & Barry, 1997; Navina Kumar et al., 2008).

The other configuration is the hybrid non-LOS topology; it does not suffer from link blocking link, but forms multipath distortion that is proportional, in parallel, to the room area. The non-directed-non-LOS or diffuse system is the most attractive indoor configuration. It works even if there is no direct link and does not need alignment

between the transmitter and receiver. The design of the photodetector is very important to receive sufficient optical power. In such case wide FOV is highly attractive with ability to avoid any obstructions for a maximum robust system. Practically, wide FOV is presented by adding a diffusion lens or by designing a light source involving LEDs array opposite to a photodetectors array. Actually, the optical signals are reflected from the ceiling of the room or any other diffuse reflector such as the; wall, room furniture and other equipment. This makes the diffuse configuration most robust and more flexible. Nevertheless, this configuration suffers from multipath signal dispersion due to the multiple delays, which causes ISI, and higher path loss than the other configurations. It makes implementation of such diffuse systems difficult for the higher transmission rates. In this case a consideration of higher degree of reflections and a high efficiency modulation technique is required (Cui et al., 2010; Zhang et al., 2012).

4.1 Indoor OWC Channel Model

VLC signals are radiated in all directions when incident on an ideal Lambertian reflector. An OWC system exploits this property to send and receive data in an indoor environment. The features of a room, for example, walls, ceiling, and office materials, can be a good approximation for an ideal Lambertian reflector (J. M. Kahn & Barry, 1997).

Practically, an optical wireless link adopts an intensity modulation and direct detection technique (IM/DD) because of its simple implementation, in which the intensity or power of the optical source is directly modulated onto the instantaneous power of the carrier, by varying the drive current. The main down-conversion technique at the receiver is direct detection (DD), in which the photo-detector produces a photocurrent proportional to the receiver instantaneous optical power (J. Kahn et al., 1992; A. Moreira et al., 1996).

The transmitted optical power $X(t)$ propagates, along a variety of paths of different lengths, with optical wireless channels subject to multipath induced distortion. The optical wireless channel can be modelled as baseband linear system using IM/DD with input power $X(t)$, output $Y(t)$, and an impulse response $h(t)$, as shown in Fig.4.2 (Carruthers & Kahn, 1997).

At the receiver the detector is illuminated by light energy, and these can include ambient lighting from other sources, formed by natural (sunlight) and artificial light sources. These sources can cause variation in the received photocurrent that is unrelated to the transmitting signal and is essentially minimizing this background light using optical filters (J. Kahn et al., 1992; A. Moreira et al., 1996).

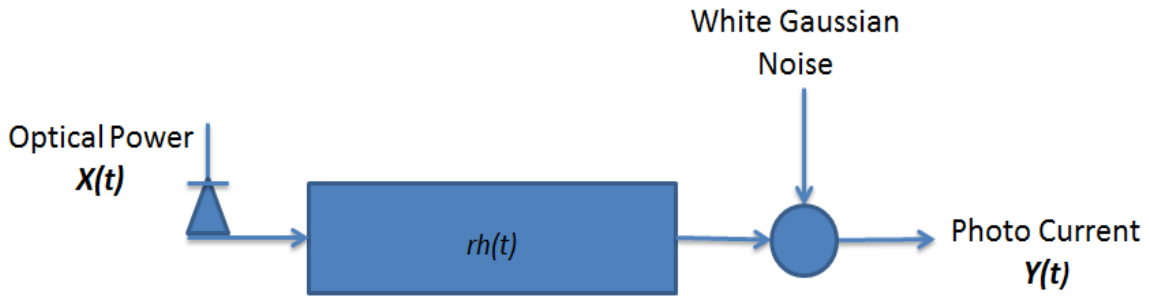

Figure 4-2-Optical Wireless Channel

The average power of this background radiation generates a DC photocurrent in the photo-detector, giving rise to shot noise $n(t)$. The shot noise can be modelled as white Gaussian and independent of the received signal. The shot noise is the dominant noise source in a typical diffuse receiver. If little or no ambient light is present, the dominant noise source is receiver amplifier noise, which is also Gaussian and signal independent. Also, artificial ambient sources can generate a periodic interference signal that are usually added to $n(t)$.Moreover, the noise also term includes the thermal noise which is normally constant and related to temperature (J. Kahn et al., 1992; A. Moreira et al., 1996).

In the photodetector, the shot noise is due to background lights inducing a current. It results in the DC photocurrent I_b, with a double sided noise power spectral density expressed as (M. J. Sibley, 1994):

$$N_0 = q.I_b \qquad (A^2/Hz) \tag{27}$$

Besides noise, there is an important path loss that can cause signal degradation, due to transmission distance and pulse delay for larger reflection time. So it is important to calculate signal to noise ratio for the system. The signal-to-noise ratio is the ratio of total electrical power to the noise power in the photodiode. In other words, in optical terms, it is a measure of optical received power as compared to the background noise. Commonly, it is written in the form of S/N or SNR and given as (J. M. Kahn & Barry, 1997; M. J. Sibley, 1994)

$$\mathrm{SNR} = \frac{2R^2{P_r}^2}{N_0 B} \tag{28}$$

where R is the photodiode Responsivity, P_r is the received optical power, N_0 is the double-side noise spectral density and B is noise bandwidth.

Mathematically, the IM/DD baseband model of the optical wireless channel, which illustrated in Fig.4.2, can be summarised as:

$$Y(t) = rX(t) * h(t) + n(t) \tag{29}$$

where r is the photo-detectorResponsivity (A/W), $h(t)$ is the channel impulse response, and the symbol * denotes convolution.

Simply stated, the receiver photocurrent $Y(t)$ is the convolution of the transmitted optical power X (t) with the channel impulse response $h(t)$, scaled by photo-detector responsivity, r, plus additive noise $n(t)$.

Generally, the channel represented by (29) is simply a conventional linear filter channel plus additive noise. However, IM/DD optical wireless channel differ from conventional electrical or radio channels, since X(t) is an optical power signal and; it must satisfy the constraints (Ghassemlooy & Hayes, 2003):

$$X(t) \geq 0 \tag{30}$$

$$P = lim_{T \to \infty} \frac{1}{2T} \int_{-T}^{T} X(t)dt \leq P_t \tag{31}$$

Where P is the transmitted optical power and P_t is the average optical power limit of the transmitter and required by eye-safety restrictions.

The constraint (31) indicates that the average optical power is given by the mean of input power signal rather than the mean square of the signal amplitude as in the case of conventional RF channel (conventional linear Gaussian noise channel) (Ghassemlooy & Hayes, 2003a; J. Kahn et al., 1992).

Then, for the optical wireless link the average received power becomes:

$$P_r = H(0).P_t \tag{32}$$

Where $H(0)$is the DC gain of the optical wireless channel, which is the Fourier transform of the impulse response $h(t)$ evaluated at zero frequency, hence

$$H(0) = \int_{-\infty}^{\infty} h(t)dt \tag{33}$$

4.2 LED Characteristics

Two basic properties of LED lights are important for VLC systems LED luminous intensity and transmitted optical power. The luminous intensity is defined as a unit of energy flux per solid angle and is normalized with visibility. Typically, LED brightness is expressed by luminous intensity. While the transmitted power is defined as the total energy radiated from an optical source (LED). In mathematical form LED luminous intensity (Komine & Nakagawa, 2004) can be

$$I = \frac{d\Phi}{d\Omega} \tag{34}$$

where Ω is the solid angle, $d\Omega$ denotes the differential solid angle and Φ is the luminous that can be specified in term of energy flux, over white light wavelength, in the following equation:

$$\Phi = K_m \int_{380}^{780} V(\lambda)\varphi_e(\lambda)d\lambda \tag{35}$$

where φ_e is the energy flux, K_m is the maximum visibility, $V(\lambda)$ is the standard luminosity curve and λ is the light wave length.

The transmitted optical power is calculated by integrated the energy flux in all directions as following.

$$P_t = \int_{\Delta_{min}}^{\Delta_{max}} \int_0^{\pi} \varphi_e d\theta d\lambda \tag{36}$$

The values of $\Delta_{\max}$ and $\Delta_{\min}$ are determined from PD sensitive curve.

The brightness of the LED over the illuminated surface is the LED illuminance. If the light source is radiated according Lambertian radiation with angle of irradiance Φ, then the luminous intensity can be expressed as

$$I(\Phi) = I(0)cos^m(\Phi) \tag{37}$$

In case of horizontal illuminance is given by

$$E_{hor} = \frac{I(0)cos^m(\Phi).\cos(\theta)}{d^2} \tag{38}$$

where $I(0)$ denotes the LED centre luminous intensity, θ is the angle of incidence and d^2 is the distance between the LED and the photodetector.

The order of Lambertian radiation m is depends on the half semi-angle illuminance,$\psi_{1/2}$, of LED.

$$m = \frac{-ln2}{\ln(\cos(\psi_{1/2}))} \tag{39}$$

However, for any LED used in offices the illuminance is limited by International Organization for Standardization (ISO) and the required illuminance is between 300 to 1500 lx (Komine & Nakagawa, 2004; J.-y. WANG et al., 2012).

4.3 Photodetector Characteristics

Photodiode is one of the most important device for any OWC, that has critical specifications which should be considered in order to have a high efficiency optical receiver, such as; Responsivity, bandwidth, response time and dark current (M. J. Sibley, 1994).

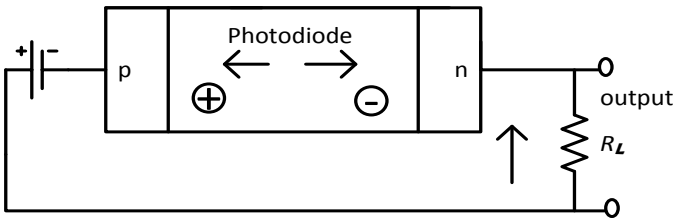

Figure 4-3 Basic Circuitry of PD

4.3.1 Responsivity:

The Responsivity is the ratio of the photocurrent that is generated at the photodetector to the power of incident light. It is expressed in units of A/W from electric current, I_p, (M. J. Sibley, 1994) as

$$I_p = \eta e \phi \tag{40}$$

Where ϕ is the photon flux and has the relation between the incident optical power to the energy of photons.

$$\phi = \frac{P}{hv} \tag{41}$$

the quantum efficiency η is defined as the relation of carrier flux generated by photodiode to the incident photon flux and can be expressed as

$$\eta = \frac{I_p/e}{p/hv} \tag{42}$$

$$I_p = \eta \frac{eP}{hv} \tag{43}$$

Therefore the responsivity is

$$R(\lambda) = \frac{I_p}{P} = \eta \frac{e}{hv} \tag{44}$$

Where P the incident power, e is the electron charge, η is the quantum efficiency of the detector, and hv is the photon energy.

The output voltage is given as

$$V_0 = PR(\lambda)R_L \tag{45}$$

where $R_L$is the load resistance and $PR(\lambda)$ is responsivity at the selected wavelength.

4.3.2 Bandwidth

The Photodiode bandwidth is an important factor when a time response for PD is required. The rise time of the PD impulse response depends on the time constant τ, which is a combination of the load resistance and diode capacitance. The rise time is that time required by the photodiode output to step from 10% to 90% of its steady state.

In optical communication systems, the bandwidth is determined by response time. The 3dB bandwidth and the rise time for the circuit are calculated as following (M. J. Sibley, 1994)

$$f_{3dB} = \frac{1}{2\pi R_L C} \tag{46}$$

$$\tau_r = \frac{0.35}{f_{3dB}} \tag{47}$$

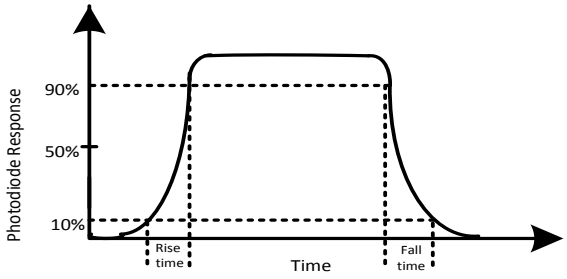

Figure 4-4 Typical response of PD to a square pulse

Most PD applications require a high speed or broadband photodetection. The two factors that control these requirements are the time of response of the photocurrent and the time constant of the PD equivalent circuit.

4.3.3 Dark Current

In most PD applications the major noise source is dark current, which is a measurable noise current. It's generated when a reverse voltage is applied on PD. A large active area of PD is often enhanced for increasing PD sensitivity as well as increasing of the dark current. In the other hand it makes it difficult trade-off these parameters (Sibley, 1994).

4.3.4 White LED

White light LEDs with a high power output and low power consumption have become more popular than lamps because of their cost and efficiency. According to the LED specifications the response time of the LED can play an important role in high speed data transmission. As the requirements for multimedia information are increased everywhere in an indoor area, demands on the data communication provider including high speed links will increase rapidly. Therefore, the concept of indoor visible light communication has attracted considerable attention and white LED is also drawing further attention (Komine & Nakagawa, 2004; O'Brien et al., 2008).
However, obtained white LEDs with high efficiency was difficult until recently. Now a mix of red, blue and green LEDs have been fabricated for producing a white light emission. Fortunately, long lifetime white LEDs with high power efficiency have become available in most markets. Consequently, the white LEDs will be used instead of incandescent or lamps in homes and offices. Many studies and researches have investigated the properties of white LEDs and confirmed they are suitable and feasible candidate for optical wireless communication systems. The proposed systems are based on propagated optical signal for data transmission and with little shadowing in a whole room becomes possible by using high power white LED, also installation of lighting equipment becomes informal (Komine & Nakagawa, 2004; Navin Kumar & Lourenco, 2010).

5 INDOOR VLC CHANNEL MODELS

In this chapter, an indoor VLC has been studied in order to investigate the channel characteristics for LOS and multipath reflections. The transmitting information is arrived and emitted into the air by LEDs. The LEDs modulate these signals related to the pulse source modulation scheme. The visible light waves are distributed over all the room; its shape is equivalent to the convolution of LED's impulse response and modulated pulses.

In order to realize the overall channel impulse response for the indoor VLC, a fixed position of the receiver and the transmitter is proposed. Thus the channel would be considered as a fixed channel, due to little variation, compared to the high speed of the binary rate. Moreover, related to the indoor optical channel characteristics the optical wireless link suffers from the effect of multiple reflections, which build up from common surfaces in the room (Barry et al., 1993; Carruthers & Kahn, 1997).

There are different models have been proposed to provide the channel characteristics of indoor VLC. The common proposed VLC system which has been considered in most of the research studies will be investigated in this thesis, the simple diagram of the VLC system is shown in Fig.5-1.

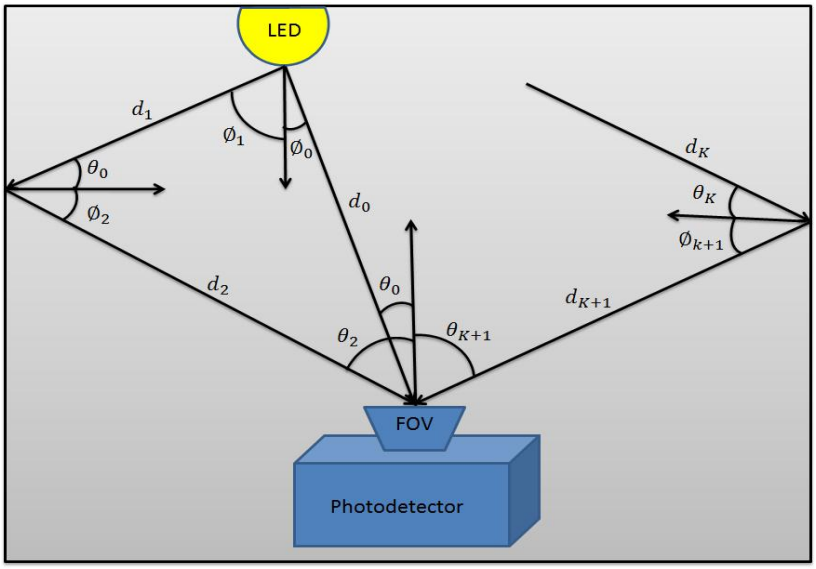

Figure 5-1 indoor VLC. Proposed system diagram

Two models have been investigated in this thesis the first one based on the different order of multiple reflections included LOS path. The second one is modelled on the impulse response related to FOV, for both LOS and non-direct-LOS.

5.1.1 VLC Impulse Response Utilizing Different order Reflections (Model 1)

The room construction, in Fig.5-1, shows a wide band non-direct source and multipath light reflections over the room. Here the reflecting surfaces include; walls, floor and furniture which are considered to be ideal Lambertian reflectors (Komine & Nakagawa, 2004; Saadi et al., 2013). Therefore, the source radiation pattern in diffuse form is given as

$$R(\phi) = \frac{m+1}{2\pi}.cos^{m}(\phi) \tag{48}$$

where m is the order of Lambertian radiation pattern. The order of Lambertian radiation m is related to the half semi-angle illuminance, $\psi_{1/2}$, of LED, and formed as

$$m = \frac{-ln2}{\ln(\cos(\psi_{1/2}))} \tag{49}$$

According to the room model with Lambertian reflectors and for a particular source *S,* and receiver *R*, and under linearity condition, the impulse response of the light wave undergoing k reflections, can be formulated as following

$$h_c(t;S,R) = \sum_{k=0}^{\infty} {h_c}^{k}(t;S,R) \tag{50}$$

For direct LOS signal the impulse response can be expressed as

$${h_c}^{0}(t;S,R) = R(\phi).\frac{A\cos(\theta)}{d^2}.V(S,R).\delta\left(t-\frac{d}{c}\right) \tag{51}$$

$V(S,R)$ is the visibility function and has value 1 and 0 for unblocked and blocked path between the source and the receiver, respectively. It can be expressed as a rectangular function (Barry et al., 1993).

$$rect(t) = \begin{cases} 1 & if|t| \le 1 \\ 0 & if|t| > 1 \end{cases} \tag{52}$$

Then

$${h_c}^{0}(t;S,R) = L_0.rect\left(\frac{\theta_0}{FOV}\right).\delta\left(t-\frac{d_0}{c}\right) \tag{53}$$

where

$$L_0 = \frac{(m+1)A_{PD}}{2\pi {d_0}^2}.cos^m(\phi_0).\cos(\theta_0) \quad (54)$$

And for undergoing K reflections with time spreading (delay) of received signals, due to multipath propagation, the impulse response can be expressed as

$${h_c}^k(t;S,R) = \int_S [L_1 L_1 \dots L_{k+1}.\rho^k.rect\left(\frac{\theta_{k+1}}{FOV}\right).\delta\left(t - \frac{d_1 + d_2 + \cdots d_{k+1}}{c}\right)]\, dA_{ref}. \qquad k \geq 1 \quad (55)$$

$$L_1 = \frac{(m+1)A_{ref}}{2\pi {d_1}^2}.cos^m(\phi_1).\cos(\theta_1) \quad (56)$$

$$L_2 = \frac{A_{ref}}{2\pi {d_2}^2}.\cos(\phi_2).\cos(\theta_2) \quad (57)$$

$$L_{k+1} = \frac{A_{PD}}{2\pi {d_{k+1}}^2}.\cos(\phi_k).\cos(\theta_k) \quad (58)$$

L_0 and $L_1 L_1 \dots L_{k+1}$ represent path loss terms for LOS and non-LOS radiations. A_{PD} is the active receiving area for PD, A_{ref} is the small active area for reflecting element and ρ is the average reflectivity of the walls. The angles of incidence and irradiance are denoted by θ_k andϕ_k, respectively. The speed of the light is c and the travel distances of the light signal to reach the detector directly or after k-bounce are d_0 and d_k, respectively. The integration in the above equation is calculated over the surface of all reflectors (K. Lee & Park, 2011; Saadi et al., 2013).

5.1.1.1 Received Power of LOS Light

Generally, VLC link includes a channel DC gain $H(0)$,when the receiver located at distance d from transmitter under the condition that the emission radiant intensity has a Lambertian pattern, and Using equation (54) (J. M. Kahn & Barry, 1997; Komine & Nakagawa, 2004), is given by

$$H(0) = \begin{cases} L_0.T_s(\theta).g(\theta), & 0 \leq \theta \leq \psi_c \\ 0, & \theta > \psi_c \end{cases} \quad (59)$$

where $\psi_c$is the FOV of the receiver, $T_s(\theta)$ denotes the gain of optical filter while $g(\theta)$ denotes the gain of optical concentrator and is given by (J. M. Kahn & Barry, 1997).

$$g(\theta) = \begin{cases} \frac{\mathrm{n}^2}{\sin^2\psi_c}, & 0 \leq \theta \leq \psi_c \\ 0, & \theta > \psi_c \end{cases} \quad (60)$$

where n is the refractive index.

Assuming the optical transmitter radiated an optical power P_t, then the received optical power can be derived by

$$P_r = H(0).P_t \tag{61}$$

If m is increased, the transmitter pattern becomes narrower; therefore more power can be received. Alternatively, optical filter and optical concentrator with high gains can be connected.

5.1.1.2 Received Power of Reflected Light

Different from LOS, in non-LOS a reflected light by the room is a key factor for received power, since the reflectors inside the room are to be considered as being diffuse reflectors, such as; walling, furniture and stuff. Therefore the path losses are completely described by the reflected power arrived at the reflection surfaces. Using equations (56, 57 & 58), the channel DC gain of VLC link after K bounces can be expressed as

$$H_{reff}(0) = \begin{cases} L_1.L_1.L_{K+1}.\rho^k.T_s(\theta).g(\theta), & 0 \le \theta \le \psi_c \\ 0, & \theta > \psi_c \end{cases} \tag{62}$$

Then the received optical power is given by

$$P_r = H(0).P_t \tag{63}$$

5.1.2 VLC Impulse Response Utilizing FOV (Model 2)

Typically, the channel linked to the active area of an optical receiver involves signal contributions due to reflectors as well as LOS signals. As in the previous section the room structure highlights the locations of the fixed transmitter and fixed receiver. Accordingly, the non-LOS channel model after unknown reflections can be characterized by two parameters, Dirac pulses with delay component ($\Delta t_{non-LOS}$) and optical multipath losses, and for LOS channel can be modelled by Dirac pulses with small delay (Δt_{LOS}). The overall VLC, $h(t)$, channel response is a LOS Dirac pulse followed by a continuous signal. In the time domain the two signals are separated and can be combined in parallel, so the impulse response of the VLC channel considered in this model can be derived in the following form (Jungnickel et al., 2002).

$$h(t) = h_{LOS}(t) + h_{diff}(t) \tag{64}$$

where the LOS channel impulse response, $h_{LOS}(t)$ is given by

$$h_{LOS}(t) = g_{LOS}\,\delta(t) \tag{65}$$

And the non-LOS channel impulse response, $h_{non-LOS}(t)$ is given by

$$h_{non-LOS} = g_{non-LOS}\,\delta(t - \Delta t_{non-LOS}) \tag{66}$$

where g_{LOS}, and$g_{non-LOS}$ are the gain and the delay of LOS and non-LOS components, respectively. $\Delta t_{non-LOS}$ denotes the delay between the arrived LOS signal and the reflected signal, while, Δt_{LOS} denotes the arrived time of the direct signal.

The impulse response of the non-LOS signal is seen as a characteristic by using a low pass filter because it is closed to that signal as evaluated by the integration of the sphere model based on small parameters. Moreover, the basic properties of visible light scattered on the sphere shape can be modelled by indoor non-LOS signal related to the intensity distribution and the gain of the optical wireless channel. Hence the total intensity due to many reflections from wide beam optical power can be expressed as (Jungnickel et al., 2002; Pohl, Jungnickel, & Von Helmolt, 2000):

$$I = \frac{I_1}{(1-\rho)} \tag{67}$$

Where I_1 is the homogeneous intensity of the first reflection across the room area.

$$I_1 = \rho_1 \frac{P_t}{A_{room}} \tag{68}$$

Hence the optical received power for non-LOS mode related to the area of the optical receiver is given by:

$$P_{\text{non-LOS}} = I * A_{PD} \tag{69}$$

A_{PD} is the active receiving area for PD, A_{room} denotes the room area and ρ is the ρ is the average reflectivity off the walls.

Therefore, the power efficiency according the non-LOS propagation related to the transmitted power can be written in the following form

$$\eta_{\text{non-LOS}} = \frac{P_{\text{non-LOS}}}{P_t} \tag{70}$$

$$\eta_{\text{non-LOS}} = \frac{A_{\text{R}} \quad \rho}{A_{Room}(1 - \rho)} \tag{71}$$

As the non-LOS signal is characteristic by low pass filter. Then the impulse response of the non-LOS signal is

$$H_{\text{non-LOS}}(f) = \frac{\eta_{\text{non-LOS}}}{(1 + \frac{\text{jf}}{f_0})} \tag{72}$$

In another expression as a function of the FOV the impulse response of non-LOS channel is given by (Jungnickel et al., 2002):

$$\eta_{\text{non-LOS}} = \frac{A_R sin^2(\text{FOV})\rho}{A_{Room}(1 - \rho)} \tag{73}$$

Including the delay time due to multipath reflection the impulse response of VLC in the room is given by

$$H(f) = \eta_{\text{non-LOS}} . \frac{\exp(-j2\pi f . \Delta t_{\text{non-LOS}})}{(1 + \frac{jf}{f_0})} \tag{74}$$

where FOV is the field of view of the detector.

Mostly, LOS channel includes less distortion compared to diffuse channel even in situation with high data rates. In the case of light source pointed downwards, the received power is given from radiant intensity equation (46) multiplied by the solid angle (Ω):

$$P_r = \frac{A_R R(\phi)}{{d_0}^2} \tag{75}$$

$$P_r = \frac{A_R(m+1)}{2\pi {d_0}^2} \tag{76}$$

Then the power efficiency according the LOS propagation related to the maximum direction transmitted power and the maximum receiver sensitivity, can be written in the following form

$$\eta_{LOS} = \frac{(m+1)A_R}{2\pi {d_0}^2} . cos^m(\phi_0) . \cos(\theta_0) \tag{77}$$

The final impulse response for indoor light propagation as a parallel combination and with a phase offset ($2\pi f.\Delta t_{diff}$) in frequency domain(Jungnickel et al., 2002; Komine & Nakagawa, 2004) can be expressed as

$$H(f) = \eta_{LOS}. + \eta_{diff}. \frac{\exp\left(-j2\pi f.\Delta t_{diff}\right)}{(1 + \frac{jf}{f_0})} \tag{78}$$

5.1.2.1 Received Power of LOS Light

Using equation (63&77), the received power for LOS light, where η_{LOS} is the VLC channel DC gain, is then expressed as:

$$P_r = \eta_{LOS}.T_s(\theta).g(\theta).P_t \tag{79}$$

5.1.2.2 Received Power of Reflected Light

Different from LOS link the received power of the reflected light (non-LOS) can be determined by using equation (63 & 74) and expressed as

$$P_r = \eta_{non-LOS}.T_s(\theta).g(\theta).P_t \tag{80}$$

And as result the total DC gain, for a VLC system includes LOS and non-LOS links, can be calculated as combined of $\eta_{LOS}. + \eta_{non-LOSff}$. Then the total received power is written as:

$$P_r = (\eta_{LOS} + \eta_{non-LOS}).T_s(\theta).g(\theta).P_t \tag{81}$$

6 VARIABLE DIPPM FOR DIMMING CONTROL

6.1 Average Power

In general each transmitted pulse requires certain energy to reach the receiving side. In such modulation schemes like OOK, the average power is denoted by P_{avr}, and if one and zero have equal probability the transmitted signal requires $2P_{avr}$ for each bit, then the transmitted signal can be written as (Alam, 2006; K. Lee & Park, 2011b)

$$x(t) = 2P_{avr} \sum a_k P(t - kT) \tag{82}$$

where P_{avr} is the transmitted average optical power.

Let the transmitted pulse $P(t,T)$ has a rectangular shape

$$rect(t) = \begin{cases} 1 & if|t| \leq 1 \\ 0 & if|t| > 1 \end{cases} \tag{83}$$

In this case P_{peak} is denoted for the transmitted power when bit "1" is sent, for the modulation scheme OOK the probability of "0" and "1" appearing is equal. Therefore, the average power of OOK can be expressed as

$$P_{ook} = \frac{P_{avr}}{2} \tag{84}$$

$$energy = \frac{P_{avr}}{2}.rect(t).T \tag{85}$$

Hence, for VLC OOK systems the transmitted signal can be written in the following form:

$$x(t) = \frac{P_{avr}}{2}.rect(t - T) * h(t) \tag{86}$$

For the DPPM modulation scheme the transmitted pulses are given by:

$$x(t) = LP_{avr} \sum a_k.rect(t - kT) \tag{87}$$

The peak to average power ratio is L=2^M, L is the number of symbol chips. The DPPM transmitter emits an optical pulse during only one of the L chips, which have a duration of T_s/L, then the L time slot T_s (Audeh & Kahn, 1995) is:

$$T_s = \frac{M.T_b}{L} \tag{88}$$

As the average power is related to the peak power, then the average transmitted power of L-PPM can be expressed as

$$P_{PPM} = \frac{P_{avr}}{2^M} \tag{89}$$

Therefore, the one single slot has energy of

$$energy = L.P_{avr}.T_s \tag{90}$$

and the other slot L-1 has no energy.
Hence, for VLC DPPM system the transmitted signal can be written in the following form:

$$x(t) = L.P_{avr}\,.rect(t-T) * h(t) \tag{91}$$

In the case of DiPPM the average transmitted power is the energy of the transmitted pulse within the DiPPM frame, according to the Table 3-1, the pulse S and pulse R in the original data are sent for a transition 01 and 10, respectively and no pulse when there is no transition for 00 or 11. Thus the probability of having a pulse becomes ½ for the peak power (M. J. Sibley, 2003b).
For the DiPPM modulation scheme the transmitted pulses are given by:

$$x(t) = P_{avr} \sum rect(t-kT) \tag{92}$$

DiPPM transmitter emits an optical pulse during and for only for S and R symbols, which have a duration of T_s:

$$T_s = T_b/2 \tag{93}$$

Therefore, the average transmitted power of DiPPM can be expressed as

$$P_{DiPPM} = \frac{P_{avr}}{4} \tag{94}$$

Therefore, the one single slot has energy of

$$energy = (S\ or\ R)P_{avr}.T_s \tag{95}$$

and the other slot with no transition has no energy.

Hence, for VLC DiPPM system the transmitted signal can be written in the following form:

For a SET pulse

$$x(t) = \frac{P_{avr}}{4}.rect(t - T_s) * h(t) \tag{96}$$

While for the RESET pulse

$$x(t) = \frac{P_{avr}}{4}.rect(t + T_s) * h(t) \tag{97}$$

6.2 Dimming Control

LED lamps have become a source of artificial illumination and related to the LED characteristic; LED has an ability of providing a high response for transmitting data via a VLC channel. In many applications, such as hospital beds, office desks and airplane seats, VLC would be used for data transmission with high efficiency, long life time, constant illumination and sufficient brightness. A combination of LED brightness control and VLC becomes essential, which can be achieved by injected a dimming control protocol within the period of transmission. The average transmitted power of an LED is the average optical intensity of the transmitted signal P, which is limited by the illumination requirements in dimmable VLC. In practice the average optical intensity cannot be changed with time, however in most situations it can be adjusted and related to the transmission mode and that used modulation schemes. The LED is illuminated by a constant current source, varying the level of this current leads to a change in the LED light emitted colour. To improve these changes a dimming control driver should be used (R. Lee, Yun, Yoo, Jung, & Kwon, 2013; Sterckx & Saengudomlert, 2011; Sugiyama et al., 2007).

However, for IM/DD the optical wireless channel differs from conventional electrical or radio channels, since X (t) is the transmitted optical power intensity; it must satisfy the constraints (Ghassemlooy & Hayes, 2003a):

$$X(t) \geq 0 \tag{98}$$

$$P_t = \lim_{T\to\infty} \frac{1}{2T} \int_{-T}^{T} X(t)dt \leq \gamma P \tag{99}$$

where the dimming level $0 \leq \gamma \leq 1$, in case of $\gamma = 1$ the LED is under full brightness and for $\gamma = 0.5$ the LED gives 50% of the brightness (Park & Kim, 2014).
In this chapter, a modulation schemes included OOK and PPM are compared with DiPPM for suitability to inject a dimming control process.

6.2.1 Variable on-off Keying (VOOK):

In the case of OOK LED brightness which can only be controlled when OOK returns to zero (RZ-OOK) is used, because using non-return-to-zero (NRZ-OOK) is supported with only 50% brightness based on the transmitted optical intensity of 2P to signify a bit one (K. Lee & Park, 2011a). The duty cycle of RZ-OOK varies as

$$0 \leq \frac{\delta = \tau_{on}}{\mathrm{T}} \leq 1 \tag{100}$$

then the dimming factor for RZ-OOK can be expressed as

$$0 < \gamma = \frac{\delta}{2} \leq \frac{1}{2} \tag{101}$$

According to this condition a Variable OOK (VOOK) coding scheme has been proposed to control the LED brightness. Changing the duty cycle (δ_d)of the transmitted pulse is considered in this process.

$$\delta_d = \tau_d/\mathrm{T} \tag{102}$$

Where τ_d denotes the ON time for the transmitted pulse. At the off time when there is no pulse transmitted, and for an interval of the duty cycle, filler bits would be injected by either zeroes or ones associated to the dimming factor. Therefore, the dimming factor for VOOK scheme is given by:

$$\gamma_{VOOK} = \begin{cases} \frac{1}{2}\delta_d & 0 < \gamma < 0.5 \\ 1 - \frac{1}{2}\delta_d & 0.5 \leq \gamma > 1 \end{cases} \tag{103}$$

As a result the average LED brightness at ON time of transmission mode becomes 0.5 when d=0 or 1.

6.2.2 Variable PPM (VPPM)

Controlling the brightness of the LED during transmission mode using PPM coding scheme has a difficulty, because PPM is not suitable for VLC. The position of transmitted pulse in PPM technique varies according to the bit information which leads to non-fixed time slots. A combination of PWM and 2-PPM is proposed and a variable PPM becomes visible (K. Lee & Park, 2011b).

The idea is that only one bit involved for each symbol slot, similar to "2-PPM, where the position of the VPPM pulse is changed with bit information as high or low, while the width of the pulse is changed according to dimming level to control the LED brightness. In addition under full brightness VPPM cannot transmit bit information. The duty cycle is equal to the data time slot unlike for VOOK.

$$0 < \gamma_{VPPM} = \delta_d < 1 \tag{104}$$

As a result VPPM can provide a flexible dimming control compared to PPM in the same time , unfortunately, insignificant spectral efficiency is produced (Noh & Ju, 2012; Noshad & Brandt-Pearce, 2014).

For any modulation scheme using a fixed time slot, the duty cycle is equal to the data duty cycle (time slot), unlike OOK.

Also, for clock recovery, VPPM has a difficulty unlike 2-PPM which can be easily recovered the clock, where the signal transition occurs at the centre of the bit information while in VPPM it is varied with brightness level (Noh & Ju, 2012).

6.2.3 Variable DiPPM (V-DiPPM)

In this section a dimming control utilizing DiPPM coding scheme has been proposed. As mentioned previously DiPPM has fixed time slot and for PCM line coded a number of like symbols is limited to n and remains constant within the time frame. As a result no fluctuation of LED illumination can be experienced by human eyes. For DiPPM scheme the position of pulses S and R within a time frame (T_b) are fixed and has a time slot T_s (pulse width)

In DiPPM S and R pulse have the equal probability of ¼. The remaining bits information where no pulses sent, has probability of $1/2$. Thus resulting average dimming becomes only 25% of the maximum. The overall time the LED light is turned for longer and so the average illumination level increases and high performance transmission can be achieved.

DiPPM waveform (Romanos Charitopoulos, 2009) is given by

$$X(t) = \frac{A\delta_d}{T} + \frac{A\delta_d}{n\pi}\left(\sin\left(\frac{n\omega\delta_d}{2}\right)\right) + \cos(n\omega(t - 1.4\delta_d) + \cos(n\omega(t - 7.4\delta_d) +$$

$$\cos(n\omega(t - 4.4\delta_d) + \cos(n\omega(t - 8.4\delta_d) \quad (105)$$

where A denotes the amplitude of the pulse, T and f $(\omega = 2\pi f)$ are the clock period and clock frequency, respectively, and δ_d (T_s) is the pulse width.

It is clear that the amplitude of the transmitted pulse is the mean factor that can be used to control LED light intensity, consequently LED dimming is controlled according to the dimming factor. The duty cycle of the DiPPM equals the time slot duration

$$\delta_d = T_s \quad (106)$$

$$0 < \gamma_{VDiPPM} = T_s < 1 \quad (107)$$

In general, for OOK and Manchester codes the maximum data rate is archived at 50% of the brightness and for 4PPM is only 25% (Kaur, Liu, & Castor, 2009). DiPPM will stay ON for 75% of the time frame, hence duty cycle increasing. Moreover, the DiPPM has a fixed transmission time so it is easy to predict this time and hence a better performance can be achieved. As a result the proposed VDiPPM can offer a flexible VLC dimming control.

7 VLC SIMULATION

7.1 VLC Simulation Model

The modelling of multipath dispersion optical channel in a room takes into account the short pulses emitted by the source. Dirac delta function is a good approximation for the impulse response; hence the receiver would receive a train of pulses as a continuous signal. The optical signal power undergoing a K reflection is considered in this simulation and the channel delay spread which is the main parameter that is used to predict the multipath power requirement (Carruthers & Carroll, 2005; Komine & Nakagawa, 2004).
The proposed model based on the optical receiver includes Si-photodiode followed by a pre-amplifier and matched filters linked to the decision circuit, is shown in Fig.7-1.The system is operated at a bit rate of 1Gbps and 100 Mbps within the range of visible light of 400nm to 740nm wavelength. In these simulations Mathcad software was used to simulate the received pulse shape through all processing starting with a convolution of transmitted pulse with VLC impulse response and ending at the output of the voltage comparator. The performance of VLC system analysis is extended in order to include the effects of pulse detection errors such as; wrong slot, erasure and false alarm and as well as the effect of intersymbol interference (ISI) on error probability.

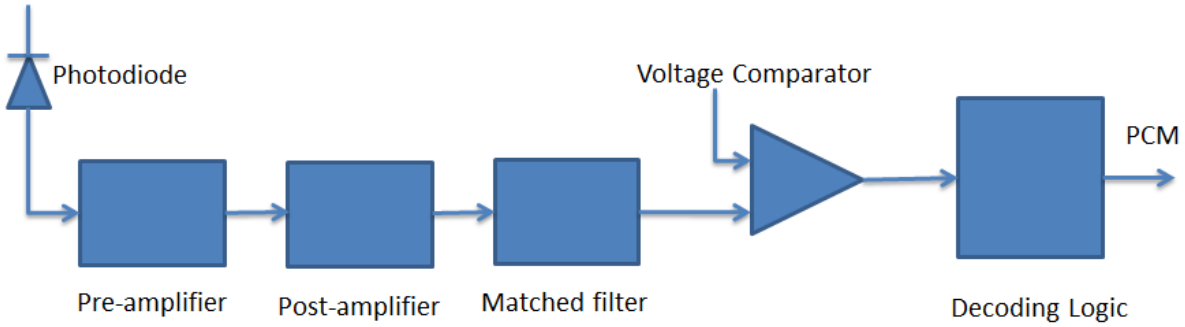

Figure 7-1 VLC Proposed Model

The average optical transmitted power is defined as a function that uses a modulation scheme (MS) to achieve a BER over a VLC channel with an impulse response $h(t)$ which includes additive white Gaussian noise of power spectral density N_0, as $P(BER, h(t), N_0, MS)$ (Carruthers & Kahn, 1997)

In this simulation, BER of 10^{-9} is used to calculate the average optical power requirements and hence the optical receiver sensitivity. The system performance is evaluated using the following algorithm:

- From knowledge of the received pulse shape and the receiver output noise ($<n^2>$), the system parameters pulse peak voltage (V_{pk}) and normalised delay spread are evaluated for a given pulses energy *b* (no. of photons) and threshold detection time t_d.
- A central decision detection strategy is applied, where $t_d = t_{pk}$ (time at the centre of the received pulse, peak time), and the smallest value of *b* is selected where *b*>0, that meets the performance criterion as given in equations (25 & 26).
- Cut-off frequency of pre-amplifier filter is selected carefully to match certain parameters ($0.5\frac{1}{T_s}$).
- The performance criterion is that the total error probability should be the same as for PCM (1 error in 10^9).
- The development of the Mathcad software simulation has been considered in order to achieve reliable theoretical and experimental results

7.2 VLC Simulation Link Setup

The optimum prediction filter for DiPPM, like DPPM, includes a noise whitened matched filter and a decision circuit, and this is utilized here to detect the shape of the received pulse.

Assume the input pulse shape $h_p(t)$ has the following property:

$$\int_{-\infty}^{\infty} h_p(t)\,dt = 1 \tag{108}$$

Therefore the output voltage of the preamplifier can be expressed as

$$v_0(t) = bhcR_0(\ Z_{pre}(t) * h_p(t)) \tag{109}$$

In presence of the VLC impulse response ($h_c(t)$) and according to the relation of the frequency response the preamplifier output voltage can be written (M. J. Sibley, 2003b)as

$$v_0(t) = \frac{b\eta q}{2\pi}\int_{-\infty}^{\infty} H_p(\omega)H_c(\omega)\, Z_{pre}(\omega)H(\omega).\, e^{j\omega t}d\omega \qquad (110)$$

where *b* denotes the number of photons per pulse (received pulse energy), R_0 is the Responsivity of the detector, *q* is the electron charge, η is the quantum efficiency of the detector and $H_c(\omega)$ is the VLC channel impulse response.

The Gaussian pulse is selected as a transmitted pulse, in the shape of

$$h_p(t) = \frac{1}{\sqrt{2\pi\alpha^2}}.\exp\left(-\frac{t^2}{2\alpha^2}\right) \qquad (111)$$

and

$$H_p(\omega) = \exp\left(-\frac{\alpha^2\omega^2}{2}\right) \qquad (112)$$

where the pulse variance α is related to the normalised system bandwidth (f_n) by

$$\alpha = \frac{0.1874\, T_b}{f_n} \qquad (113)$$

By assuming that the optical receiver has a single pole response f_c of -3 dB bandwidth, with a mid-band transimpedance R_T, and by using the matched filter at the receiver side ($H_p(\omega)$), the output voltage of the optical receiver at the output of the matched filter is derived as:

$$v_0(t) = \frac{b\eta q}{2\pi}\int_{-\infty}^{\infty} \frac{R_T}{\left(1+\frac{j\omega}{\omega_c}\right)}.\exp\left(-\frac{\alpha^2\omega^2}{2}\right).\exp\left(-\frac{\alpha^2\omega^2}{2}\right).H_c(\omega).e^{j\omega t}d\omega \qquad (114)$$

$$= \frac{b\eta q R_T}{2\pi}\int_{-\infty}^{\infty} \frac{1}{\left(1+\frac{j\omega}{\omega_c}\right)}.\exp(-\alpha^2\omega^2)..H_c(\omega).e^{j\omega t}d\omega \qquad (115)$$

From equation (22) the receiver noise obtained at the output of matched filter is

$$n_0{}^2 = \frac{S_0}{2\pi}\int_{-\infty}^{\infty} |\ H_p(\omega).Z_{pre}(\omega)\ |^2\, d\omega \qquad (116)$$

7.3 VLC Simulation Results Using Model (1)

The optical channel response model, for a diffuse VLC indoor optical wireless link adopted here, is based on the propagation model (1) which described in section 5.1.1.

Table 7-1 shows the propagation parameters used to generate the impulse response for indoor VLC link. These parameters adopted here are selected according to experimental

and simulation in many studies that proposed for indoor VLC channel the results (John R. Barry, 1993; Komine & Nakagawa, 2004; Saadi et al., 2013).

Table 7-1 Propagation Parameters for Model (1)

parameter	values
Irradiance angles, deg	$\phi_0 = 25,\ \phi_1 = 40,\ \phi_2 = 35,$
Incidence angles, deg	$\theta_0 = 15,\ \theta_1 = 25,\ \theta_2 = 20,$
Area of reflecting element, cm	$A_{ref} = 0.85$
Photodiode area, cm	$A_{PD} = 0.18$
Average wall reflectivity	$\rho = 0.8$
LOS distance, cm	$d_0 = 90$
Non-LOS distance, cm	$d_1 = 75,\ d_2 = 75$
Half semi-angle, deg	$\psi_{1/2} = 50$

The impulse response of the VLC channel in convolution with the transmitted Gaussian pulse is plotted in Fig.7-2. The figure shows that the received pulse due to the first reflection (non-LOS) has low power related to the LOS signal. This turns out that when the light undergoes two or more bounce, the reflected received power can be ignored due to weakness. According to the results in the LOS impulse arrives at time zero and carries 79% percent of the total power whereas for 6% (JR Barry, JM Kahn, WJ Krause, E Lee, 1993). A similar conclusion is determined where the rate of non-LOS light is small enough compared to with LOS light which are 3.6% and 95% of the total power, respectively (Borogovac et al.; Carruthers & Carroll, 2005; Komine & Nakagawa, 2004) and .

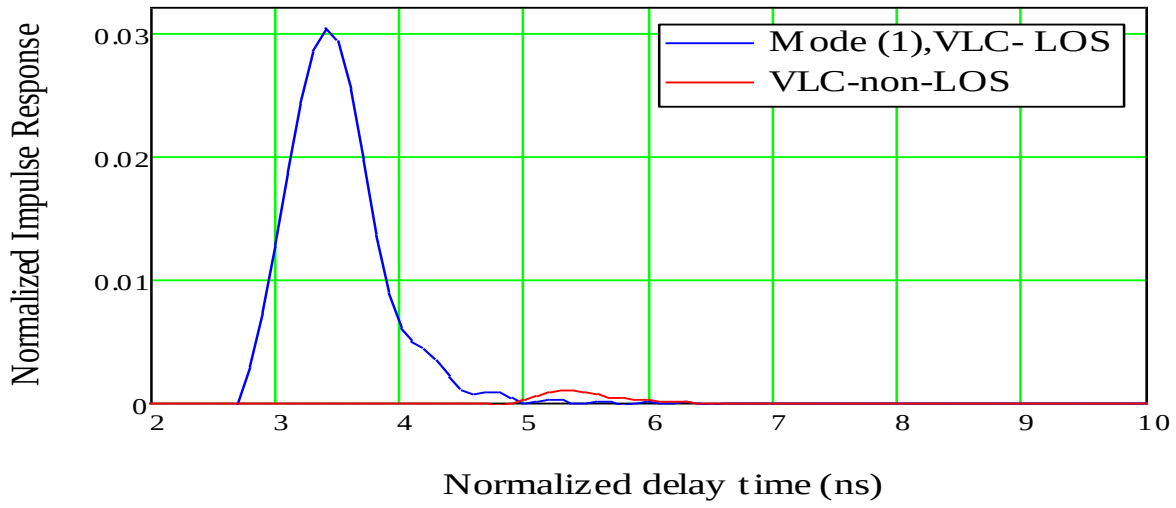

Figure 7-2 Impulse response of the VLC channel

By using equations (54, 55) for VLC impulse response for model (1), LOS and non-LOS are convolved in time and in parallel combination. In this case the shifting property of the Dirac-delta function can be used based on the definition of the Fourier transform, thus equation (116) can be rewritten as

$$v_0(t) = \frac{1}{2\pi}\int_{-\infty}^{\infty} \frac{1}{\left(1+\frac{j\omega}{\omega_c}\right)} . \exp(-\alpha^2\omega^2).[(L_0 \exp(-j\omega.\Delta t_{LOS}) + (L_1.L_2.\rho.\exp(-j\omega.\Delta t_{diff}))] . e^{j\omega t} d\omega \quad (117)$$

$$v_0(t) = \frac{1}{2\pi}\int_{-\infty}^{\infty} \frac{1}{\left(1+\frac{j\omega}{\omega_c}\right)} . \exp(-\alpha^2\omega^2).[(L_0 \exp(t - j\omega.\Delta t_{LOS}) + (L_1.L_2.\rho.\exp(t - j\omega.\Delta t_{diff}))] . d\omega \quad (118)$$

.

The simulation based on the parameters of the preamplifier and optical receiver as displayed in Table.7-2, data relating to a commercial receiver is used. The Thorlabs FDS025 photodiode is used for 1 Gbps simulation with a bandwidth of 7.5 GHz within a wavelength range of 400 to 1100 nm, 650 nm is assumed here. Double-sided equivalent noise spectral density of $50x10^{-24}$ A^2/Hz is used referenced to the preamplifier input. The preamplifier which utilized is a Philips CGY2110CU Transimpedance Preamplifier. Mathcad software has been written for VLC communication link. The channel link is completely described by the output shape pulse getting by equation (118).

The simulation results have been considered for two propagation topographies, diffuse and non-LOS. According to the amplitude of the obtained pulse shape, the errors probabilities of the received pulse are calculated for the modulation sequences based on the receiver noise at BER of 10^{-9}. The calculations have been carried out with a zero interval guard and the coding schemes are injected by two interval guards. The number of photons per pulse has been obtained, and the average received power is determined, then the receiver sensitivity is calculated in dBm.

In addition, the VLC channel path losses are calculated in order to determine the average transmitted power that is required from an LED to enhance the system performance.

Since in indoor VLC systems the LED light arrives at the receiver front-end in direct LOS and after multiple reflections, many parameters influence the receiver capability, such as; receiver field-of-view (FOV), angle of incidence and angle of irradiance. In addition to

the distance from the receiver surface to the light source and room futures (reflected surfaces).

In fact based on these distances the propagation delay of the detected received pulse at the optical receiver front-end is limited. The calculations find out the propagation delay time for LOS was 3 ns, while for non-LOS was 5 ns.

Table 7-2 System Parameters for VLC Simulation

System Parameters	
Number of like symbols in PCM	n=10
Number of PCM bits, data rate	N=3, 1 Gbps
Quantum efficiency	η=100%
Electron charge	$q=1.602\text{x}10^{-19}$ coulombs
Planck's constant	$h=6.624\text{x}10^{-34}$ Js
Velocity of light	$3\text{x}10^{8}$ *m/s*
Photon-energy	$h.c/\lambda$
Philips CGY2110CUTransimpedance Preamplifier	
Bandwidth	10 GHz
Equivalent noise spectral density N_0	$50\text{x}10^{-24}$ A^2/Hz
Si Photodiode Thorlabs FDS025	
Wavelength Range (λ)	400 to 1100 nm
Selected Wavelength (λ_p)	650 nm
Responsivity R(λ_p)	0.48 A/W
Dark Current I_D	35pA
Photodiode Load Resistor R_L	50 Ω
Bandwidth	*7.5 GHz*

7.3.1 Simulation Results for 1Gbps DiPPM:

In this section, the simulation has been performed for VLC system using DiPPM modulation technique operating at 1Gbps. Mathcad software was written to simulate the DiPPM system (Appendix-A1).Table.7-3 displays the simulation results for DiPPM without a guard interval and with two guard intervals. When the diffuse link is applied the obtained receiver sensitivities are -21.79 dBm and -27.618 related to the average received power of 6.62 μW and 1.73 μW, respectively.

When non-LOS is applied the predicted sensitivity becomes -6.88 dBm and -12.69 dBm associated with the average received power of 200.53 μW and 53.77 μW, respectively. And this in turn based on the amplitude of the received signal, where Fig.7-3 and Fig.7-4 shows that the amplitude of non-LOS signal is very small compared to that of diffuse signal and arrived later at 5 ns.

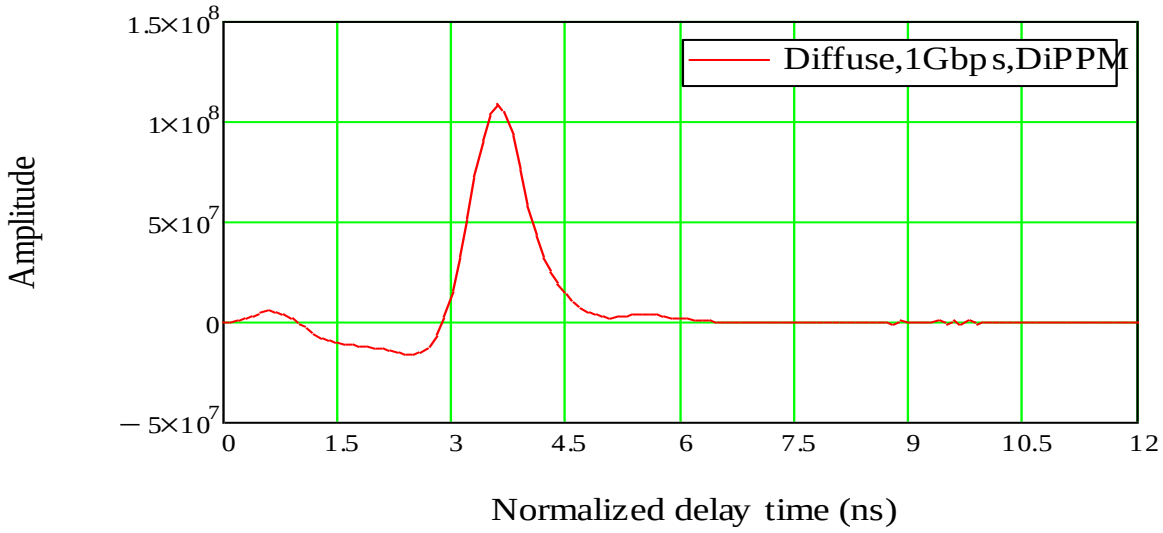

Figure 7-3-Received Pulse for Diffuse Link

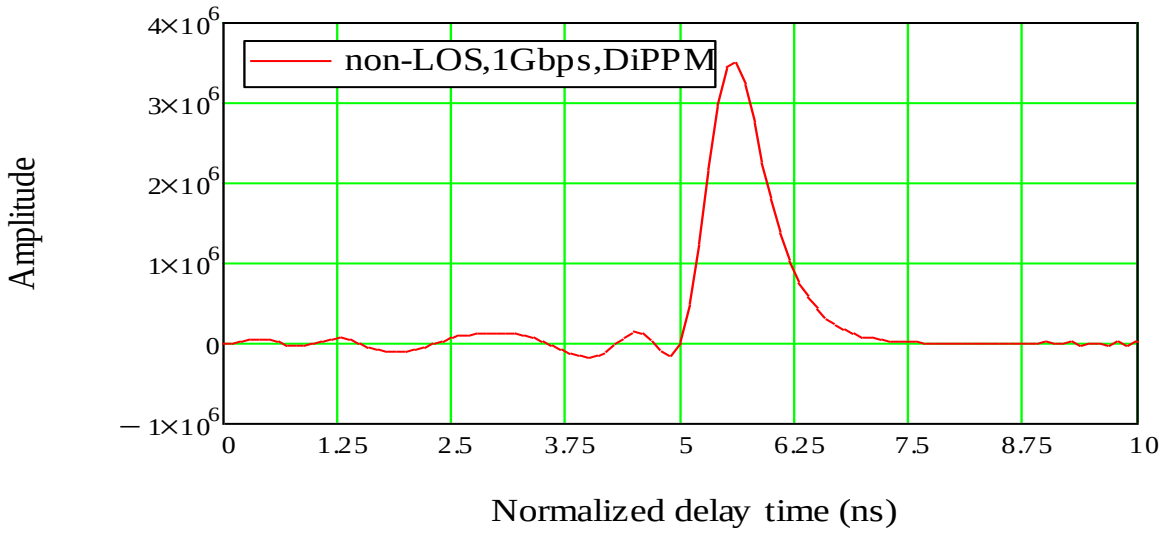

Figure 7-4-Received Pulse for Non-LOS Link

Also, the results clearly show that using interval guards can reduce the effect of ISI and increase the sensitivity of the optical receiver, as shown in Fig.7-5 and Fig.7-6. Hence a better VLC system performance can be achieved.

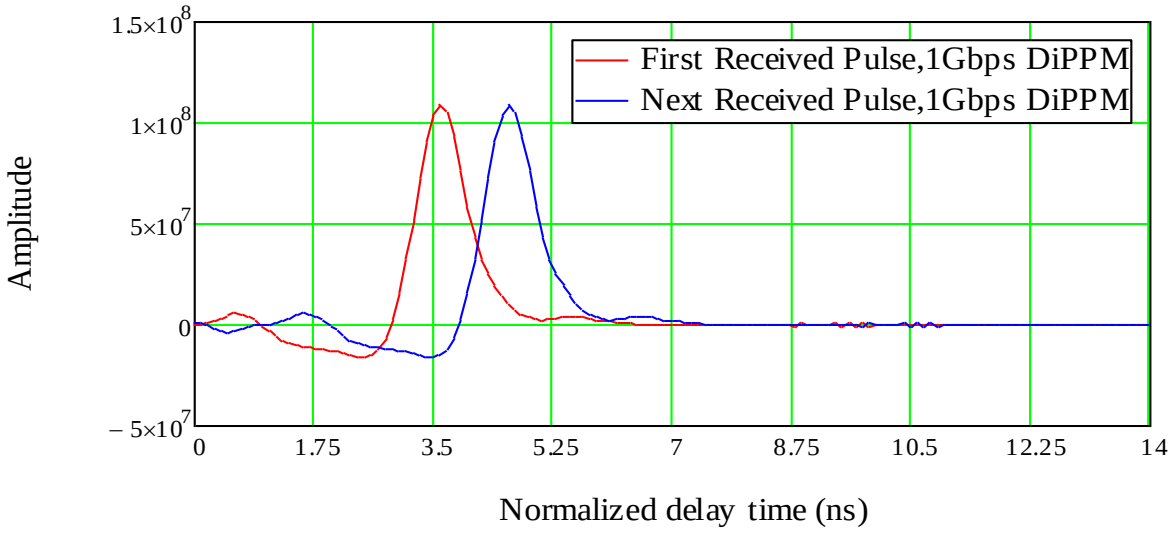

Figure 7-5 Response of DiPPM with zero guards

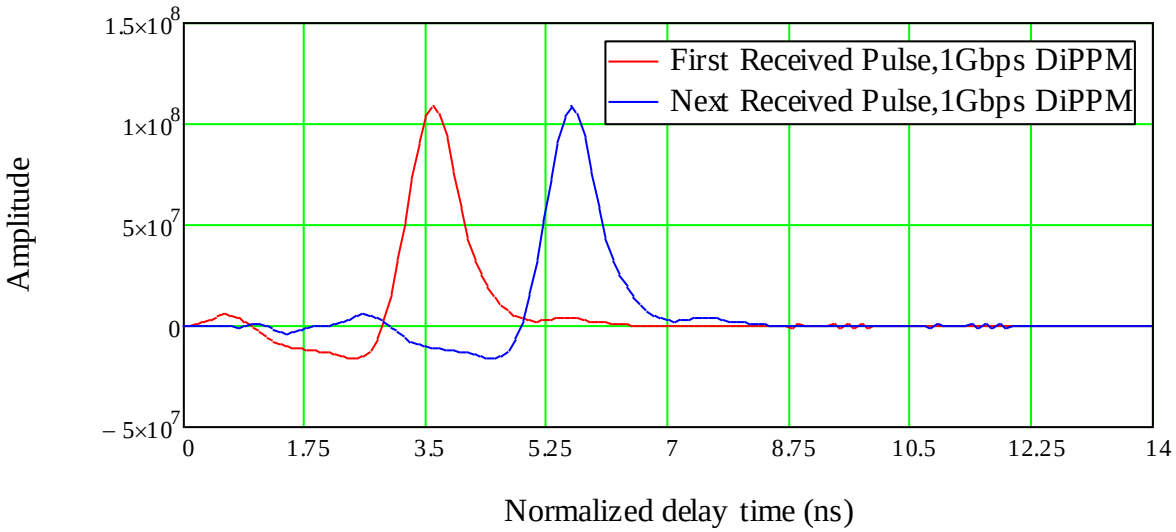

Figure 7-6-Response of DiPPM with two guards

Using the path loss values, the minimum transmitted power required for diffuse signal is 0.85 mW and 0.24 mW for both with zero guard and two guards, respectively. This is comparable to non-LOS, where 888.00 mW and 230.00 mW are required.
Detailed results show a different temporal evaluation of the DiPPM system when LOS link is blocked, however a different sensitivity. This because of the received power when light is reflected for non-LOS model is very weak and leads to a high error probability.
In this case using an LED with enough power can enhance VLC system performance.

Table 7-3-Simulation Results for DiPPM

DiPPM 1 Gbps	Diffuse (LOS & non-LOS)		Non-LOS	
	zero guard	two guards	zero guard	two guards
Number of Photons	$3.15x10^5$	$1.65x10^5$	$9.76x10^6$	$5.11x10^6$
Average received power	6.62 μW	1.73 μW	200.53 μW	53.77 μW
Sensitivity, dBm	-21.79	-27.61	-6.88	-12.69
Path Losses. dB	21.11		36.36	
Average transmitted power required,	0.85 mW	0.24 mW	888 mW	230 mW

7.3.2 Simulation Results for 1Gbps DPPM

In order to get the same BER performance of the two different modulations the same parameters are applied on DiPPM and are used for DPPM. The simulation has been performed for the DPPM system operating at 1 Gbps data rate. By using Mathcad software the simulation has been run (Appendix-A2)
Table 7-4, demonstrates the simulation results for DPPM system without a guard interval and with two guard intervals.
For the diffuse type the receiver sensitivity achieved -16.24 dBm and -19.37 which was calculated according the average received power of 23.79 μW and 11.57 μW, when a number of photons about $2.33x10^5$ and $1.89x10^5$ were received, respectively. Once only

non-LOS is examined the offered sensitivity is reduced and -1.35 dBm and -4.47 dBm related to the average received power of 733.70 μW and 356.90 μW, with a high number of photons of $7.19x10^6$ and $5.83x10^6$, respectively. Fig.7-7 and Fig.7-8 show the difference in amplitude between diffuse signal and non-LOS signal

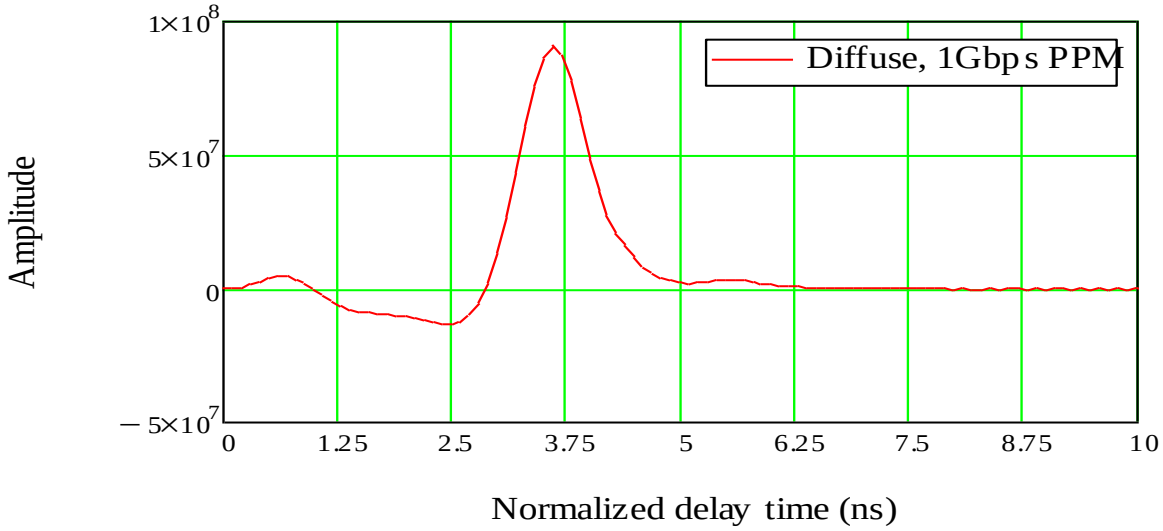

Figure 7-7-Received Pulse of Diffuse Link model (1)

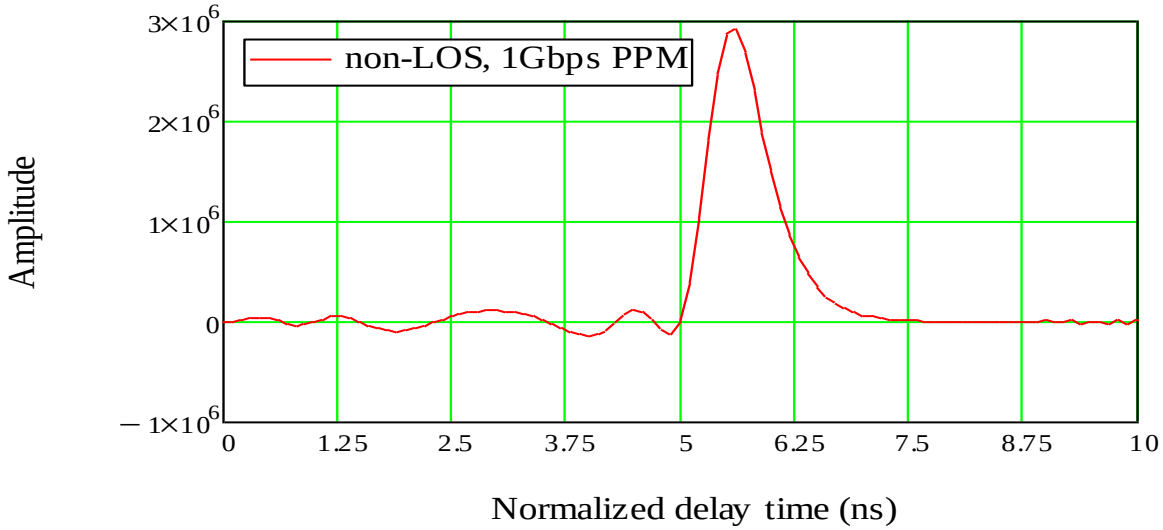

Figure 7-8-Received Pulse of non-LOS Link model (1)

As guard intervals are inserted to the frame of coding pulses the effect of ISI is decrease and improves the receiver sensitivity, a pulse with and without guard intervals are plotted in Fig.7-9 and Fig.7-10.

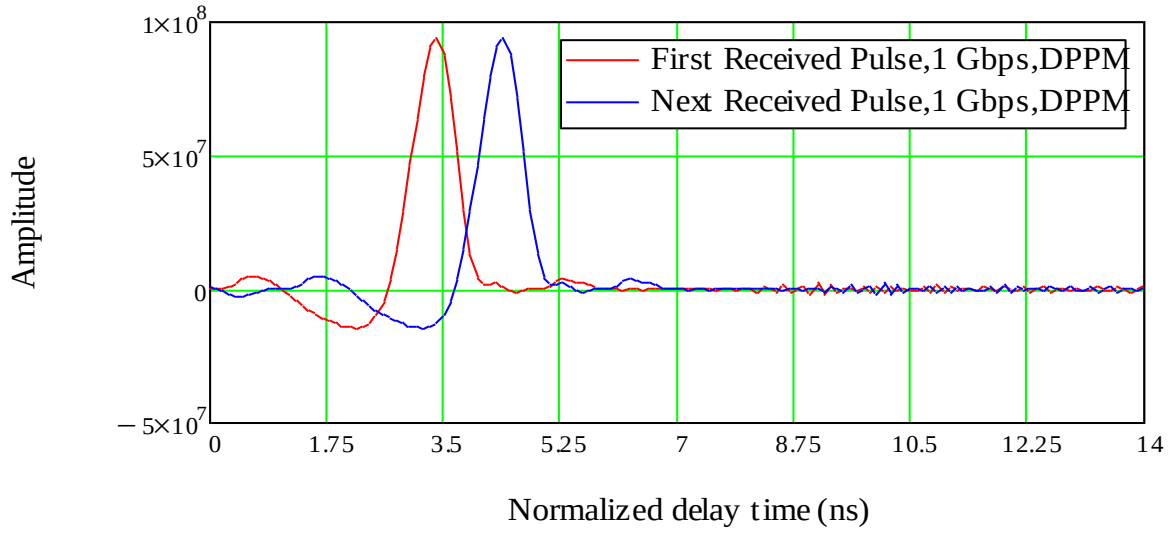

Figure 7-9 Response of DPPM with zero guards

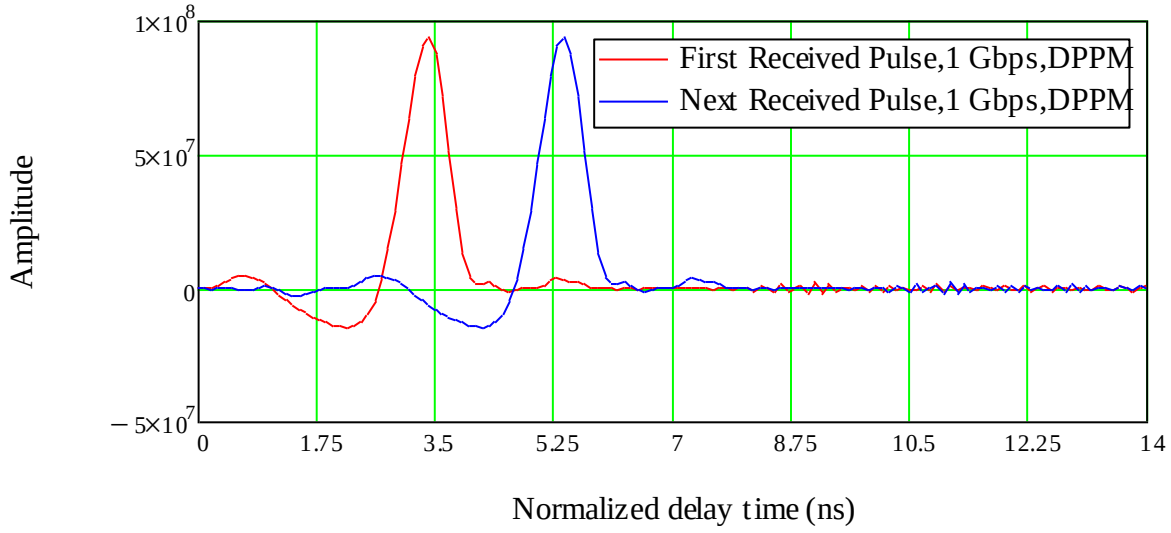

Figure 7-10 Response of DPPM with two guards

Next, according to the path losses calculation, 21.11 dB for diffuse link and 36.36 dB for non-LOS link, the minimum transmitted power required for a diffuse link is about 3.07 mW and 1.49 mW with zero guard interval and two guard intervals, respectively. In case of non-LOS the minimum transmitted power required is 3.17 mW and 1.54 mW.

Table 7-4 Simulation Results for DPPM at 1 Gbps

DPPM 1 Gbps	Diffuse		Non-LOS	
	zero guard	two guards	zero guard	two guards
Number of Photons	$2.33\text{x}10^5$	$1.89\text{x}10^5$	$7.19\text{x}10^6$	$5.83\text{x}10^6$
Average received power	23.79 μW	11.57 μW	733.70 μW	356.90 μW
Sensitivity, dBm	-16.24	-19.37	-1.35	- 4.47
Path Losses. dB	21.11		36.36	
Average transmitted power required,	3.07 mW	1.49 mW	3.17 W	1.54 W

7.4 VLC Simulation Results Using Model (2)

The VLC model adopted here is considered by the channel impulse response of model 2. From equation (78), $H_c(f)$ is given by

$$H_c(\omega) = \eta_{LOS}.\exp(-j2\pi f.\Delta t_{LOS}).+\eta_{diff}.\frac{\exp(-j\omega.\Delta t_{diff})}{(1+\frac{\mathrm{j}\omega}{\omega_0})} \quad (119)$$

Table 7-5 shows the propagation parameters which used to generate the impulse response for indoor VLC link. These parameters adopted here are selected according to experimental and simulation in many studies that proposed for indoor VLC channel the results (John R. Barry, 1993; Jungnickel et al., 2002; Pohl et al., 2000)

Table 7-5 Propagation Parameters for model (1)

parameter	values
Irradiance angles, deg	$\phi_1 = 25$
Incidence angle, deg	$\theta_1 = 20$
Area of room, m	$A_{room} = 25$
Photodiode area, cm	$A_R = 0.018$
Average wall reflectivity	$\rho = 0.8$
LOS distance, cm	$d = 70$
FOV, deg	80
Half semi-angle, deg	$\psi_{1/2} = 50$

The VLC channel response is plotted in Fig.7-11. It shows both the LOS amplitude and the non-LOS amplitude. It is clear the optical power due the multipath reflection is lower than that due to LOS propagation.

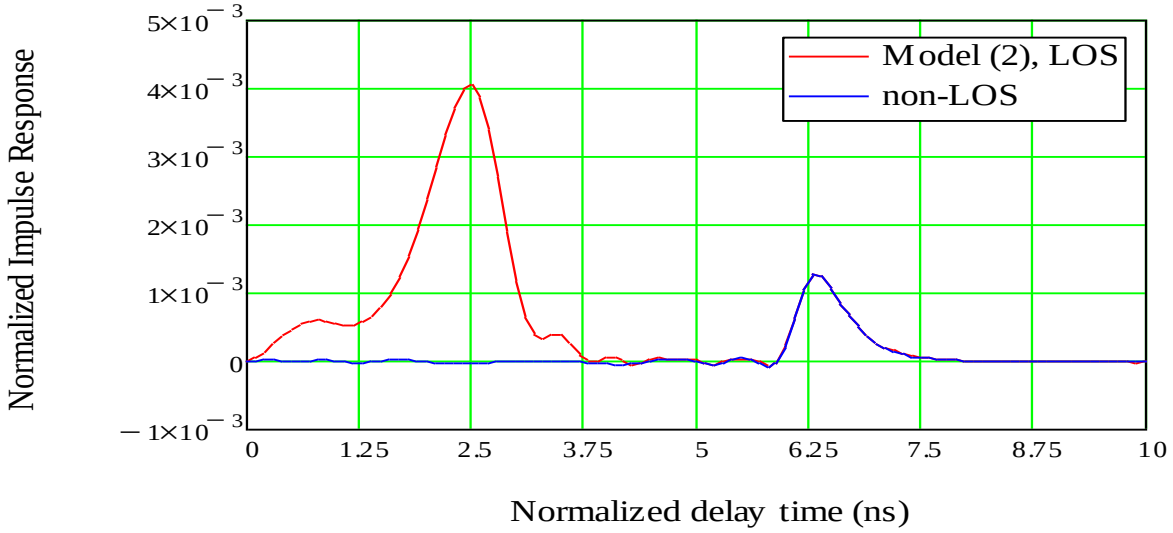

Figure 7-11-VLC channel response

Therefore, using equation (117) the pulse shape at the threshold detector is given by

$$v_0(t) = \frac{b\eta q R_T}{2\pi}\int_{-\infty}^{\infty}\frac{1}{\left(1+\frac{j\omega}{\omega_c}\right)}.\exp(-\alpha^2\omega^2).\left[\eta_{LOS}.\exp(-j2\pi f.\Delta t_{LOS}).+\eta_{diff}.\frac{\exp\left(-j\omega.\Delta t_{diff}\right)}{\left(1+\frac{j\omega}{\omega_0}\right)}\right].e^{j\omega t}d\omega \quad (120)$$

$$v_0(t) = \frac{b\eta q R_T}{2\pi}\int_{-\infty}^{\infty}\frac{1}{\left(1+\frac{j\omega}{\omega_c}\right)}\exp(-\alpha^2\omega^2)\left[\eta_{LOS}\exp(j\omega(t-\Delta t_{LOS}))\right. + \left.\eta_{diff}\frac{\exp\left(j\omega(t-.\Delta t_{diff})\right)}{(1+\frac{j\omega}{\omega_0})}\right]d\omega \quad (121)$$

The simulation established with the parameters of the preamplifier and optical receiver that displayed in Table 7-6. The Thorlabs SM05PD1A photodiode is used for 100 Mbps within a wavelength range of 350 to 1100 nm, however 650 nm is assumed here. A Philips transimpedance preamplifier TZA3043 is selected. with a double-sides equivalent

noise spectral density of $16x10^{-24}$. The Mathcad software has been used for writing the programme codes to implement VLC communication link for both DiPPM and DPPM systems operating at 100 Mbps (Appendix-A3 & A4.). The channel link is completely described by the output shape pulse getting by equation (121).

Table 7-6 System parameters for VLC Simulation

System Parameters	
Number of like symbols in PCM	n=10
Number of PCM bits, data rate	N=3, 100 Mbps
Quantum efficiency	η=100%
Electron charge	$q=1.602x10^{-19}$ coulombs
Planck's constant	$h=6.624x10^{-34}$ Js
Velocity of light	$3x10^{8}$ *m/s*
Photon-energy	$h.c/\lambda$
TZA3043 Preamplifier	
Bandwidth	4 GHz
Equivalent noise spectral density N_0	$16x10^{-24}$ A^2/Hz
Thorlabs SM05PD1A photodiode	
Wavelength Range (λ)	350 to 1100 nm
Selected Wavelength (λ_p)	650 nm
Responsivity R(λ_p)	0.48 A/W
Dark Current I_D	35pA
Photodiode Load Resistor R_L	50 'Ω
Bandwidth	*7.5 GHz*

In this simulation a visible light impulse response includes diffuse and non-LOS propagations model have been investigated. It is different from model (1), the non-LOS propagation adopted here for model (2) is for unlimited number of reflections that the light undergoes, as shown in Fig.7-11 non-LOS pulse has significant amplitude compared to the amplitude of the diffuse signal when compared with Fig.7-2 in model (1).

The same investigation for model (1) is repeated for model (2). The received pulse, the number of photons per pulse, the errors probabilities BER of 10^{-9}, the average received power and hence the received sensitivity have been examined for DiPPM and DPPM VLC systems.

According to the model (2) structure, the VLC channel path losses has been calculated in order to determine the minimum average transmitted power that is required for enhancing the system performance. The results show 24.227 dB when a diffuse link is applied and while for non-LOS link is 32.67 dB.

As mentioned previously, many parameters influencing the receiver capability, such as; receiver field-of-view (FOV), angle of incidence, angle of irradiance and the distance between the receiver front-end and the transmitter and for all other reflectors. The delay propagation time is assumed for this mode unlike model (1) where the delay time for both LOS and non-LOS signals can be calculated according to specific equations. Here is assumed to be for LOS as 2 ns and for non-LOS 6 ns (John R. Barry, 1993; R. KIZILIRMAK, 2013).

7.4.1 Simulation Results for 100 Mbps DiPPM

The simulation for DiPPM VLC system operating at 100 Mbps data rate to achieve BER of 10^{-9} has been run, Fig.7-12 and Fig.7-13 show the received pulse at the output of the matched filter for both links diffuse and non-LOS, individually.

Table 7-7 displays the simulation results for DiPPM when two guard intervals are added and also with zero guard intervals as well. For the diffuse link the predicted sensitivities are -20.30 dBm and -25.00 dBm according to the average received power of 9.34 μW and 3.20 μW, respectively. Whereas, for non-LOS link the sensitivities are -12.10 dBm and -1.92 dBm, corresponding to the average received power of 61.63 μW and 16.14 μW, respectively.

Table 7-7 Simulation Results for DiPPM at 100 Mbps

DiPPM 100Mbps	Diffuse		Non-LOS	
	zero guard	two guards	zero guard	two guards
Number of Photons	4.44×10^6	2.99×10^6	29.29×10^6	15.35×10^6
Average received power	9.34 μW	3.20 μW	61.63 μW	16.14 μW
Sensitivity, dBm	-20.30	-25.00	-12.10	-17.92
Path Losses. dB	28.27		35.54	
Average transmitted power required, mW	6.27	2.12	221.00	58.00

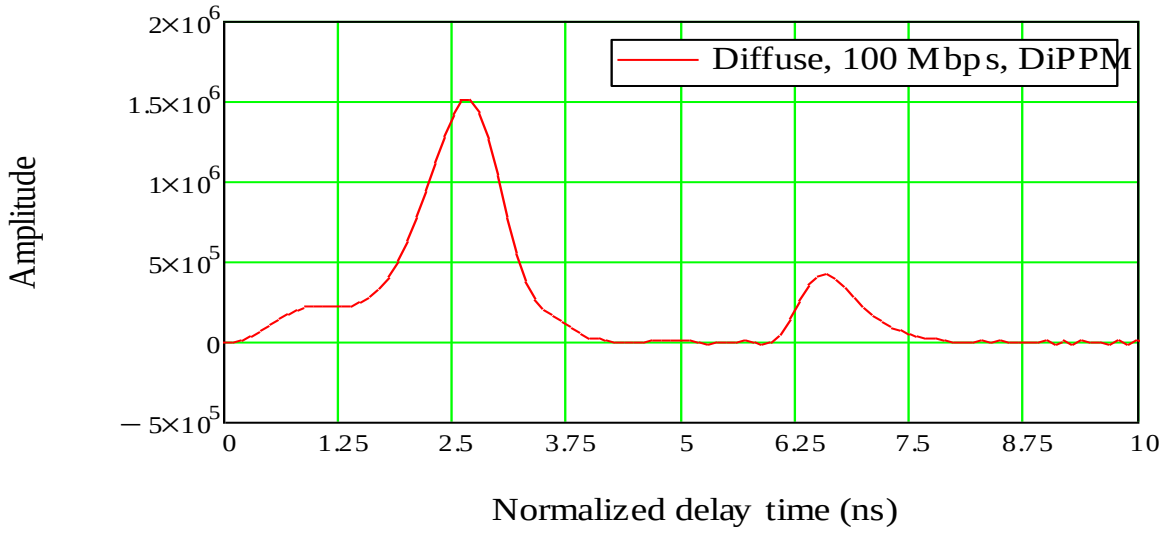

Figure 7-12-Received Pulse of Diffuse Link model (2)

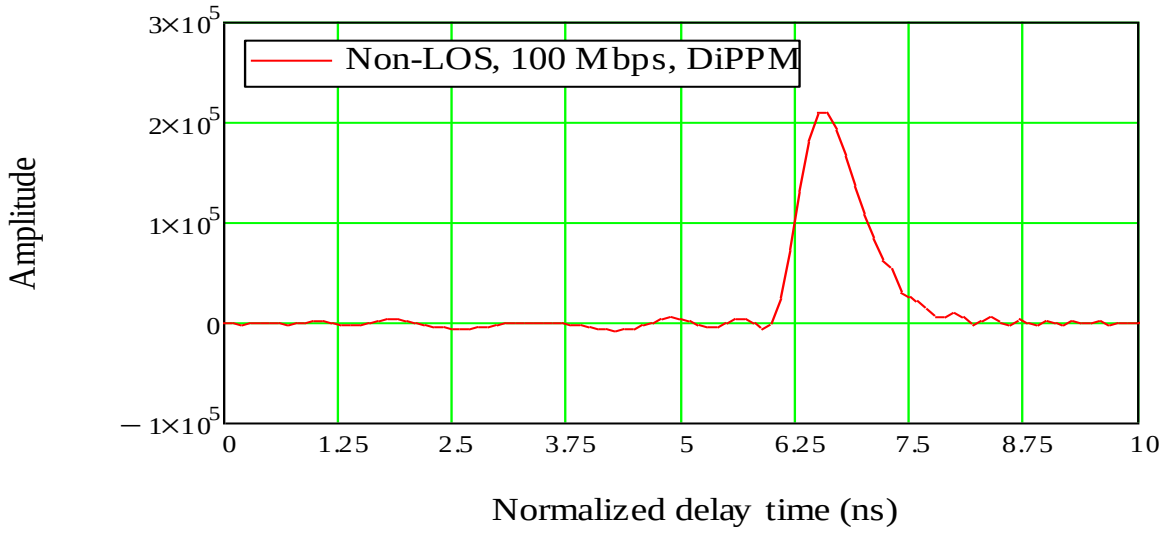

Figure 7-13-Received Pulse of Non-LOS Link model (2)

The effect of ISI is reduced when two interval guards have been added as the receiver sensitivity is improved. And this in turns is shown in Fig.7-14 and Fig.15 where the two adjacent pulses are separated with enough time.

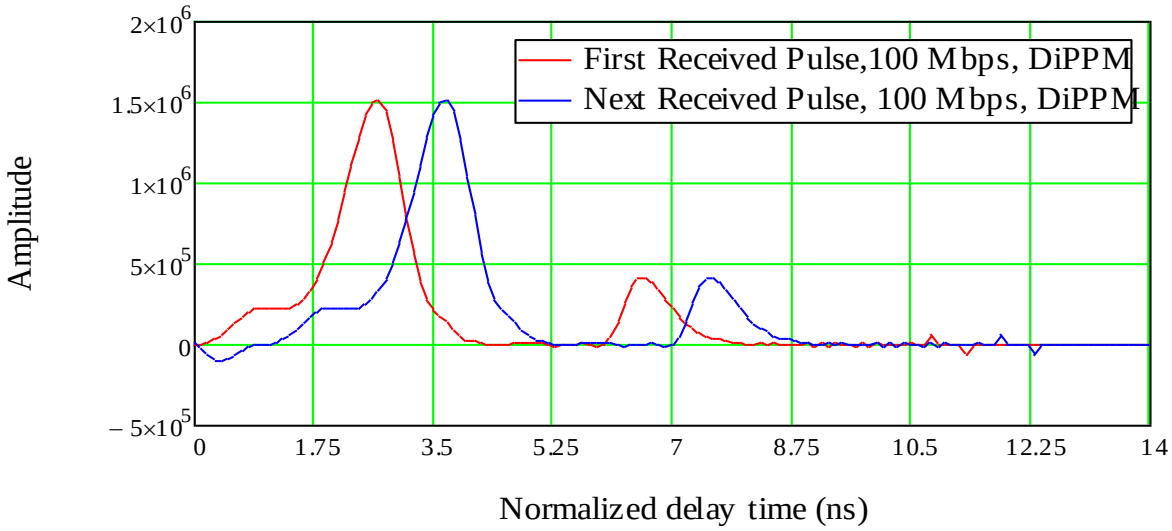

Figure 7-14-Response of DiPPM with zero guard

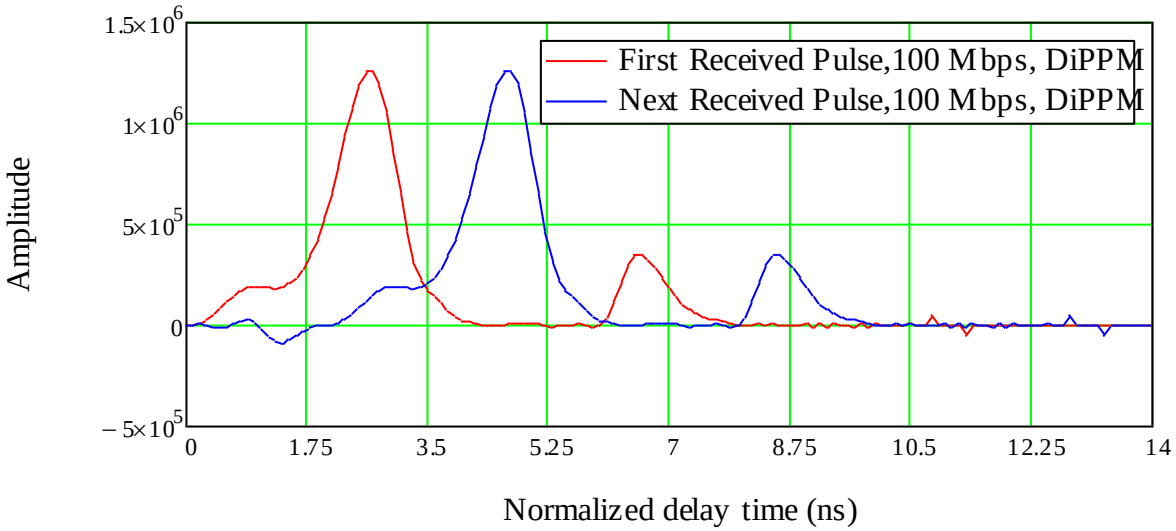

Figure 7-15 Response of DiPPM with zero guards

For power efficiency, the minimum transmitted power required has been obtained. In the case of diffuse link the results show that, for the two situations with zero guard intervals and with two guard intervals, the minimum transmitted power is 6.27 mW and 2.12 mW, respectively. This in comparison to non-LOS, minimum transmitted power is 221.00 mW and 58.00 mW, respectively.

In fact using only a non-LOS propagation link for evaluation of the DiPPM system offers low receiver sensitivity and limits the system performance. This is because the received power when light is reflected from non-LOS model is small. However, model (2) receiving more optical power than model (1) is used only for non-LOS link on the same path loss.

7.4.2 Simulation Results for 100 Mbps DPPM

In this section the simulation for DPPM VLC system operating at 100 Mbps to achieve BER of 10^{-9} has been run, Fig.7-16 and Fig.7-17 show the received pulse at the output of the matched filter for link diffuse and non-LOS links, individually. In Table.7-8 the detailed results show that, with zero guard intervals, the diffuse link offering a sensitivity of -15.17 dBm for average received power of 30.38 μW, while non-LOS link offering sensitivity of -9.61 dBm for average received power of 109.40 μW, respectively.

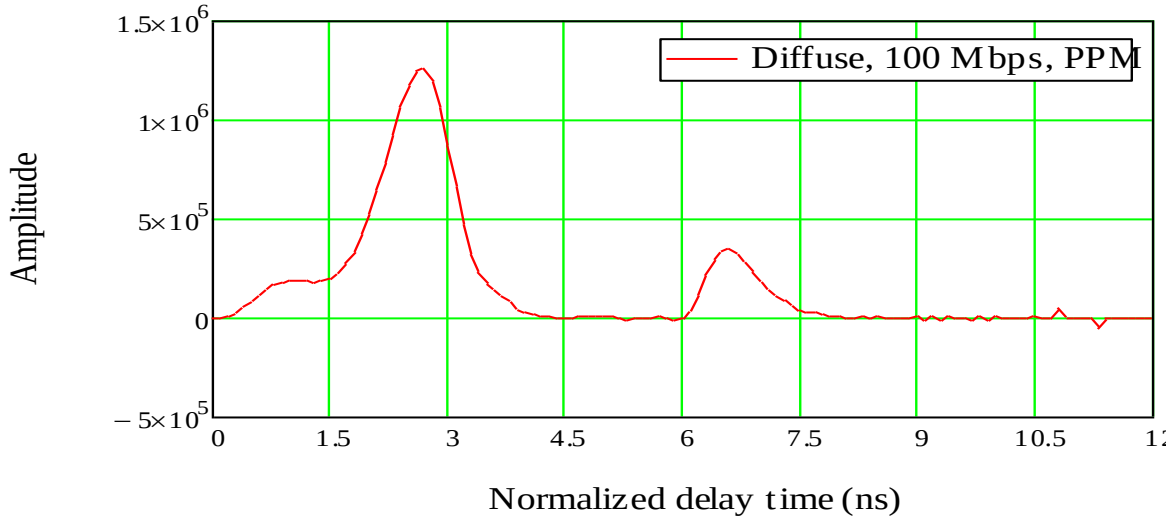

Figure 7-16-Received Pulse of Diffuse Link model (2)

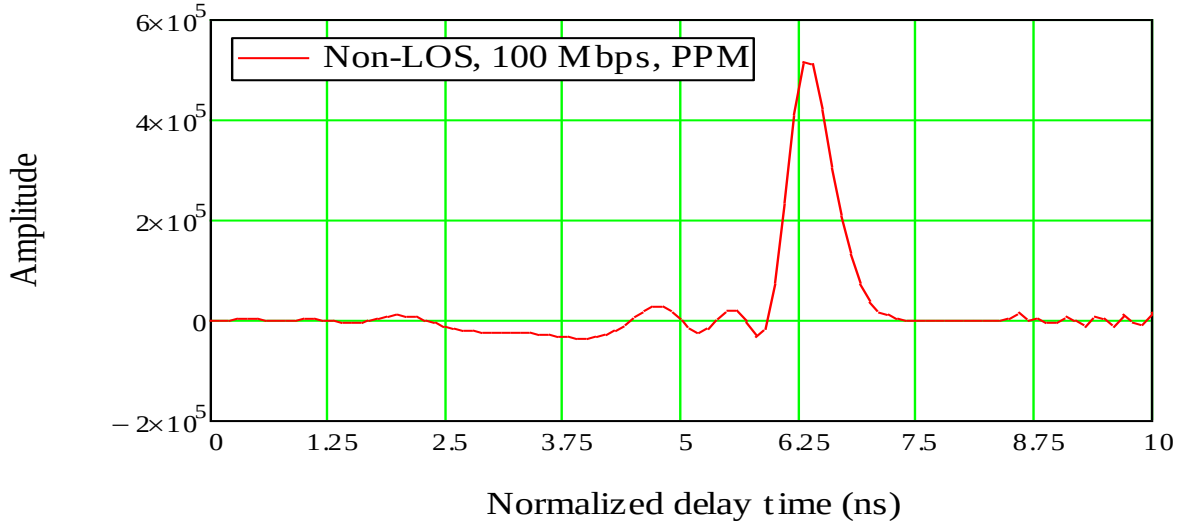

Figure 7-17-Received Pulse of Non-LOS Link model (2)

In order to minimize the ISI degrading two interval guards are adding which in typical improve the receiver sensitivity and system efficiency. Fig.7-18 and Fig.7-19 show the two received adjacent pulses after adding two interval guards, which in turn increases the receiver front-end capability for detecting the received pulse without error. In this case the system can offer better sensitivity, as the results show that the obtained sensitivity is -18.30 dBm for diffuse link and -12.74 dBm for a non-LOS link.

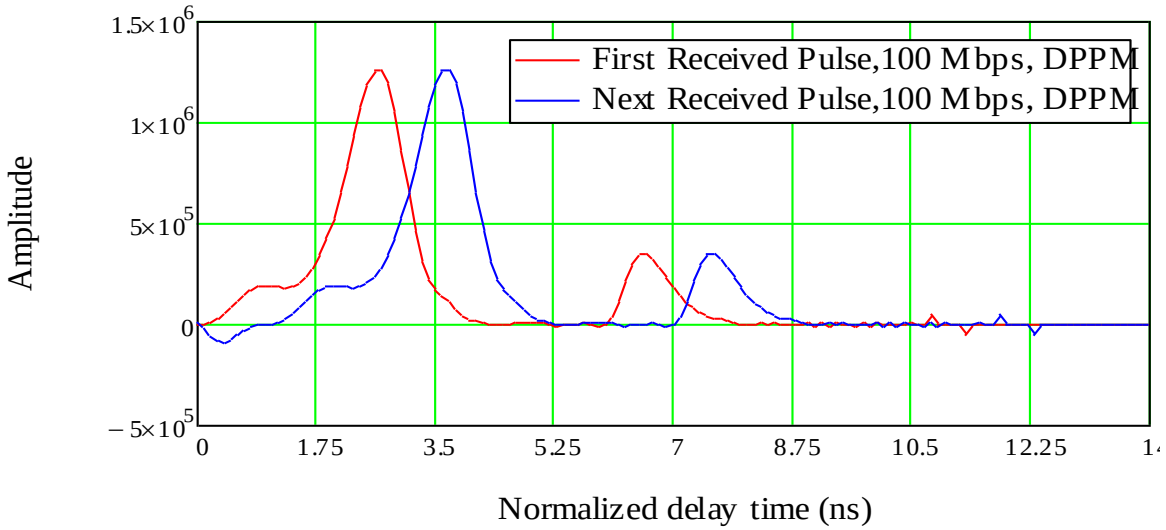

Figure 7-18 Response of DPPM with zero guard

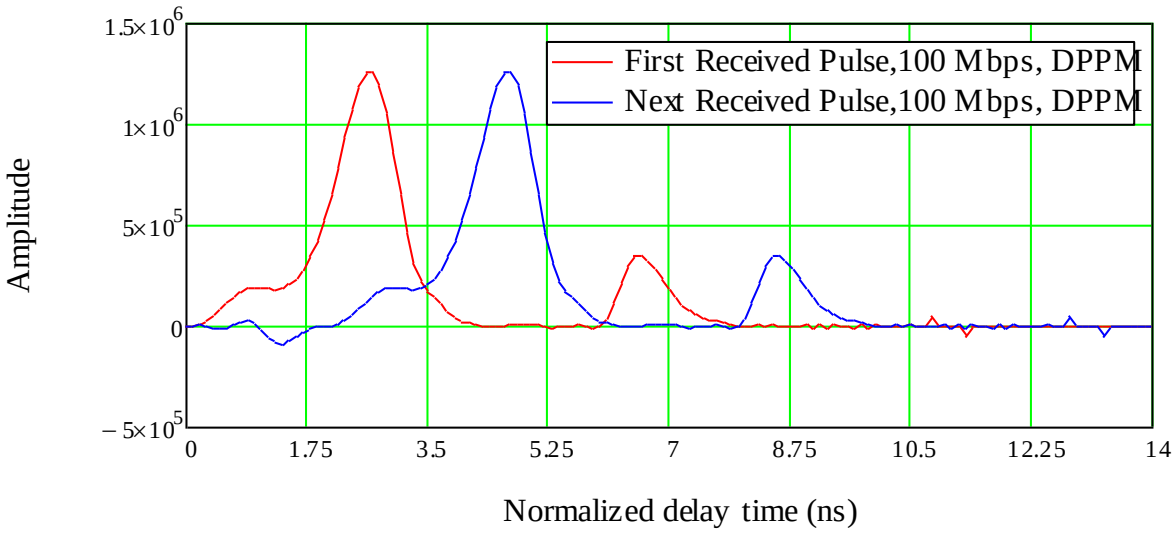

Figure 7-19 Response of DPPM with two guards

Besides that, the minimum transmitted power required is determined for both propagation links, diffuse and non-LOS. When the DPPM with zero guard intervals is used

the minimum transmitted power required is 20.00 mW and 392.00 mW. Whereas, when two guard intervals are added the minimum transmitted power required becomes less and is 9.97 mW and 190.00 mW, respectively. As a result, a better VLC system performance can be obtained

Table 7-8 Simulation Results for DiPPM at 100 Mbps

DPPM 100 Mbps	Diffuse		Non-LOS	
	zero guard	two guards	zero guard	two guards
Number of Photons	$2.98x10^6$	$2.42 x10^6$	$10.72x10^6$	$8.69x10^6$
Average received power	30.38 μW	14.78 μW	109.40 μW	53.32 μW
Sensitivity, dBm	- 15.17	-18.30	-9.61	- 12.74
Path Losses. dB	28.27		35.54	
Average transmitted power required, mW	20 00mW	9.97 mW	392.00mW	190 00mW

The comparison of simulation results for both modulation technique DiPPM and DPPM are displayed in Table 7-9 for diffuse (LOS & non-LOS) and in Table and 7-10 for non-LOS only, both operating at 1 Gbps data rate, while for 100 Mbps are displayed in Table 7-11 for diffuse (LOS & non-LOS) and in Table 7-12 for non-LOS only, both operating at 100 Mbps.

Table 7-9 Comparison between DiPPM and DPPM over diffuse VLC, 1 Gbps

Diffuse (LOS & non-LOS) 1 Gbps	DiPPM		DPPM	
	zero guard	two guards	zero guard	two guards
Number of Photons	$3.15x10^5$	$1.65x10^5$	$2.33x10^5$	$1.89x10^5$
Average received power	6.62 μW	1.73 μW	23.79 μW	11.57 μW
Sensitivity, dBm	-21.79	-27.61	-16.24	-19.37
Path Losses. dB	21.11			
Average transmitted power required,	0.85 mW	0.24 mW	3.07 mW	1.49 mW

Table 7-10 Comparison between DiPPM and DPPM over non-LOS VLC, at 1 Gbps

Non-LOS only 1 Gbps	DiPPM		DPPM	
	zero guard	two guards	zero guard	two guards
Number of Photons	$9.76x10^6$	$5.11x10^6$	$7.19x10^6$	$5.83x10^6$
Average received power	200.53 μW	53.77 μW	733.70 μW	356.90 μW
Sensitivity, dBm	-6.88	-12.69	-1.35	- 4.47
Path Losses. dB	36.36			
Average transmitted power required,	888 mW	230 mW	3.17 W	1.54 W

Table 7-11 Comparison between DiPPM and DPPM over diffuse VLC, at 100 Mbps

Diffuse (LOS & non-LOS) 100 Mbps	DiPPM		DPPM	
	zero guard	two guards	zero guard	two guards
Number of Photons	$4.44x10^6$	$2.99x10^6$	$2.98x10^6$	$2.42\ x10^6$
Average received power	9.34 μW	3.20 μW	30.38 μW	14.78 μW
Sensitivity, dBm	-20.30	-25.00	- 15.17	-18.30
Path Losses. dB	28.27			
Average transmitted power required, mW	6.27	2.12	20 00mW	9.97 mW

Table 7-12 Comparison between DiPPM and DPPM over non-LOS VLC, at 100 Mbps

non-LOS only 100 Mbps	DiPPM		DPPM	
	zero guard	two guards	zero guard	two guards
Number of Photons	$29.29x10^6$	$15.35x10^6$	$10.72x10^6$	$8.69x10^6$
Average received power	61.63 μW	16.14 μW	109.40 μW	53.32 μW
Sensitivity, dBm	-12.10	-17.92	-9.61	- 12.74
Path Losses. dB	35.54			
Average transmitted power required, mW	221.00	58.00	392.00mW	190.00mW

7.5 Conclusion

In order to examine the system performance based on evaluation of the optical receiver sensitivity, 1 Gbps diffuse VLC system using DiPPM and DPPM, at BER of 10^{-9} has been simulated. The comparison shows the average received optical power required for DiPPM is lower than by 17.17 μW and 9.84 μW that required for DPPM for both zero guard and two guard intervals, correspondingly. Thus the optical receiver used with DiPPM offers best sensitivity of -21.79 dBm and -27.61 dBm and this in turn compared with DPPM that offered less sensitivity and are -16.24 dBm and -19.37 dBm when zero guard and two guards intervals are injected, respectively. Also, the results found that the average transmitted power required for the optical for both DiPPM and DPPM modulations is different over the same path losses of 21.11 dB It is calculated as 0.24 mW for two guards and 0.85 mW for zero guard when DiPPM is applied, while for DPPM is 1.49 mW and 3.07 mW over the same path losses, respectively. For non-LOS VLC system the simulation results show that according to the average received power required DiPPM needs less power than DPPM. Where at zero guard the average received power is 200.53 μW for DiPPM and 733.70 μW for DPPM while for two guards is only 53.77 μW for DiPPM and 356.90 μW for DPPM. The related evaluated sensitivity obtained by DiPPM is -6.88 dBm compared to the -1.35 dBm for DPPM both with zero guard. When the two guards is applied the evaluated sensitivity is -12.69 dBm and -4.47 when DiPPM and DPPM are used, respectively. In the two cases an improvement in sensitivity has been represented when DiPPM is utilized over a VLC system. In addition, the results obtained by the simulation determined that for optical source the transmitted power required is different for both modulations DiPPM and DPPM as excepted to be only 230 mW for two guards and 888 mW for zero guard when DiPPM is applied over the calculated path losses of 36.36 dB, while for DPPM is more and to be 1.54 W and 3.17 W over the same path losses, respectively.

At low data rate of 100 Mbps and with at BER of 10^{-9} , a similar results are obtained when DiPPM is applied over VLC system compared to DPPM. The DiPPM system offers a better sensitivity than DPPM system. When a diffuse propagation is considered, the results show that the DiPPM outperforms DPPM at zero guard and two guards for the sensitivity by 5.13 dBm and 6.70 dBm, respectively. Also, the related average received power required for DiPPM is less compared to that required for DPPM and calculated as 9.34 μW for DiPPM and 30.38 μW and this based on the technique of the DiPPM scheme. Whereas for evaluated the system performance according the average transmitted power required for each modulation technique. The DiPPM excepted required power is clearly less than for DPPM, as for DiPPM can be 6.27 mW and for DPPM can be 20.00 mW over the same path losses of 28.27 dB. When the non-LOS propagation is simulated the sensitivity in comparison between the DiPPM and DPPM systems is outperform by 2.49 dBm and 5.18 dBm when zero guard and two guards are used, respectively. It is also shown that the DiPPM is collected small amount of optical power compared to that collected by DPPM, as clarified previously this is due to the unique technique used by DiPPM. The average received powers obtained by DiPPM are 61.63 μW for zero guard and 16.14 μW for two guards, while for DPPM are 109.40 μW for zero guard and 53.32 μW for two guards. Also in terms of transmitted power required, the DiPPM required lower power than DPPM and are predicted of 171 mW is required by DPPM over DiPPM when only zero guard is applied, while for two guards is reduced to 132 mW.

8 EVALUATION OF VLC PERFORMANCE

Typically, high data rates are potentially available using optical radiation. This technology can use with the visible spectrum and so LEDs can be utilized for high data transmission as well as for lighting rooms. Obviously high sensitive receivers are essential for these types of communications.

8.1 Optical receiver:

The basic structure of an optical receiver is shown in Fig.8-1. The PIN photodiode and preamplifier have received a great deal of attention if it is to be used in an optical wireless system as a photodetector for high speed response. The resultant noise in the receiver is noise generated by the preamplifier first stage and noise produced by the photodiode, and the dark current is based on the bandwidth noise factors achieved (Brundage, 2010; M. J. N. Sibley, 1995).

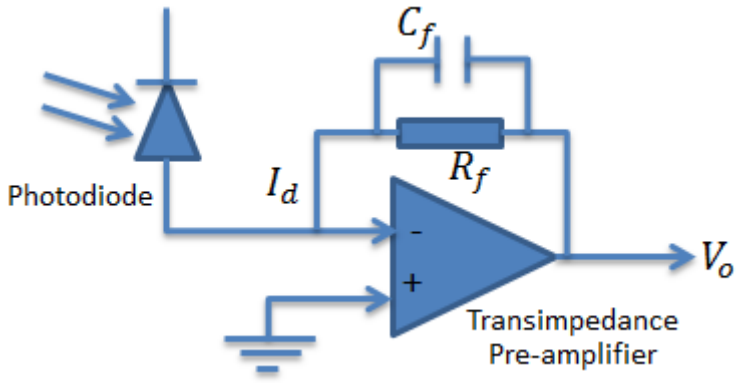

Figure 8-1 Basic structure of optical receiver

8.2 Numerical Evaluation

The evaluation of the VLC system is performed for both DiPPM and digital PPM systems to verify the system performance based on the receiver sensitivity calculation. The flow chart in Fig.8.2 shows the method of how the mean optical received power is determined and then the receiver sensitivity in dBm is obtained. Appendix B1-B8 describe a Mathcad program used for the numerical calculations of VLC receiver sensitivity that utilizes DiPPM and DPPM coding schemes when operated at 1 Gbps and 100 Mbps.

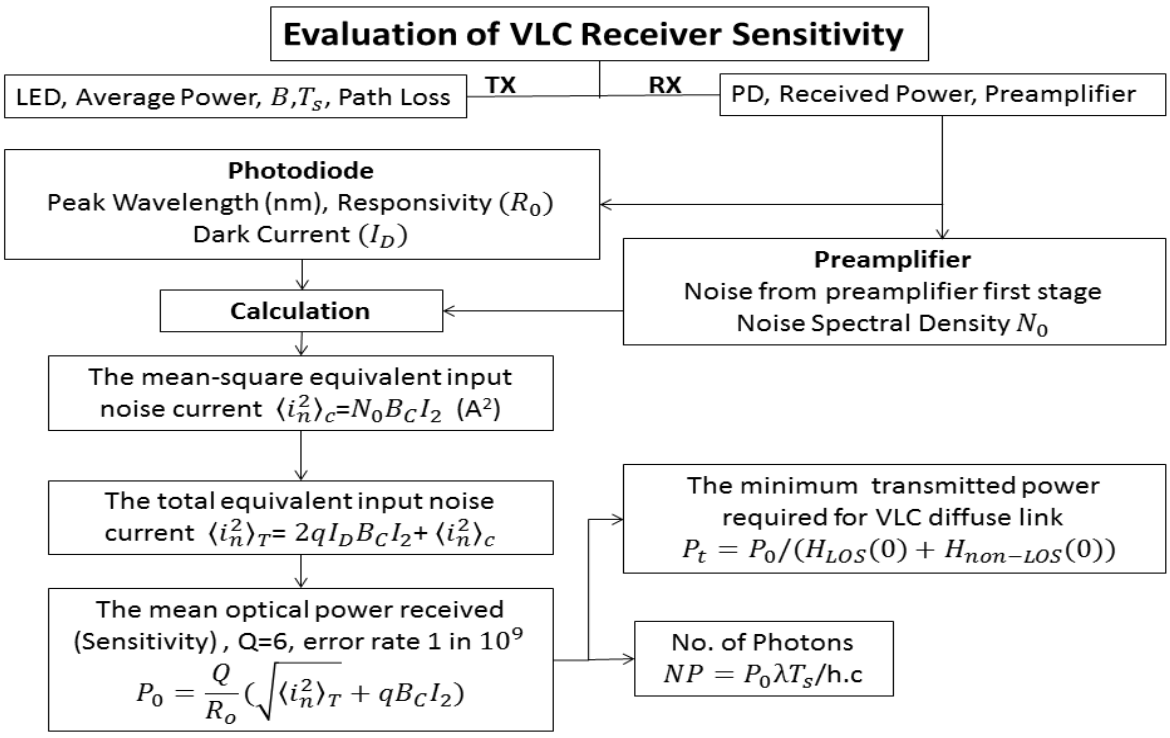

Figure 8-2-Receiver Sensitivity Determination

The calculation is processed according to the structure of the following chart in Fig.8-2, which is described in the following steps:

1- Determine the input noise spectra density at the input of the preamplifier, which is essential to calculate the mean-square equivalent input noise current. Usually, the factory includes the value of the input noise spectral density in a data sheet.

2- Determine the value of the mean-square equivalent input noise current, which depends on the noise current related to the first stage amplifier (noise spectral density) and the system bandwidth. Also it is affected by the bandwidth noise factor (I_2).

3- Calculate the total equivalent input noise current which mainly includes the noise due to the dark current from the photodiode and first stage preamplifier noise.

4- As a result the mean optical power received is then determined at BER of 10^{-9}. The calculation is related to the photodiode responsivity and the system bandwidth.

5- The sensitivity of the receiver is then obtained in dBm.

6- The number of the received photons is then find out according to the selected wavelength, the wavelength used here is 650 nm.

7- In addition, the minimum transmitted power that required for offering the obtained sensitivity at the receiver front-end is calculated according to the path loss of the proposed VLC propagation model.

8.2.1 Total receiver noise:

The photodiode noise falls into two main noise sources dark current noise and signal the preamplifier noise, so the total noise is expressed as:

$$\langle i_n^2 \rangle_T = 2qI_D B_C I_2 + \langle i_n^2 \rangle_c \qquad A^2 \qquad (122)$$

And the mean-square equivalent input noise is

$$\langle i_n^2 \rangle_c = N_o B_C I_2 \qquad A^2 \quad (123)$$

B_C is the bit rate of the modulation coding schemes, which are 2B and $\frac{2^3}{3}B$ for DiPPM and DPPM, respectively, and B is the original PCM bit rate, $K_B = 1.38 * 10^{-23} J/K$ is the Boltzmann's constant, $T = 300$ Kelvin denotes the absolute temperature, R_L is the load resistor usually 50 ohms, I_D denotes the value of photodiode dark current and q denotes the value of the electron charge $1.602 * 10^{-19} C$.

The noise bandwidth factor (I_2) depends on the shape of the input received pulses.

In general, the optical receiver uses a pre-detection filter where the output pulses have a raised-cosine spectrum. When the Gaussian shape pulse is assumed, the normalised FT of the its pulse is given (M. J. N. Sibley, 1995) by

$$H_p'(y) = \frac{1}{T}.\exp -\left((2\pi\beta y)\right)^2/2 \qquad (124)$$

Where β is related to the measure of the pulse width, and is used to calculate I_2.

From table-11 for full-width Gaussian input pulse β =0.1 and the value of I_2 is 0.376, and for high pulse dispersion β =1 and the related value of I_2 is 0.564.

Table 8-1 Gaussian Input Pulses

β	0.1	0.2	0.3	0.4	0.5	…	1
I_2	0.376	0.379	0.384	0.392	0.403	…	0.564

8.3 Sensitivity of the Optical Receiver:

The sensitivity of the optical receiver is the ratio of received optical power to the transmitted optical power. The mean optical power required can be expressed (M. J. N. Sibley, 1995) as

$$P = \frac{Q}{R_o}\left(\sqrt{\langle i_n^2 \rangle_T} + qB_C I_2\right) \quad (125)$$

Where R_o denotes the photodiode Responsivity and Q denotes the signal-to-noise parameter.

The output photo diode current is given by

$$I = \frac{Q}{R_o}\left(\sqrt{\frac{4K_B T}{R_L} B_C I_2}\right) \quad (126)$$

Then the received optical power can be expressed as

$$P_o = \frac{I}{R_o} \quad (127)$$

Thus, the number of the received photons is given by

$$NP = P_o \lambda \frac{T_s}{hc} \quad (128)$$

Where λ denotes the operation wavelength, h denotes Plank's constant ($6.624 * 10^{-34}\, JS$), $c$denotes the light velocity ($3 * 10^8 m/s$) and T_s denotes the slot time for used schemes, in this case and for 3 bits PCM, which are $\frac{T_b}{2}$ and $\frac{3.T_b}{2^3}$ for DiPPM and DPPM, respectively.

8.4 Results and Discussion:

Mathematical evaluation has been examined for indoor VLC system utilizing two modulations techniques, DiPPM and DPPM. Both have been applied over the VLC system operating at 1 Gbps and 100 Mbps, 3 bits of original PCM rate is considered. Q is chosen by relating to a BER of 10^{-9} and has value of 6.

To evaluate the receiver sensitivity, the equivalent input noise current should be known and then the optical received power determined. Table 8, display the values of the noise bandwidth factor (I_2), related to β.that is required for this calculation When ISI is present the value of (I_2) is high (0.564) and while the effect of ISI is ignored the value of (I_2) is small (0.376).

8.4.1 Numerical Evaluation of VLC system at 1 Gbps:

For the VLC system operating at 1 Gbps, the preamplifier Philips CGY2110CU was used with a bandwidth of 10 GHz and a white noise spectral density of $50x10^{-24}$ A^2/Hz at the input. It was matched to a Thorlabs FDS025 photodiode with a resposivity of 0.4 A/W at the selected wavelength of 650 nm. Mathcad software has been written for the calculation processor (Appendix-B1-B4) for both DiPPM and DPPM system.

The detailed results, in Table 8-2, show that the optical receiver obtains the lowest noise of $37.60x10^{-15}$ A^2/Hz when operated with DiPPM compared to the DPPM which is $50.13x10^{-15}$ A^2/Hz. As the effect of ISI is introduced the total input noise becomes $56.40x10^{-15}$ A^2/Hz for DiPPM and $75.20x10^{-15}$ A^2/Hz for DPPM which indicates that even with ISI DiPPM produces low noise. Because the DiPPM technique has a capability to offer fixed and low data rate speeds and therefore a lower and fixed bandwidth can be offered in comparison to the DPPM technique. This is in turn gives an improvement in receiver sensitivity.

Table 8-2 -1Gbps, VLC System Performance without ISI, error rate 1 in 10^9

Without ISI $\beta = 0.1,\ I_2 = 0.376$ **for 1Gbps**	**DiPPM**		**DPPM**	
The total equivalent input noise current	$37.60x10^{-15}$		$50.13x10^{-15}$	
Mean Optical received Power Required, μW	2.91		3.36	
Sensitivity, dBm	-25.36		-24.74	
Number of Received Photons NP	$4.76x10^3$		$4.12x10^3$	
VLC Link Path Loss, dB	Diffuse	Non-LOS	Diffuse	Non-LOS
For Model 1	21.11	36.36	21.11	36.36
Minimum Average Optical Transmitted Power required, mW	0.38	12.59	0.43	14.54

Original results present that the best sensitivity is offered by the optical receiver when DiPPM is applied, as a low optical power is required for the DiPPM than DPPM at the selected BER of 10^{-9}. The results show when ISI is ignored the predicted sensitivity is -25.36 dBm and -24.74 dBm for DiPPM and DPPM, respectively. When, ISI is present the sensitivity is -24.48 dBm for DiPPM and -23.85 dBm for DPPM. These results are then related to the optical received power which as determined for DiPPM is 2.91 μW and 3.57

μW with ISI and without ISI, respectively. Whereas, the optical received power for DPPM with ISI is 3.36 μW and without ISI is 4.12 μW.

Table 8-3-1Gbps, VLC System Performance with ISI, error rate 1 in 10^9

With ISI, $\beta = 1,\ I_2 = 0.564$ for 1Gbps	**DiPPM**		**DPPM**	
The total equivalent input noise current	56.40×10^{-15}		75.20×10^{-15}	
Mean Optical received Power Required, μW	3.57		4.12	
Sensitivity, dBm	-24.48		-23.85	
Number of Received Photons NP	5.83×10^3		5.05×10^3	
	Diffuse	Non-LOS	Diffuse	Non-LOS
VLC Link Path Loss, dB For prototype 1	21.11	36.36	21.11	36.36
Minimum Average Optical Transmitted Power required, mW	0.46	15.41	0.53	17.81

Next, in terms of evaluating power efficiency, the path losses for VLC system have been calculated using the VLC model (1), and the obtained results are 21.11 dBm and 36.36 dBm for using diffuse link and non-LOS link, in that order. From Table 8-2 and Table 8-3, the calculation highlights a difference in the required optical transmitted power when DiPPM system is used compared to when using a DPPM system. Hence, the minimum average transmitted power required, to enhance the indoor VLC system, for DiPPM is 0.38 mW for diffuse link without ISI and 12.59 mW for non-LOS. While for DPPM it is 0.43 mW for diffuse link and 14.54 for non-LOS link, without ISI.

As the effects of ISI are included, the minimum average transmitted power required for DiPPM is obtained for diffuse and non-LOS links as 0.46 mW and 15.41 mW, respectively. Whereas when DPPM is operated with the minimum average transmitted power required for both diffuse and non-LOS links these are 0.53 mW and 17.80 mW, respectively.

This explains that the optical receiver operating with DiPPM has a capability to collect a large number of photons compared to when operating with DPPM. The technique of DiPPM offers a wider time slot than the technique used for DPPM. The received photons number for DiPPM and DPPM in case of ISI is ignored and are 4.760×10^3 and 4.12×10^3,

respectively. Whereas, in the case of ISI being present the received photons numbers are $5.83x10^3$ for DiPPM and $5.05x10^3$ for DPPM.

Also, it is clear that most of the average power supported by direct LOS link because of the multipath reflection enforced the received signal is very weak. However, the DiPPM system gives a higher sensitivity than DPPM, even when only the non-LOS link is applied. In some cases using a concentrator of high gain or wide receiver area can give a better system performance.

8.5 Numerical Evaluation of VLC system at 100 Mbps

In this evaluation the processor for the calculation will follow the same flow chart shown in Fig.8-2. The calculations have been done for VLC systems operation at the original PCM data rate of 100 Mbps and a wavelength of 650 nm. The commercial preamplifier used here is a Philips TZA 3043 with a bandwidth 1.2 GHz and a noise spectral density of 16x10-24 A2/Hz when referred to the input. The Thorlabs SM05PD1A photodiode with resposivity of 0.45 A/W at the selected wavelength was used. The Mathcad software used for this evaluation is written in (Appendix-B5-B8).

From Table 8-4 & 8-5, the detailed results show that DiPPM produces the lowest noise of $1.20x10^{-15}$ A^2 compared to the DPPM of $1.60x10^{-15}$ A^2. As the effect of ISI is introduced the total input noise becomes $1.81x10^{-15}$ A^2 for DiPPM and $2.41x10^{-15}$ A^2. This is in turn gives different receiver sensitivity.

According to the original results, the best sensitivity is offered by the DiPPM system is -33.35 dBm without ISI and -32.47dBm with ISI. Whereas, for DPPM system the sensitivity is lower and -32.72 dBm without ISI and -31.84 dBm with ISI. This sensitivity is related to the obtained optical received power which is required for the DiPPM and DPPM systems at error rate of 1 bit in 10^9. The results show when that ISI ignored the predicted main optical received power is 0.46 μW and 0.53 μW for DiPPM and DPPM respectively. When, ISI is introduced the main optical received power is 0.56 μW for DiPPM and 0.65 μW for DPPM.

In order to evaluate the VLC system in terms of power efficiency, the path losses for diffuse link and non-LOS link for both DiPPM and DPPM systems have been determined using model (2), and the obtained results are 28.27 dB when applied with a diffuse link and 35.54 dB when applied with a non-LOS link. The results show that the required optical transmitted power when DiPPM system is used is lower than that required by using a DPPM system. For DiPPM and without ISI is 0.311mW over diffuse link and 1.66 mW over a non-LOS link, although when ISI it is introduced it is 0.38 mW over a diffuse link and 2.03 over non-LOS link. Also, the required optical transmitted power when DPPM is applied over diffuse and non-LOS links and ISI is ignored, the results are 0.36

mW and 1.91 mW, respectively. If ISI is present the results were 0.44 mW and 2.34 mW for each link, individually.

Table 8-4 100 Mbps-VLC System Performance without ISI, error rate 1 in 10^9

Without ISI, $\beta = 0.1$, $I_2 = 0.376$ For 100 Mbps	DiPPM		DPPM	
The total equivalent input noise current	1.20×10^{-15}		1.60×10^{-15}	
Mean Optical received Power Required μW	0.46		0.53	
Sensitivity, dBm	-33.35		-32.72	
Number of Received Photons NP	7.57×10^3		6.55×10^3	
VLC Link Path Loss, dB for prototype 2	Diffuse	Non-LOS	Diffuse	Non-LOS
	28.27	35.54	28.27	35.54
Minimum Average Optical Transmitted Power required, mW	0.311	1.66	0.36	1.91

Continuation, the number of the received photons has been collected by DiPPM and DPPM. The results are 7.57×10^3 and 9.27×10^3 for DiPPM without ISI and due to ISI effects, respectively. As for DPPM the obtained photons number are 6.55×10^3 and 8.03×10^3 with and without ISI, in that order.

Table 8-5 100 Mbps-VLC System Performance with ISI, error rate 1 in 10^9

With ISI, , $\beta = 1$, $I_2 = 0.564$ 100Mbps	DiPPM		DPPM	
The total equivalent input noise current	1.81×10^{-15}		2.41×10^{-15}	
Mean Optical received Power Required, μW	0.56		0.65	
Sensitivity, dBm	-32.47		-31.84	
Number of Received Photons NP	9.27×10^3		8.03×10^3	
VLC Link Path Loss, dB for Model 2	Diffuse	Non-LOS	Diffuse	Non-LOS
	28.27	35.54	28.27	35.54
Minimum Average Optical Transmitted Power required, mW	0.381	2.03	0.44	2.34

8.6 Conclusion

Based on the calculation, it is clear that for both high (1 Gbps) and low (100 Mbps) the related input noise current generated by DiPPM receiver is less than that generated by DPPM and this leads to give a different sensitivity at the front-end receiver. Without intersymbol interference (ISI) the sensitivity is greater than that evaluated when the ISI is presented in both cases where DiPPM and DPPM are applied over the VLC system. This is in turn gives different receiver sensitivity and is evaluated as -33.35 and -32.72 for DiPPM and DPPM, according to the average received power and at high and low data rate, for selected BER of 10^{-9}, respectively. The obtained results show that DiPPM collected more optical power than DiPPM and hens the transmitted power required is less than that for DPPM by 1.35 mW when diffuse link is used while 1.55 mW when only non-LOS is used.

As the intersymbol interference is presented the generated noise becomes high. Thus the obtained sensitivity by DiPPM in comparison to DPPM systems is outperforming by 0.62 dBm for both high and low data tare. It is also shown that the transmitted optical power required by DiPPM is lower compared to that collected by DPPM, when the diffuse path is introduced the difference of the required transmitted power becomes high to that when only non-LOS is introduced, as clarified previously this is due to the unique technique used by DiPPM.

9 DESIGN CONSTRUCTION OF INDOOR VLC SYSTEM

The next stage of this project was the design and construction where the VLC system will needed to be integrated into a lab area. The system to be worked and with correct alignment between the receiver and the transmitter should be available, when the communication link is started and the data are sent. The receiver must be selected to fully respond to the transmitter data rate, the transmitter needs to operate at high speed and within a distance as far as possible from the receiver. Then, the construction of all the test equipment and the software implementation and the downloading on to the interface board (FPGA) have to be tested for both DPMM and DiPPM before the measurements can start. The experimental tests are performed in order using the following approach:

- Examine the DiPPM coding scheme in real time transmission mode, over a visible light link that has not yet been experimentally evaluated.
- Verify the stability of the communication link in order to receive the DiPPM transmitted signal and compare with the original PCM bits.
- Measure the photodiode current in order to calculate the received power and hence evaluate the system performance including the receiver sensitivity for a certain bit error rate (BER) in comparison with another coding scheme (DPPM).

9.1 System Architecture

The block diagram of the proposed VLC system is illustrated in Fig.9-1. The system is made of necessary the components to set up with the communication link for data transmission and data receiving. The computer, using Quartus-II software, sends a sequence of information bits through the interface unit to the LED transmitter. The LED emits an optical power related to the modulated signal. The transmitted power carrying information bits then passes through wireless optical channel. The receiver collects the incident power, converts it to original electrical signal and returns it to the receiving point.

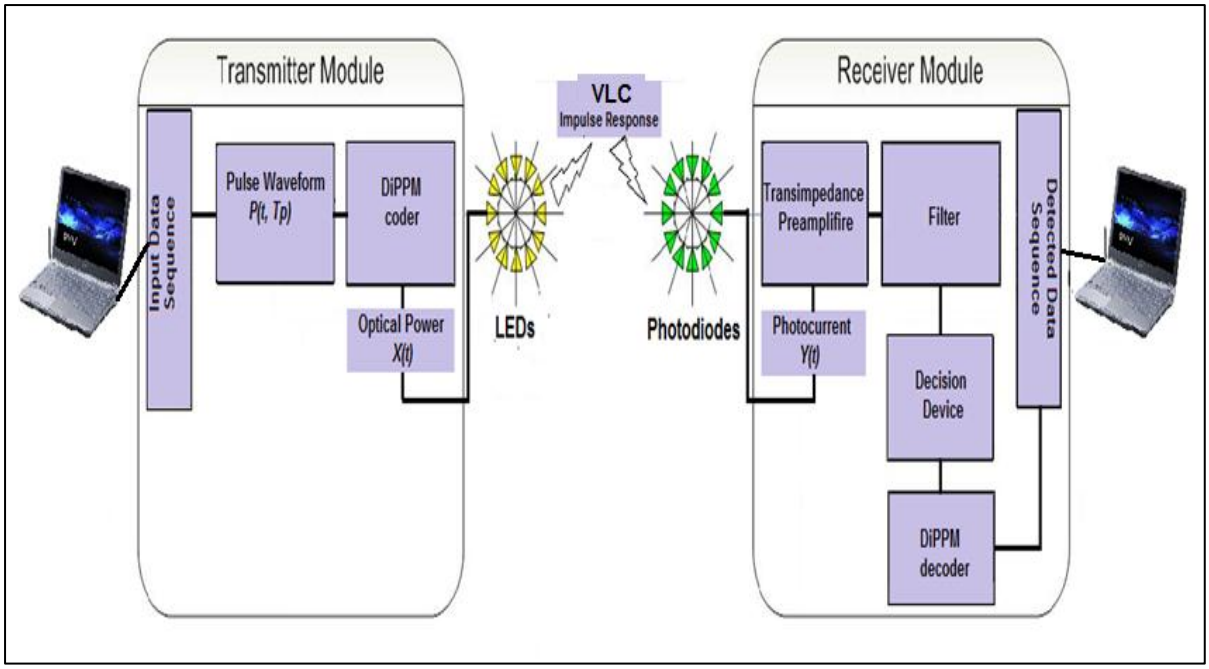

Figure 9-1 Block diagram of the proposed VLC system

The following tools and hardware equipment were used for the system design:

VHDL Language

One programming language that can be used for logic circuits is the Very High Speed Integrated Circuit (VHSIC) Hardware Description Language (VHDL). The VHDL is made for digital systems designing that uses a physical hardware implementation, thus it is not for general purpose use compared to other language like Java and C. It is fabricated under IEEE standards and has the ability to support design hierarchy in different methodologies (Benjadid, 2012)

In general, designing a full electronic system becomes more complex due to the increase of the gate counts and hardware implementation. However, VHDL offers a top-down methodology for a simulation model that helps the designer to start utilizing a specific code that is written by VHDL for a certain system, and enables carrying out real time tests before the building up of a hardware design. In addition, provided simulations performance helps to identify any errors and give a chance to the designer to correct the errors in advance, and it is in turn useful less design time is available (Hunter & Johnson, 1995).

Field Programmable Gate Arrays (FPGA)

It is a highly sophisticated hardware electronic board that is used in design fields for digital electronic circuits. Utilizing FPGA can offer low levels of external noise systems and small delays within the operation taken in the transmission part. Typically, FPGA is used to improve performance of system design even with multiplication. Practically, FPGA has a capability to be controlled by various software such as; Quartus, Xilinx.
Cyclone IV GX FPGA is one of different models of FPGA development boards used for the hardware platform. The facilities of this type are; high speed, high efficiency, low power consumption and large memory interface. In addition Cyclone IV GX FPGA can be used as an interface unit for a transmission system, where the bins are allocated and the full design is downloaded. The general purpose microcontroller included in FPGA allows the design models to be partitioned for different tasks and so the simulators in such cases can be verify the used results in advance (ALTERA, 2013).

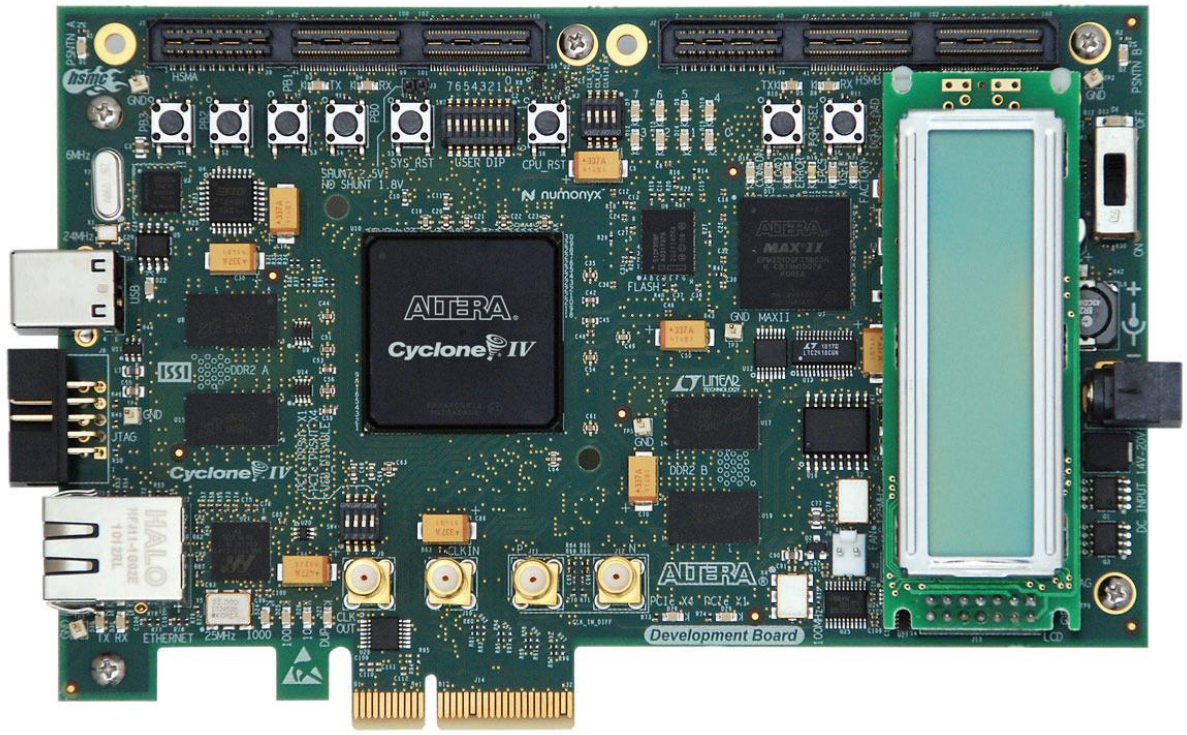

Figure 9-2 Cyclone IV GX FPGA

PRBS Signal Generator

Every communication system transmits data bits, where binary data is needed. What is important is how the data bits are generated. In some design implementation of PRBS

block it can generate sequences of binary data for zeroes and ones. For example a VHDL has a capability for providing PRBS sequences on software function instead of using a signal generator device. Alternatively, since the communication system is designed for performance over a certain BER, and then a signal generator with error detection facilities is required. The capability of BER measurement and analysis at the selected data rate are available. Detecting errors for any communication link is very important because no practical coding schemes can correct all the errors for transmitted pulses (Benjadid, 2012).

9.2 Optical Transmitter

In addition to data generation, a VLC system requires a transmitting part that can project the data over the wireless optical channel. It consists of an LED which is a photon source and the main part of the transmitting block. There are different types of LEDs which are classified according to the wavelength and response time. LEDs response times are normally higher than or equivalent to the transmission data rates. Typically, using LEDs for transmission need a driver current circuit. The LED driver is an electrical circuit that used to regulate and provide a constant power to the LED where it can emit with enough light intensity. LED driver circuit can offer a dimming control while the LED is used for illumination and data transmission and therefore a better LED performance can be achieved (Komine & Nakagawa, 2004) .

In practical terms, the VLC transmitter has a critical part to play which provides a combination of the AC current (data signal) and the DC bias current. Moreover, the LED is a source of photons and must be worked under the correct voltage and current in order to emit the required optical intensity for link setup. Typically, a bias Tee device is used where the adjustment of LED bias current is isolated and independent of the AC current signal (Lo, 2004). Alternatively, in our design a high speed driver circuit is built up. It offers an adjustable current combined with the data signal current. The DC bias current is controlled and stabilized according to the LED forward current.

9.3 Optical Receiver

In any optical system the optical receiver is the most important element which must sense the optical power and convert it to an electrical current proportional to the variation of the optical power. Generally, the intensity of the light near the receiver is often very low due to link loss and signal multipath distortions, so the choice of the photodetector must meet the requirements of the communication system such as: high sensitivity at the required wavelength, high efficiency for converting optical power

(photons) to electrical power (electrons), fast response time at the required data rate, low noise (minimum error), high reliability and low cost and in general high quality have performance (M. J. N. Sibley, 1995).

Generally, an optical receiver is the end destination of data information which has been transmitted over an optical link channel. The optical receiver consists of a photodetector, preamplifier, and current to voltage circuitry. However, the optical receiver converts the received optical energy into an electrical signal with sufficient amplification to allow the signal to be processed by other electronics components (Brundage, 2010)

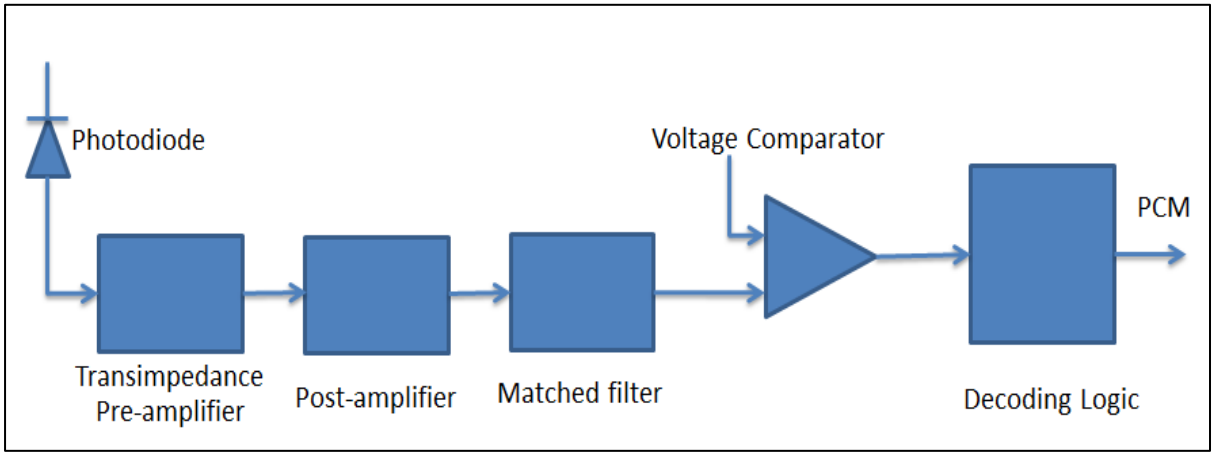

Figure 9-3-Optical receiver

Typically, a transimpedance is the first block immediately following the photodiode to which converts and amplifies the PD current into voltage. By the way, the received signal after it is converted to current a signal become extremely small. Moreover, the voltage is amplified by the pre-amplifier and the DC component is eliminated (M. J. N. Sibley, 1995). Finally, the signal passing through the threshold crossing detector (voltage comparator) is then processed for decoding, as shown in Fig.9-4.

9.3.1 Transimpedance Pre-Amplifier

The basic idea of converting the photodiode current is described by the current to voltage circuit in Fig.9-4. The voltage across the resistor is produced while the current flows through the resistor. The output voltage is limited by the load resistance, since a very high resistance is possible in available design but the flow of the current would be reduced and the corresponding output voltage, so a lower gain would be achieved. In addition a problem is experienced when the photodiode reaches the saturation state, as this appears when the output load voltage is equivalent to the photodiode reverse biased voltage. Though, at high data rate the response time is a key factor, and with high load

resistors time response becomes slow due to the photodiode parasitic capacitance. Therefore, the trade-off cannot be ignored between the gain and response time, where the time constant is equal the photodiode capacitance times the value of the resistor R.

$$t = RC \tag{129}$$

Typically, a development circuit called a transimpedance amplifier become available; it consists of a resistor in parallel with a capacitor which is connected across an op-amplifier. From the schematic circuit in Fig.9-5, in this case the parasitic capacitance can be removed by connecting negative pin to the photodiode, as result a large gain at high response time can be achieved. The R value used to determine the total gain of the transimpedance amplifier and the output voltage is expressed as (Brundage, 2010; M. J. N. Sibley, 1995).

$$V_o = I_d R \tag{130}$$

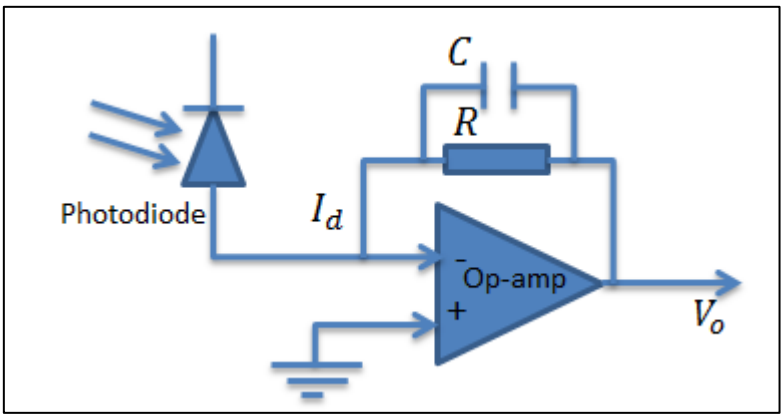

Figure 9-4-transimpedance amplifier

9.3.2 Voltage Comparator

In most communication system at the receiver output the comparator is used to guarantee that the receiver outputs are zero and high volts where two signals are taken in by the comparator and compares them and then decide which signal is larger. The received data pulse after amplification processing is applied into the input of the comparator. Inside the comparator the received data signal is converted into voltage levels and which usually TTL signal. Typically, the TTL signal is required from the comparator output in order to satisfy the logic circuit requirements that 0 and +5 volts. The TTL signal depends on the amplitude of the input signal related to the reference signal at the comparator. If the input signal is lower than the reference voltage is then the TTL output detected as low and vice versa. This is described in Fig.9-6 where an arrived signal is the top-trace and the TTL output is the lower trace and the mid line

denotes the level of the reference voltage at the comparator (Brundage, 2010; M. J. N. Sibley, 1995).

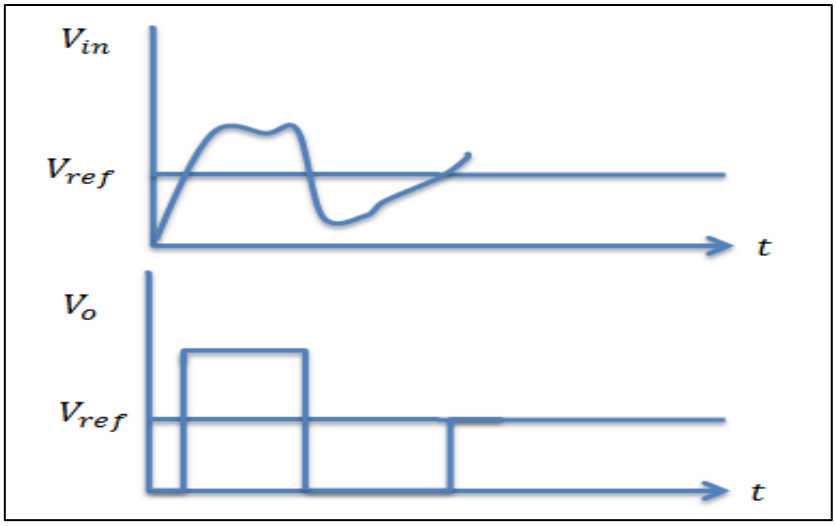

Figure 9-5-Comparator Input/Output

9.4 Fabrication of the Experimental Devices

The experiments were carried out for the indoor VLC link in wide room with dimensions of (11.0x8.9x3.0m) in order to work on everyday life environment, where interference from the background light and a multipath distortion are included. The room is a lab area where instruments and devices are everywhere and fluorescent lambs are hung on the ceiling.

Fig.9-7 shows the photograph of the full system the tools and devices as were they assembled. The FPGA (Cyclone IV GX) development board connected to the PC through a USP cable which used for downloading, the output/input pins are used for sending and receiving the data stream. For flexibly transmission the LED is mounted on a metal holder and linked to the driver circuit board while the LED emits bits of information. Whereas, the photodiode is placed faced towards the LED and is at a proper distance, as shown. In the top of the photodiode at the right distance the optical concentrator is held to enable a good reception, since the photodiode effective is very small under a wide spectrum of visible light. The tool set-up is placed as seen in Fig.9-7 where the oscilloscope, pattern test set (pattern generator/error detector), pico-ammeter and the power suppliers were placed on the work bench. All the components were located near each other and a short connection cables were used in order to reduce the stray capacitance due to electronic boards.

In the performing measurement the transmitter is pointed straight downward and the receiver is pointed straight upward where the incident angle is to a minimum value. The TX (LED) is located at 30 cm over the desk while the RX (PD) is located on the desk.

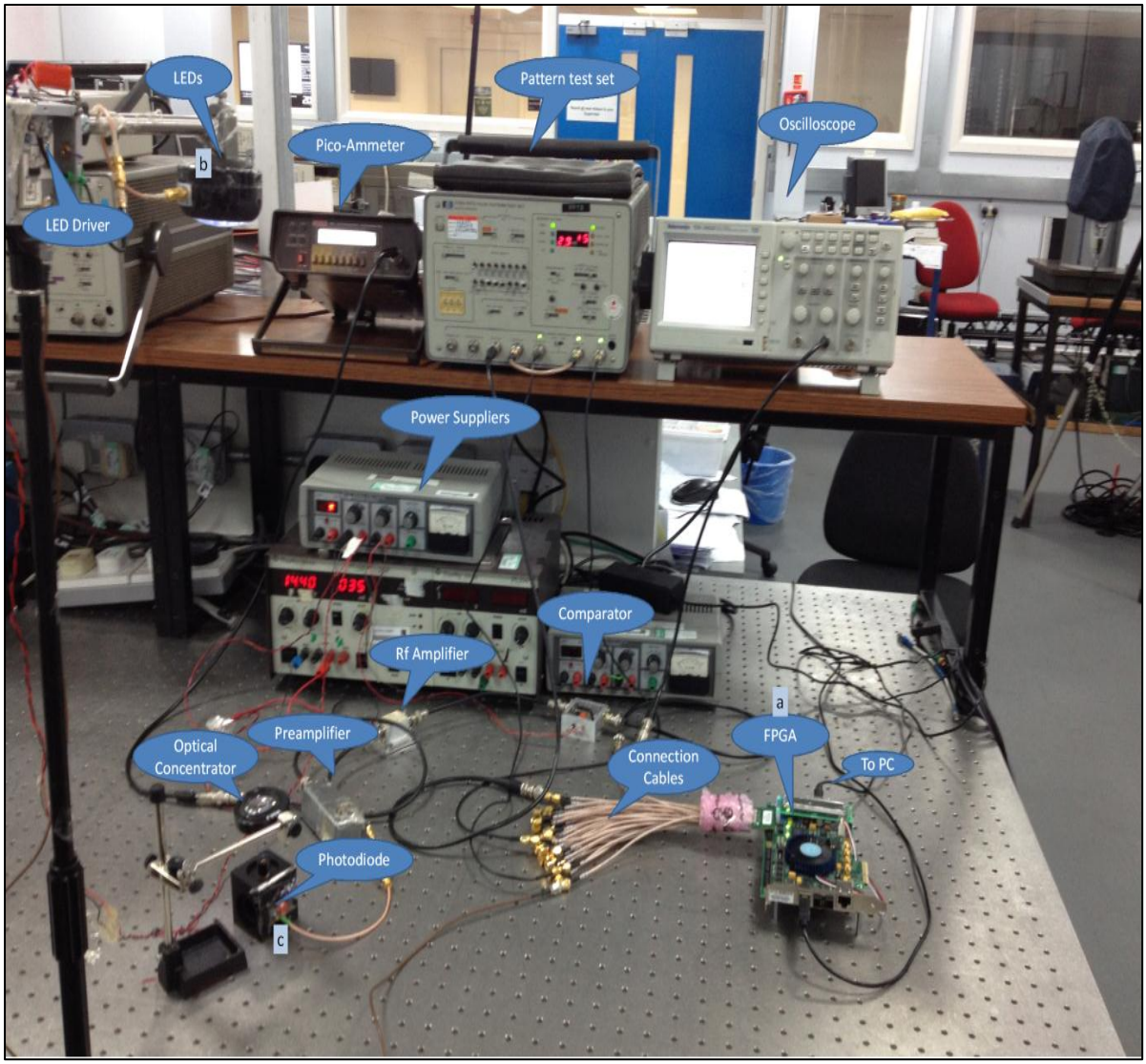

Figure 9-6-Indoor VLC System

9.4.1 Fabrication of the Optical Transmitter

The first step for the transmitter design is to decide if the selected emitter can meet the requirements and overcome the constraints of a working VLC system. In order to simplify the system design and for low cost a very popular commercial white LED has been used. Furthermore, there are many reasons for chosen LEDs as the light source instead of using light bulbs and fluorescent lamps. The first reason is that LED has advantages of low power consumption. The second reason is that LED has a long lifetime

while in operation. More important, LED can offer high speed switching under enough brightness. The selected LED is a LIVARNO Z31792 with white phosphorous light. It is filled with 24 white diodes, and each has 0.06W output power (LED: 24x0.06=1.44 W) and have identical specifications. The benefit of utilizing many LEDs instead of using one LED is to overcome the optical power losses and maximize light illumination coverage area. Since the objectives are to be able to illuminate the desk surface and transmit data at the same time. The LEDs are driven by 50mA and provide a full beam angle of 160^0

9.4.1.1 LED Drive Circuit

In reality, designing a LED driver proved to be more difficult than that was theoretically planned. A high speed NAND gates (SN74ACTQ00) LED driver is used in our design, the parameters of the circuit is located in operation manual. Theoretically, the circuit can drive LEDs up to 100 Mbps depends on the capability of the LED. The selected commercial white LED is operated with a constant current source up to 1 Mbps, since development driver circuit connected to the LED has been driven up to 16 Mbps.

According to the schematic diagram of LED drive circuit in Fig.9-8, the final design and the implantation is based on the empirical values of some components. These values have been calculated according to our current model application, where high enough current level is applied to the LED in order to achieve high data rate with sufficient illuminance. In the same time the a higher LED current should be limited by choosing the final resistor values greater than that calculated and the final value of the capacitor (C4) less than. As seen in the schematic diagram using a combination of RC is used to reduce the LED switching time and hence the rise time which increase the data rates (semiconductor, 2008).

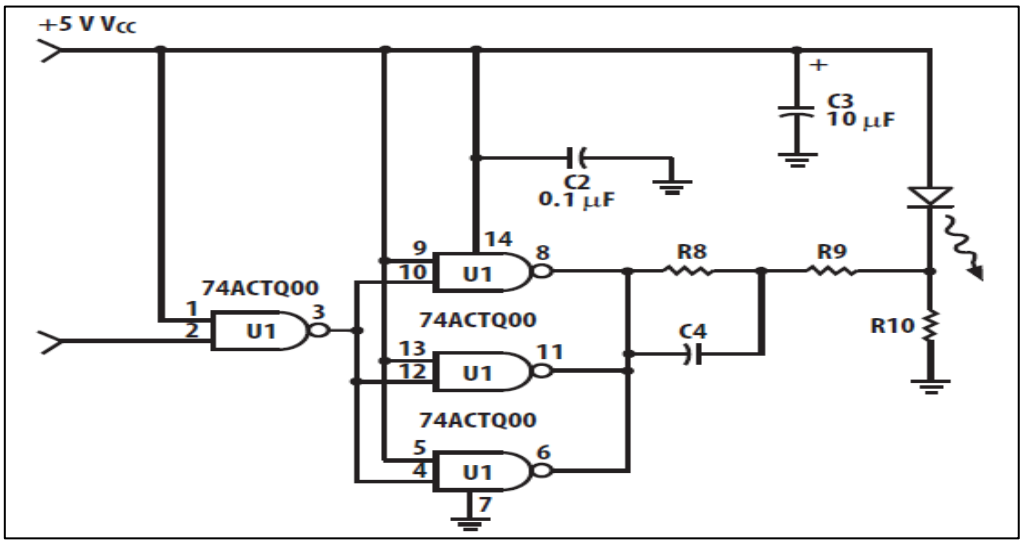

Figure 9-7-LED Driver Schematic Diagram

9.5 Fabrication of the Optical Receiver

The Thorlabs Si SM05PD1A photodiode is used in our model with a responsivity of 0.45 A/W at 650 nm wavelength. It has been selected to achieve full response to the transmitted data rate that used for the practical test. The photodiode appears wired up with the rest of the components. The transimpedance preamplifier is always the second block and follows the photodiode, as shown in Fig.9-6, as it is used to amplify the small photodiode output current and converts it to voltage. Then the signal passed through the post amplifier with gain of 30 dB for amplification, the post amplifier is placed close up to the preamplifier as displayed in Fig.9-6 and then connected to the voltage comparator of which the final stage of the received signal which entered the FPGA interface board unit and is streamed to the digital signal processing steps.

9.6 System Implementation

FPGA and Quartus II

The programming code for both DiPPM system and DPPM system was programmed by using a Very High Speed Integrated Gate Circuits (VHSIC) Hardware Description Language (VHDL). The VHDL code used for DiPPM is presented in (Appendix-C1),(Romanos Charitopoulos, 2009) and the VHDL code used for DPPM is presented in (Appendix-C2, (Benjadid, 2012). Quartus II 11.1 software was used to generate VHDL codes and it creates on the required system blocks; included coder, decoder, input and output pins linked to FPGA interface board. Following this, the complete code for the system is then downloaded into the FPGA by using Quartus II 11.1 software. The FPGA (Cyclone IV GX-EP4CGX150DF31C7) is used for this model, see Fig.9-3.

Pseudo Random Bit Sequence (PRBS) Generation:

The pulse pattern test (*HP* 3780A) generates the PRBS pulses of n=9, so the number of the pulses is 512, it has option of either using an internal clock for a low data rate or an external clock for inputs for a high data rate operation. The output of the PRBS generator is then connected through the FPGA interface pins that are allocated for PCM input data. The PCM input data is first coded by coding blocks according to the modulation technique.

Data transmitting:

The output pulses of the coding block are then used to drive the LED source through the LED driver circuit. As the data sequences passes through to the LEDs, The LEDs emit

pulses according to the data patterns. The original information that is carried by the coding pulses is then propagated with the LED flux intensity through the indoor optical wireless channel. At the photodiode the output current is measured and the received pulses are amplified and are at that time also displayed by the oscilloscope.

Data Receiving:

At the receiver the detected weak signal is delivered into the preamplifier, as it needs an amplification to allow following and next signal processing steps. Then at the next stage the RF amplifier is used within the system to provide a high level of 30dB gain. After, the signal is arrived at the input of the voltage comparator, which mainly used as a decision circuit to recover the input signal. The recovered data is inserted into the input of the interface unit (FPGA) according to the allocated pins. The received data is sequentially passed through the FPGA and linked into the decoder block.
Finally, in order to verify that the whole VLC system is established with a communication link and is ended without any missing information, the received data sequence bits is compared to the original PCM data bits by using two methods to demonstrate the results: SignalTap II Analyzer on Quartus II tools and the screen on the oscilloscope (TDS1002B).
Next, the decoding sequence bits are sent back through the FPGA bins and connected to the input of the pulse pattern test on the receiver section. In order to measure the error rate some errors are injected into the original PCM bits reference.

9.7 Simulation Testing Results

The simulation is performed after the complete VLC system is implemented and other devices were also developed and connected to each other. The simulation has been done for both DiPPM and DPPM systems over the indoor optical link as following.

9.7.1 DiPPM System Results:

The schematic diagram of the full DiPPM system is shown in Fig.9-8. The whole blocks are linked together, some output pins and input pins are signed, for signal out and signal in, respectively. The encoding PRBS is connected to the LED through the FPGA. Whereas the input pins one connects the PRBS sequence and the other is for connecting the receiver output into a DiPPM decoder input. The full DiPPM system results are demonstrated as the following.

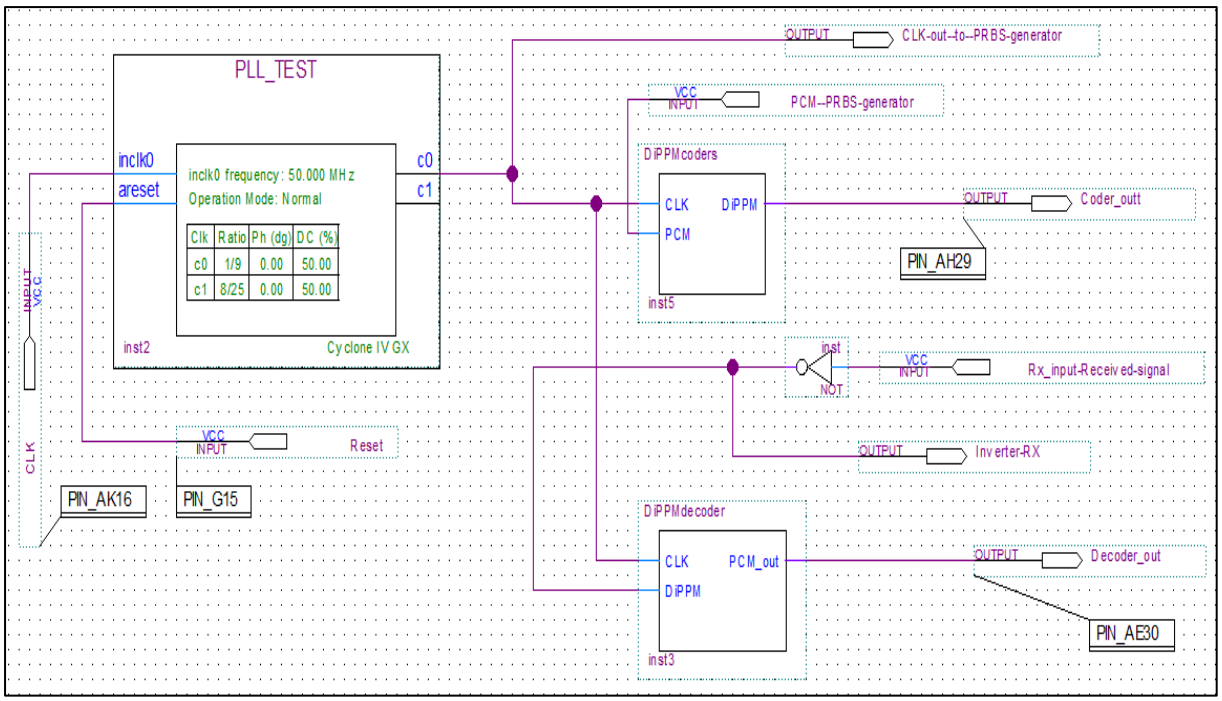

Figure 9-8 -Full Schematic Diagram of DiPPM system

Fig.9-9 displays the output sequence of the DiPPM encoded pulses thorugh the FPGA ouput pins (top trace) and the measured received sequence via LED at the output of the voltage comparator (bottom trace). The results show that the oscilloscope aprears with both signals having full matching and no error has been detected.

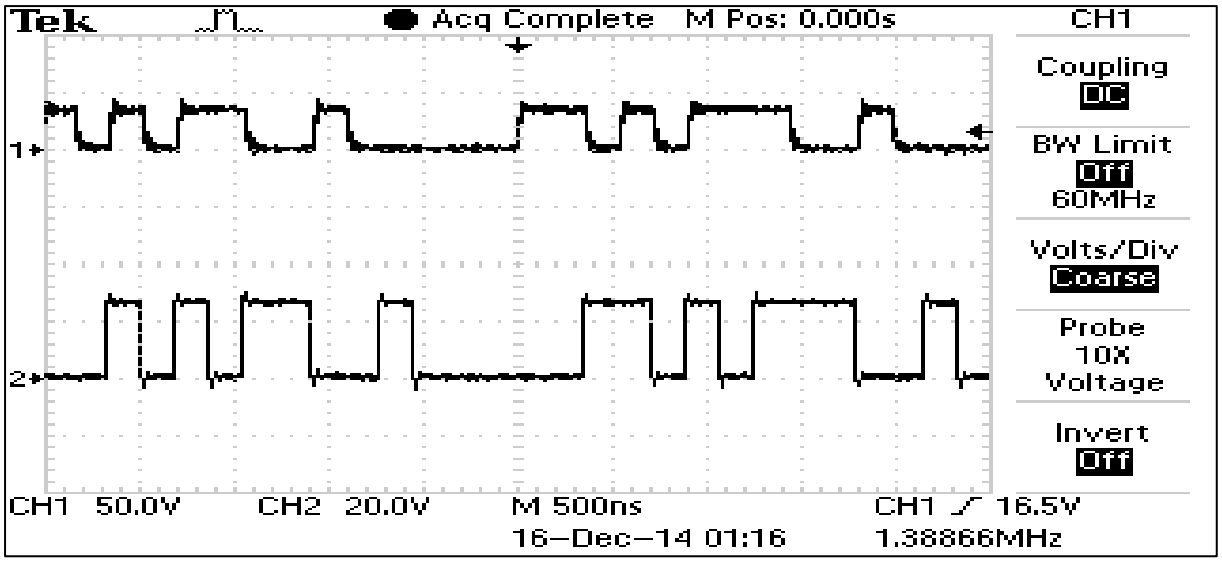

Figure 9-99 Coder output (top trace), Received coder sequence (bottom trace)

Fig.9-10 shows the final result of the DiPPM indoor VLC system. The Quartus II software generated the codes and sent it through the FPGA to the LED transmitter circuit. The emitted pulses propagated on an indoor VLC channel and then which was decoded by the Quartus II software, after it arrived at the photodetector.

The detailed results show the transmitted pulses have been produced back without missing any information for the PCM data sequences.

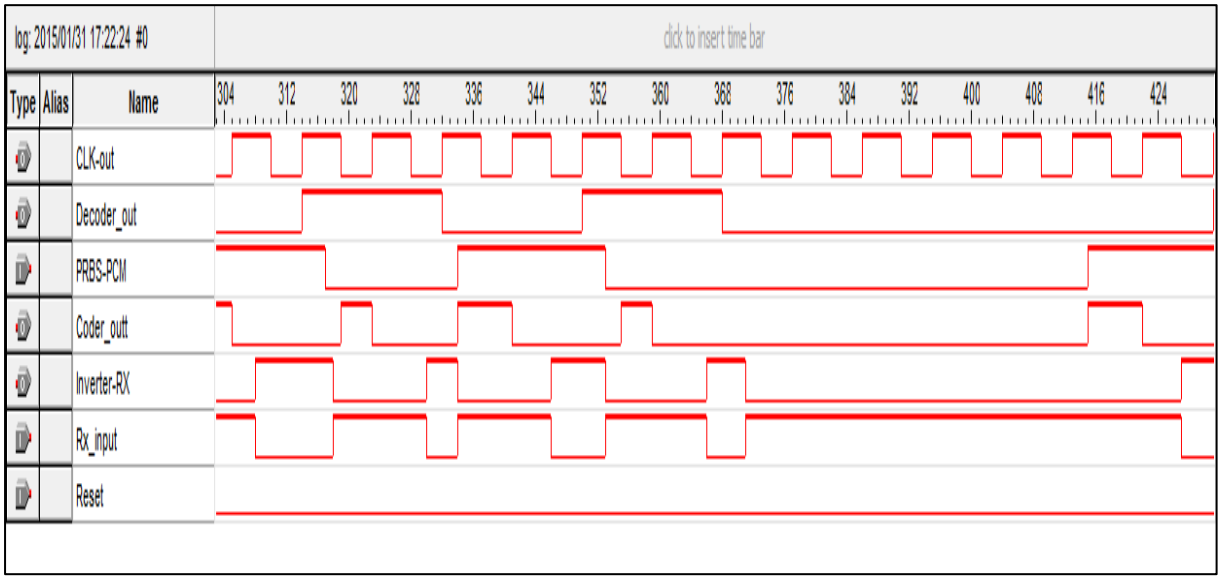

Figure 9-10-DiPPM System results

9.7.2 DPPM system Results:

The schematic diagram of the full digital pulse position modulation (DPPM) system is shown in Fig.9-11. The whole blocks are linked together including the coder, parallel to linear and linear to parallel convertors and a decoder. A Similar idea to the DiPPM system is used in this test simulation. Where, the encoding PRBS (PCM) connected to the LED through the FPGA, the LED emits the sequennce of the DPPM encoded pulses. At the receiver the optical pulses after detection returend back to the decoding block a gain through the FPGA and hence compared to the original PCM pulses. The full DiPPM system results are demonstrated as the following.

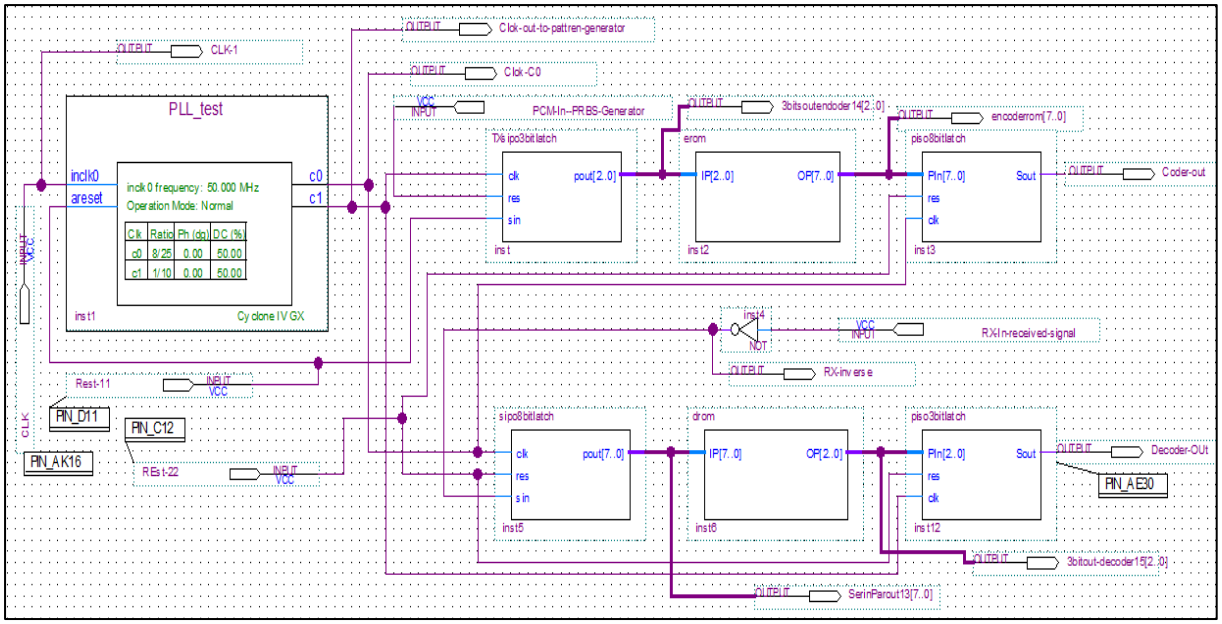

Figure 9-10-Full Schematic Diagram of DPPM system

The output sequennce of the DPPM encoded pulses and the measured received sequence via LED is displays in Fig.9-12. The results show that the oscilloscope aprears with both signals having full matching and no error has been detected after the signal propagated thorugh the VLC channel.

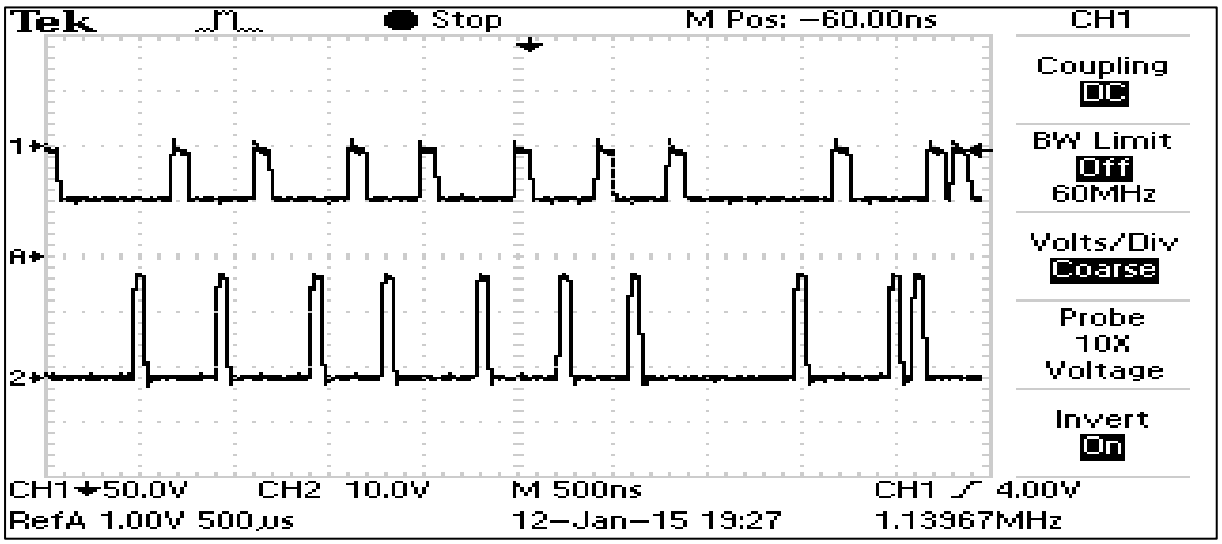

Figure 9-11 Coder output (bottom trace), Received coder sequence via LED (top trace)

Fig.9-13 shows the final result of the DPPM indoor VLC system. The results show that the transmitted encoded data has been detected back and compared to the original PCM data sequence. Also it shows that both the transmitted and the received pulses have been detected without missing out any information.

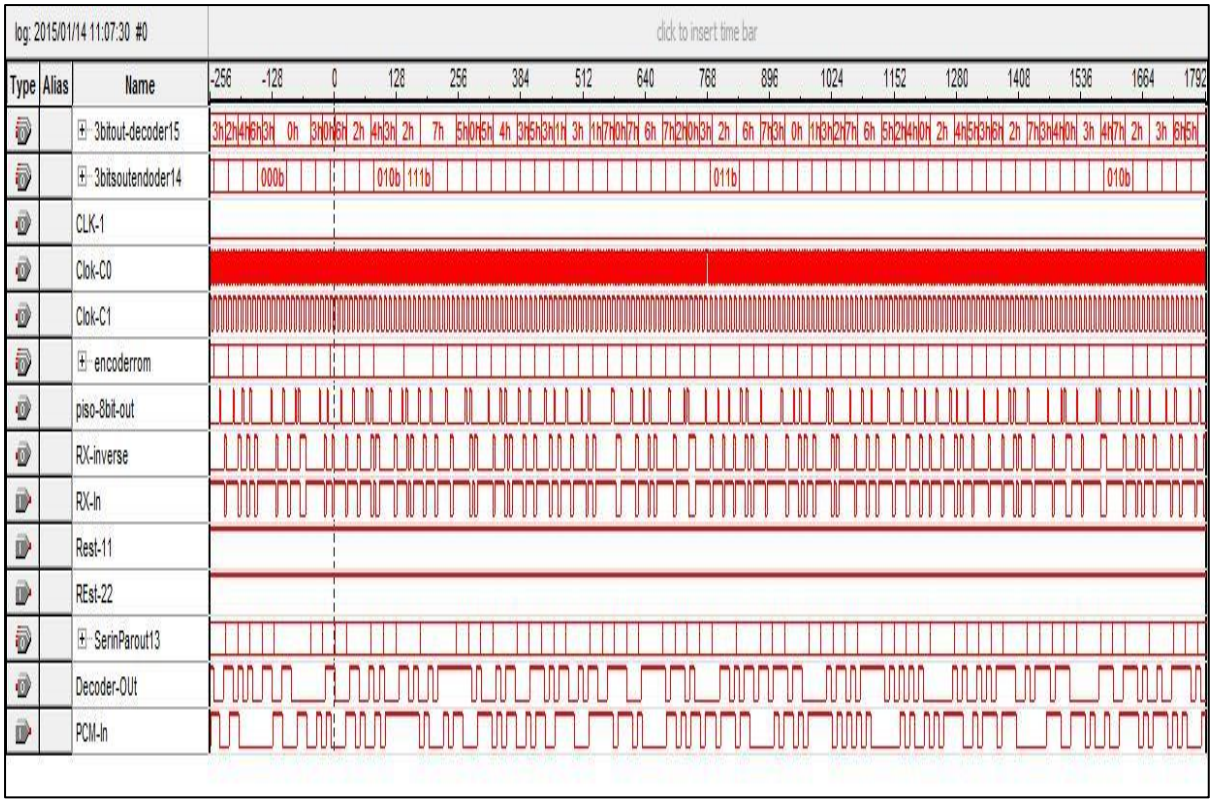

Figure 9-12-DPPM System results

9.8 Measurements and Evaluations:

Typically, in order to evaluate the performance of an indoor VLC system the measurement test has been performed while the VLC system was in operation. The tests are carried out in the following steps:

1. Transmitter and Receiver setup test: It is an essential test which is performed of the beginning of the measurements to ensure that the LED emits the data bits information. The test is typically taken after driving the LED by current source (constant current) and connecting it to the data sequences source at a selected data rate.

   We did this test by connecting the photodetector to the display of the oscilloscope and compared the received pulses with the transmitted pulse (Coder output) as shown in Fig.42 and Fig.44 for DiPPM and DPPM systems, respectively.
2. Receiver Sensitivity Measurement: Practically, the receiver sensitivity is measured in terms of received optical power as a minimum amount that is required for the photodetector to meet system performance criteria over a specific bit error rate. The BER is main critical factor in any optical link, in other words it is essential to have a distinct BER before starting the measurements. A valid measurement

needs a number of errors at least in order of tens. Indicating BER is important, because measurements can take a very long time for low error(JDSU, 2009).

$$\text{BER= error bits/total bits} \tag{131}$$

$$\text{BER = error bits/ T.B} \tag{132}$$

where T is the gating time that is required for finishing the test.

In some cases and for BER of 10^{-12} if the selected data rate is 100 Mbps and the number of the errors is 10 errors, the gating time can be then calculated as

$$T= 10/(100x10^{6}x10^{-12}) = 10000 \text{ s}$$

In our test we take this into account as these could leads to impracticable results and so an error rate of 10^{-7} has been used here.

3. The ambient light Measurement: this is a background current due to the natural and artificial light that is received by the photodiode. It is a Dc current that produces a shot noise power at the photodiode which is a deterministic signal. Typically, as the received power is going to be measured, it is important to introduce the shot noise power in our VLC system measurements. As the shot noise power is directly proportional to the ambient light and it can then be straight forwardly be obtained as a resulting of the conversion process, where the incident optical power is converted to background current. Hence, the total photodiode output current is

$$I_d = I_p + I_a \tag{133}$$

where I_p is a current related to the optical received power transmission light and I_a is the ambient background light (A. J. Moreira, Valadas, & de Oliveira Duarte, 1995)

4. Due to the wide band spectrum of VLC, it is difficult to measure the received optical power. Instead we measure the output current of the photodiode and by using the responsivity of photodiode the received optical power can be calculated. The receiver responsivity is a main factor used to measure its sensitivity to the LED light at a certain wavelength, which is the ratio of the measured photodiode current to the incident optical power, which is expressed as in equation (127).
5. The sensitivity of the receiver can be determined in dBm by the following equation

$$sensitivity = P(dBm) = 10log_{1o}(1000.P(W)/1W) \tag{134}$$

6. In normalisation of VLC performance the receiver sensitivity is to be specified in terms of the number of photons per bit interval that is required at the receiver for the decision circuit output. Which in reality is related to the received optical power and expressed as average sensitivity (M. J. N. Sibley, 1995)

$$N_p = \frac{Photons}{bit} = \frac{energe/sec}{(energy/photon)(bit/\sec)} = \frac{P_r.\lambda.T_s}{hc} \quad (135)$$

7. Typically, the quantum efficiency is defined as a conversion efficiency of the photodiode when it converts photon to electron (M. J. N. Sibley, 1995). And is given by

$$ή = \frac{I_p/q}{P_0/hv} * 100 \quad (136)$$

In general, the quantum efficiencies for the photodiodes are in the range of 60 to 80%.

8. For more precision, the measurements have been done, for both DiPPM and DPPM systems with the same tools and same FPGA board. The data rate used in this test is limited by the LED bandwidth, original PCM data rate is selected for 5.5 Mbps for both DiPPM and DPPM coding schemes.

Table 9-1 LED Parameters

Parameters	LED chip
Number of LEDs	24
Output power, W	1.44 (each 0.06W)
full beam angle	160^0
Input current	50mA

9.8.1 Measurements Results for DiPPM system:

DiPPM coding scheme operating at 11Mbps

In order to measure the photodiode (I_p) current two steps are used:

1- We measure the ambient current (I_a) in absence of the LED emission

$$I_a = 5.66\,\mu A \quad (137)$$

2- Average measured total current received by the photodiode with an optical concentrator:

$$I_{tot} = 13.71\ \mu A \tag{138}$$

Then the difference is the output photodiode current related to the received optical power, from table 14, the average photodiode current is

$$I_p = I_{tot} - I_a \tag{139}$$

$$I_p = 13.71 - 5.66 = 8.50\ \mu A \tag{140}$$

3- Calculation of the receiver sensitivity:

The receiver sensitivity is calculated by using equation (127) in the following steps:

1- We calculate the average optical received power by using the Responsivity of the PD, from the data sheet and using the curve of Responsivity vs wavelength for 650 nm. The Responsivity is 0.45 A/W.

2- Using equation (127) the optical received power is:

$$P_0 = \frac{I_p}{R_0} \tag{141}$$

$$P_0 = \frac{8.50}{0.45} * 10^{-6} \tag{142}$$

$$P_0 = 18.89\ \mu W \tag{143}$$

3- The receiver sensitivity in dBm is

$$sensitivity = P(dBm) = 10log_{1o}(1000.P(W)/1W) \tag{144}$$

$$sensitivity\ = 10log_{1o}(1000 * 18.89\ * 10^{-6}/1W) \tag{145}$$

$$sensitivity\ = -17.24\ dBm \tag{146}$$

4- Using equation (135) the number of photons is

$$N_p = \frac{18.89.10^{-6}.\lambda.T_s}{hc} \tag{147}$$

$$N_p = 5.62.10^6 \quad (148)$$

5- By using equation (136) the quantum efficiency is

$$\acute{\eta} = 85.85\ \% \quad (149)$$

Table 9-2- Measurements Results for VLC DiPPM System

Photodiode Current, μA DiPPM	I_p		
	13.71	13.71	13.71
Received Power, μW	18.89		
Sensitivity, dBm	-17.24 dBm		
Number of Photons	$5.62.10^6$		
Quantum Efficiency	85.85%		

9.8.2 Measurements Results for DPPM system

For the DPPM we did apply the same procedures for the same error rate of 1 in 10^7. DPPM coding scheme operating at 16 Mbps, the results are:

1- We measure average ambient current (I_a) in absence of LED emission

$$I_a = 5.66\ \mu A \quad (150)$$

2- We measure the average total current received by photodiode

$$I_{tot} = 15.88\ \mu A \quad (151)$$

Then the

$$I_p = I_{tot} - I_a \quad (152)$$

$$I_p = 15.88 - 5.66 = 10.22\ \mu A \quad (153)$$

3- the optical received power is:

$$P_0 = \frac{I_p}{R_0} \tag{154}$$

$$P_0 = \frac{10.22}{0.45} * 10^{-6} \tag{155}$$

$$P_0 = 22.71\ \mu W \tag{156}$$

4- Then sensitivity in dBm is :

$$sensitivity\ = 10log_{1o}(1000 * 22.71\ * 10^{-6}/1W) \tag{157}$$

$$sensitivity\ = -16.44\ dBm \tag{158}$$

5- Using equation (135) the number of photons is

$$N_p = \frac{22.71.10^{-6}.\lambda.T_s}{hc} \tag{159}$$

$$N_p = 5.065.10^6 \tag{160}$$

6- By using equation (136) the quantum efficiency is

$$ή = 85.85\ \% \tag{161}$$

Table 9-3- Measurements Results for VLC DPPM System

Photodiode Current, μA	I_d		
DPPM	15.90	15.87	15.88
Received Power, μW	22.71		
Sensitivity, dBm	-16.44 dBm		
Number of Photons	$5.065x10^6$		
Quantum Efficiency	85. 58%		

9.9 Conclusion

The measurements have been done for both DiPPM and DPPM systems in order to examine the optical receiver for enhancing the VLC system performance. The photodiode current is measured in average for more accurate as the environment and the background light may affect the measurements. According to the Pico-ammeter measurements the average photodiode current is $8.50\,\mu A$ for DiPPM which less than that for DPPM of 10.22 μA. Thus, based on the responsivity of the photodiode the obtained average received power for DiPPM is $18.89\,\mu W$ while for DPPM is $22.71\,\mu W$. This in turn that more optical power is required by DPPM when it is applied over VLC link compared to that required by DiPPM, therefore a greater sensitivity can be achieved with DiPPM system. The calculation of the average received power in dBm determine the related sensitivity which is $-17.24\,dBm$ and $-16.44\,dBm$ for DiPPM and DPPM, respectively Also, the obtained results show that the number of photons collected by DiPPM is high than that collected by DPPM, which means less and sufficient incident optical power can be received by DiPPM in comparison to the DPPM, and this show how the DiPPM modulation technique is different from DPPM modulation technique.

10 CONCLUSIONS

The objectives of this thesis were carried out and the main conclusions are:

- A detailed investigation of indoor VLC channel using two modulation techniques DiPPM and DPPM was implemented in order to exam the indoor VLC performance. The effects of the ISI have been introduced over the propagation models, the equivalent input noise current generated by optical receiver is presented when the sensitivity is evaluated. Theoretical and practical results have been presented in this thesis.
- Mathematical models and software simulations were developed and evaluated for DiPPM and DPPM VLC systems, based on the received pulse shape, in order to examine the receiver sensitivity using the equivalent PCM error probability for a specific BER. Both systems were operating at 100 Mbps and 1 Gbps for a BER of 10-9.

  The simulation has been done at high data rate (1Gbps) based on VLC channel model(1) propagation and low data rate (100 Mbps) based on VLC channel model(2) propagation, for both DiPPM and DPPM system at BER of 10-9. The detailed results show that an improvement in DiPPM VLC system performance is achieved when compared to the DPPM VLC system. Sensitivity calculation have been carried out by Mathcad software, the predicted sensitivity over diffuse link at 1 Gbps data rate for DiPPM is -21.79 dBm and -27.61 dBm and for DPPM is -16.24 dBm and -19.37 dBm when zero guard and two guards intervals are injected, respectively. While over the non-LOS link only the evaluated sensitivity is reduced compared to the diffuse link and for DiPPM is -6.88 dBm where for DPPM becomes -1.35 dBm, with zero guard. When the two guards is applied the evaluated sensitivity is reduced to -12.69 dBm and -4.47 for DiPPM and DPPM, respectively

As the 100 Mbps data rate is applied the obtained sensitivity and when a diffuse propagation link is considered, the results show that the DiPPM outperforms DPPM at zero guard and two guards by 5.13 dBm and 6.70 dBm at a sensitivity of -20.30 dBm and -25.00, respectively. While over non-LOS propagation link the sensitivity in comparison between the DiPPM and DPPM systems is outperform by 2.49 dBm and 5.18 dBm when zero guard and two guards are used, at a sensitivity of -12.10 and -17.92, respectively.

The different values for the evaluated sensitivity is based on the received optical power required by the modulation scheme and hence system performance and that related to the unique technique used by modulation scheme.

- Original results of numeral calculation of the average received power have been evaluated for both systems to form a comparison in order to obtain the receiver sensitivity as referred to the input noise. Both systems have been tested on different data rate of 100 Mbps and 1 Gbps for a BER of 10-9. The predicted results show that the DiPPM VLC system required a low incident optical power and offers lower noise bandwidth. The total equivalent input noise current generated by DiPPM receiver has small value in comparison to that generated by DPPM referred to the same preamplifier at wavelength of 650 nm. The numerical calculations show that when both systems are operating at high data rate the equivalent input noise current is 37.60×10^{-15} and 50.13×10^{-15} as ISI is ignored and when ISI is presented the value is 56.40×10^{-15} and 75.20×10^{-15} for DiPPM and DPPM, in that orders. At low data rate is 1.20×10^{-15} and 1.60×10^{-15} without ISI and if the ISI is introduced the value becomes high of 1.81×10^{-15} and 2.41×10^{-15} for DiPPM and DPPM, respectively. Thus DiPPM system outperforms DPPM with greater sensitivity of -25.36 dBm (without ISI) and -24.48 (with ISI) at 1 Gbps and -33.35 dBm (without ISI) and -32.47 dBm at 100 Mbps.

- The real-time transmission has been completed for indoor VLC system utilizing two modulation techniques, DiPPM and DPPM. Quartus II 11.1 software was used

to generate VHDL codes. FPGA development board (Cyclone IV GX) has been used as main interface unit in this system. The system performance was examined in order to determine the outperformance of a DiPPM VLC system when compared to the DPPM VLC system. The measurements were performed by using LED white light as optical transmitter faced to photodiode optical receiver on desk. Due to the LED bandwidth limitation the operating PCM data rate was 5.5 Mbps and the achieved BER was 10^{-7}. The original results for the measurements determined that the average photodiode current produced by using DiPPM was $8.50\,\mu A$ and by using DPPM was 10.22 μA. The calculation steps have been done related to the responsivity of the photodiode and found that the average received power collected by DiPPM is less than that collected by DPPM and outperforming by $3.82\,\mu W$. The number of photons collected by DiPPM ($5.62.10^6$) is higher than that collected by DPPM ($5.065.10^6$), this in turns indicated that the DiPPM receiver has a capability to receive a sufficient incident optical power at the selected BER. Thus a better sensitivity was achieved with DiPPM system ($-17.24\,dBm$) while with DPPM system is only $-16.44\,dBm$.

- The conclusion showed that the simulation and numerical calculation results agreed as well as the real-time measurements. A higher VLC system performance is achieved by using DiPPM coding scheme compared to DPPM VLC system.
- Dimming control is a key factor that brings up a fixed illumination whilst LED emit bits of information. A proposal called variable DiPPM (VDiPPM) is developed for dimming control while the DiPPM VLC system is in operation. DiPPM offers a fixed time slot and so a dimmable VLC would be available and has a simple construction than that used in a DPPM VLC system. A flexible dimming control comparison is provided by changing the amplitude of the transmitted pulse.
- Finally indoor optical wireless transmission can be embedded into full communication system utilizing DiPPM over visible light for high data rate .

Further Work

The conclusion of this thesis demonstrated that the experimental results proved the theoretical and simulation results where the DiPPM offers a better VLC system performance when compared with the original DPPM system. This in turn the DiPPM modulation technique has a capability to be suitable for indoor wireless visible light communication and has a flexible dimming control base on its technique as its offers a fixed time slot and low number of transmitted pulses, S,R or N(no pulses). The system

used a white LED as a light source with a low transmitted power and the illumination is covers small desk which provides enough light for study place.

According to the conclusion the following further research is proposed:

The developments of the solid state lighting offers advantageous in the field of visible light LED such as; high brightness, low power consumption and low cost. Since the researches have turned to use this technology the demand of the new mobile wireless generation require this everywhere. Hence, a complete DiPPM VLC system with high output LED is suggested to be the objective of new research where a high sensitivity is required. The system can be implemented indoor for big halls in universities or in the manufacture or conference rooms.

- In this thesis the performance has been evaluated for DiPPM VLC system using only one transmission channel. VLC systems also consist of multiple-input-multiple-output (MIMO) utilizing a DiPPM coding scheme. In such cases and in compared with MIMO-OFDM system in order to obtain sensitivity and accuracy of the transmission could be investigate.
- In order to examine the error correction over the transmission additional coding schemes could be used with DiPPM VLC systems, such as ; Reed Solomon and MLSD as this can enhance the system performance.

Appendices

Appendix-A1

Simulation of DiPPM VLC receiver sensitivity, operating at 1 Gbps data rate and 3 PCM bits. using photodiode (FDS025, Thorlabs) and preamplifier (Philips CGY2110CU) Model (1)

Number of like symbols in PCM

$n := 10$

offset

$i := 0, 1 .. 30$ $\quad v_i := v_{off} + \frac{i}{1000}$

Quantum energy

$\eta q := 1.6 \cdot 10^{-19}$

This is the wavelength of operation $\lambda := 650 \cdot 10^{-9}$

$$photon\_energy := \frac{6.63 \cdot 10^{-34} \cdot 3 \cdot 10^{8}}{\lambda}$$

Resposivity

$$R_o := \frac{\eta q}{photon\_energy}$$

Preamp noise at input - double sided

$S_o := 50 \cdot 10^{-24}$

Bit rate

$B := 1 \cdot 10^{9}$

PCM bit time

$$T_b := \frac{1}{B}$$

Slot time

$$T_s := \frac{T_b}{2 + gu}$$

Preamp

$$f_c := 0.5 \cdot \frac{1}{1}$$

$\omega_c := 2 \cdot \pi \cdot f_c$

$$H_{pre}(\omega) := \frac{1}{1 + j \cdot \frac{\omega}{\omega_c}}$$

Pulse shape

Area of the reflecting element

$A_{ref1} := 0.085$ m

photodiode area

$A_{PD} := 0.018$

irradiance angles $\phi_0 := 25$ $\phi_1 := 40$ $\phi_2 := 35$

incidence angles $\theta_0 := 15$ $\theta_1 := 25$ $\theta_2 := 20$

Half semi-angle $\varphi := 50$

Lambertian order $m := \frac{-\ln(2)}{\ln(\cos(\varphi \cdot deg))}$

average wall reflectivity $\rho := 0.8$

LOS distance $d_0 := 0.90$

NonLOS distance $d_1 := 0.750$ $d_2 := 0.75$

LOS channel DC gain $L_0 := \frac{A_{PD} \cdot (m + 1) \cdot \left(\cos\left(\phi_0 \cdot deg\right)\right)^m \cdot \cos\left(\theta_0 \cdot deg\right)}{2 \cdot \pi \cdot {d_0}^2}$

NonLOS channel DC gain $L_1 := \frac{A_{refl} \cdot (m + 1) \cdot \left(\cos\left(\phi_1 \cdot deg\right)\right)^m \cdot \cos\left(\theta_1 \cdot deg\right)}{2 \cdot \pi \cdot {d_1}^2}$

$L_2 := \frac{A_{PD} \cdot \cos\left(\phi_2 \cdot deg\right) \cdot \cos\left(\theta_2 \cdot deg\right)}{\pi \cdot {d_2}^2}$

$cc := 3 \cdot 10^8$

Propagation delay for LOS signal $\Delta t_{los} := 10^9 \cdot \frac{d_0}{cc}$ $\Delta t_{los} = 3$ ns

Propagation delay for non-LOS signal $\Delta t_{diff} := 10^9 \cdot \frac{(d_1 + d_2)}{cc}$ $\Delta t_{diff} = 5$ ns

VLC impulse response

$$h_{LOS}(t) := \left[\int_0^{2 \cdot t} \mathrm{Re}\left(L_0 \cdot \exp\left(i \cdot \omega \cdot \left(t - \Delta t_{los}\right) \right) \right) d\omega \right]$$

$$h_{nonLOSf}(t) := \left[\int_0^{2t} \mathrm{Re}\left(1 \cdot \rho \cdot L_1 \cdot L_2 \cdot \exp\left(i \cdot \omega \cdot \left(t - \Delta t_{diff}\right) \right) \right) d\omega \right] \qquad t := 0, 0.1 .. 14$$

$$h(t) := \left[\int_0^{2t} \mathrm{Re}\left(L_0 \cdot \exp\left(i \cdot \omega \cdot \left(t - \Delta t_{los}\right) \right) + \left(\rho \cdot L_1 \cdot L_2\right) \cdot \exp\left(i \cdot \omega \cdot \left(t - \Delta t_{diff}\right) \right) \cdot \left(H_{pre}(\omega)\right) \right) d\omega \right]$$

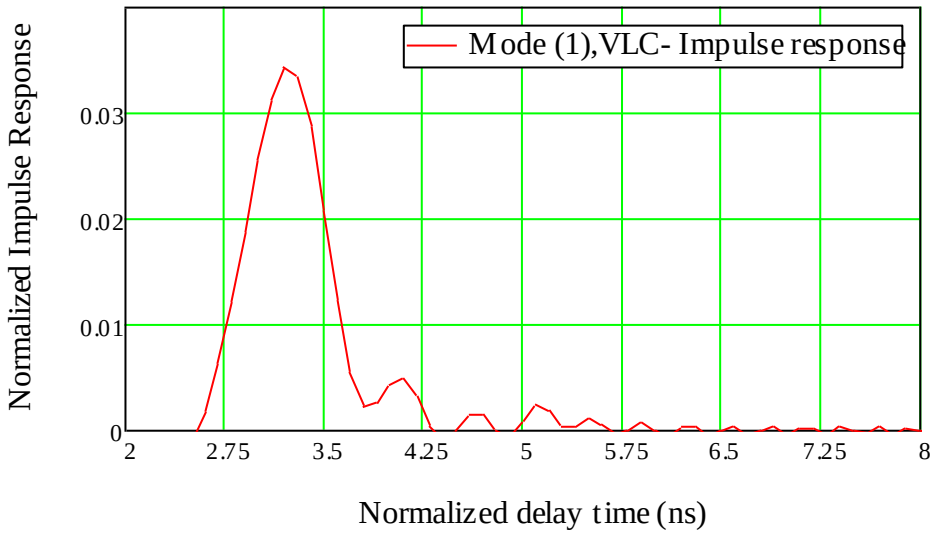

Gaussian Transmitted Pulse

$$\alpha_p := \frac{0.1874 T_b}{f_n} \qquad f_n \equiv 0.71$$

$$Pulse(t) := \frac{1}{\sqrt{2\cdot\pi}\cdot\alpha_{pn}\cdot 1}\cdot\exp\left(\frac{-t^2}{2\cdot\alpha_{pn}^2}\right)$$

Matched Filter

$$Pulse_{matched}(t) := \left(2\cdot\int_0^t Pulse(\tau)\cdot Pulse(t-\tau)\,d\tau\right)$$

Received Pulse Shape

$$V_0(t) := \left(\frac{2}{T_s}\cdot\int_0^t h(\tau)\cdot Pulse_{matched}(t-\tau)\,d\tau\right)$$

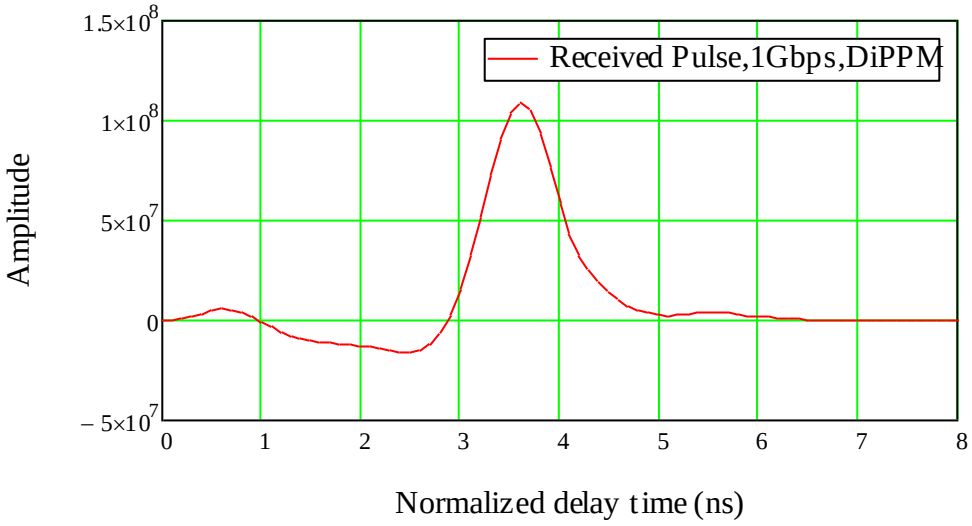

$I_0(t) := V_0(t)$

$$I_1(t) := \frac{d}{dt} I_0(t)$$

$t := 3.5$

Guess at the peak time

This is the peak time

$$t_{pk} := \text{root}\left(I_1(t)\cdot T_s^{\,2}, t\right)$$

$t_{pk} = 3.605$

This is the peak voltage

$v_{pk} := I_0(t_{pk})$ $\quad v_{pk} = 1.09\times 10^{8}$

receiver noise

$$noise := \frac{2}{2\cdot\pi}\cdot\int_0^{\frac{1}{T_s}\cdot 10^3}\left[\left|\frac{1}{1+j\cdot\frac{T_s\cdot\omega}{\omega_c}}\cdot\exp\left[-\left(T_b\cdot\alpha_{pn}\right)^2\cdot\frac{\omega^2}{2}\right]\right|\right]^2 d\omega$$

Erasure of pulse

$$Q_{e_i} := \eta q\cdot\frac{v_{pk} - v_i\cdot v_{pk}}{\sqrt{S_o\cdot noise}}$$

$$P_r(b,i) := \frac{1}{2}\cdot\text{erfc}\left(\frac{Q_{e_i}\cdot b}{\sqrt{2}}\right)$$

$$P_{er}(b,i) := 2\cdot\sum_{x=0}^{n-1}\left[\left(\frac{1}{2}\right)^{x+3}\cdot P_r(b,i)\cdot(x+1) + \left(\frac{1}{2}\right)^{n+2}\cdot P_r(b,i)\cdot(n+1)\right]$$

False alarm

False alarm when pulse appears in slot R can spread into S-slot of following symbol P_{efISI} or into previous S-slot of same symbol P_{efISI} , $v_{oISI1} := Vo(td - Ts)$ and $v_{oISI1} := Vo(td - Ts)$

$$v_{oISI1\_Ts_i} := v_i\cdot I_0\left(\frac{T_s\cdot t_{pk} - T_s}{T_s}\right)$$

$$v_{oISI2\_Ts_i} := v_i\cdot I_0\left(\frac{T_s\cdot t_{pk} + T_s}{T_s}\right)$$

$$Q_{eISI1_i} := \eta q\cdot\frac{v_i\cdot v_{pk} - v_{oISI1\_Ts_i}}{\sqrt{S_o\cdot noise}}$$

$$P_{efISI1}(b,i) := \frac{1}{2}\cdot\text{erfc}\left(\frac{Q_{eISI1_i}\cdot b}{\sqrt{2}}\right)$$

$$Q_{eISI2_i} := \eta q \cdot \frac{v_i \cdot v_{pk} - v_{oISI2\_Ts_i}}{\sqrt{S_o \cdot noise}}$$

$$P_{efISI2}(b, i) := \frac{1}{2} \cdot erfc\left(\frac{Q_{eISI2_i} \cdot b}{\sqrt{2}}\right)$$

$$P_{efR}(b, i) := \left[\sum_{x=0}^{n-1} \left[\left(\frac{1}{2}\right)^{x+3} \cdot P_{efISI1}(b, i) \cdot (x) + \left(\frac{1}{2}\right)^{n+2} \cdot P_{efISI1}(b, i) \cdot (n)\right]\right] \ldots + \sum_{x=0}^{n-1} \left[\left(\frac{1}{2}\right)^{x+3} \cdot P_{efISI2}(b, i) \cdot (x+1) + \left(\frac{1}{2}\right)^{n+2} \cdot P_{efISI2}(b, i) \cdot (n+1)\right]$$

False alarm no ISI occurs between S and R and the error appears within the run of N-symbols where k is the symbol position

False alarm between R and S pulses - N to SET

$$Q_{NS}(b, i) := \eta q \cdot \frac{v_i \cdot v_{pk}}{\sqrt{S_o \cdot noise}}$$

$$P_{NS}(b, i) := \frac{1}{2} \cdot erfc\left(\frac{Q_{NS}(b, i) \cdot b}{\sqrt{2}}\right)$$

$$P_{eNS}(b, i) := \sum_{y=3}^{n-1} \sum_{k=2}^{y-1} \left[\left(\frac{1}{2}\right)^{y+3} \cdot P_{NS}(b, i) \cdot (y + 1 - k)\right] + \sum_{k=2}^{n-1} \left[\left(\frac{1}{2}\right)^{n+2} \cdot P_{NS}(b, i) \cdot (n + 1 - k)\right]$$

False alarm between S and R pulses - N to R

$$Q_{NR}(b, i) := \eta q \cdot \frac{v_i \cdot v_{pk}}{\sqrt{S_o \cdot noise}}$$

$$P_{NR}(b, i) := \frac{1}{2} \cdot erfc\left(\frac{Q_{NR}(b, i) \cdot b}{\sqrt{2}}\right)$$

$$P_{eNR}(b, i) := \sum_{x=3}^{n-1} \sum_{k=2}^{x-1} \left[\left(\frac{1}{2}\right)^{x+3} \cdot P_{NR}(b, i) \cdot (x + 1 - k)\right] + \sum_{k=2}^{n-1} \left[\left(\frac{1}{2}\right)^{n+2} \cdot P_{NR}(b, i) \cdot (n + 1 - k)\right]$$

$$P_{fN}(b, i) := P_{eNS}(b, i) + P_{eNR}(b, i)$$

$$P_{efN}(b,i) := \left[\sum_{x=1}^{n-1}\left[\left(\frac{1}{2}\right)^{x+3}\cdot\sum_{k=1}^{x}\left[P_{fN}(b,i)\cdot(x+1-k)\right]\right]\right]\ldots$$
$$+\left(\frac{1}{2}\right)^{n+2}\cdot\sum_{k=1}^{n}\left[P_{fN}(b,i)\cdot(n+1-k)\right]+\sum_{x=2}^{n-1}\left[\left(\frac{1}{2}\right)^{x+3}\cdot\sum_{k=2}^{x}\left[P_{fN}(b,i)\cdot(x+1-k)\right]\right]..$$
$$+\left(\frac{1}{2}\right)^{n+2}\cdot\sum_{k=2}^{n}\left[P_{fN}(b,i)\cdot(n+1-k)\right]$$

Total False-alarm

$$P_{ef}(b,i) := P_{efN}(b,i) + P_{efR}(b,i)$$

Total Error for 1 in 10^9 errors

$$P_{eb}(b,i) := P_{er}(b,i) + P_{ef}(b,i)$$

$$pc(b,i) := \left(\log\left(P_{eb}(b,i)\right) + 9\right)$$

Find the root to give 1 in 10^9 $a_i := \text{root}(pc(b,i),b)$ $b \equiv 1\cdot10^5$

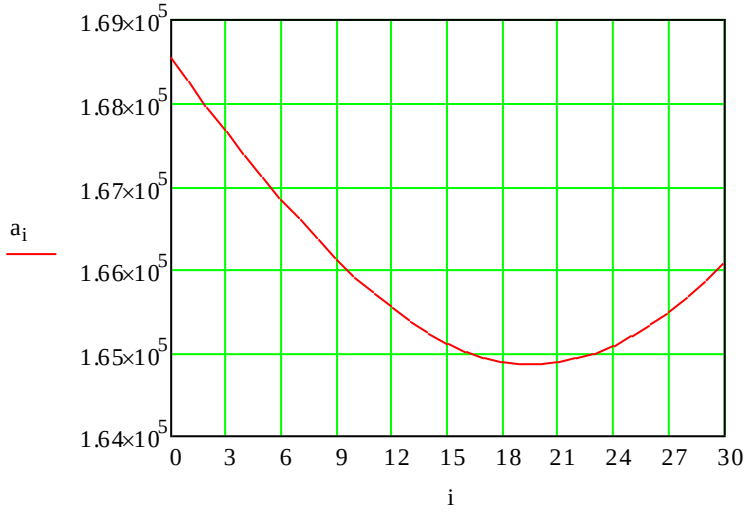

$a_i =$

$1.686\cdot10^5$
$1.682\cdot10^5$
$1.68\cdot10^5$
$1.677\cdot10^5$
$1.674\cdot10^5$
$1.671\cdot10^5$
$1.668\cdot10^5$
$1.666\cdot10^5$
$1.663\cdot10^5$
$1.661\cdot10^5$
$1.659\cdot10^5$
$1.657\cdot10^5$
$1.655\cdot10^5$
$1.654\cdot10^5$
$1.652\cdot10^5$
...

$v_{off} \equiv 0.49$

Guard intervals $gu \equiv 2$

Number of photons $minimum = min(a)$ $minimum = 1.649\times10^5$

Average received optical power

$$P_{rv} := \frac{\text{minimum}}{((gu + 2))} \cdot \text{photon\_energy} \cdot \left(\frac{1 + n}{8 \cdot n}\right) \cdot B$$

$$P_{rv} = 1.734 \times 10^{-6}$$

$$dBm := 10 \cdot \log\left[\frac{\text{minimum}}{((gu + 2))} \cdot \frac{\text{photon\_energy}}{10^{-3}} \cdot \left(\frac{1 + n}{8 \cdot n}\right) \cdot B\right]$$

$$dBm = -27.609 \text{ dB}$$

Calculate the required transmitted power

Total channel DC gain

$$DC_{gainTot} := \left(L_0 + \rho \cdot L_1 \cdot L_2\right)$$

Path loss for diffuse signal

$$DC_{dBmTot} := -10\log\left(DC_{gainTot}\right)$$

$$DC_{dBmTot} = 21.106$$

Path loss for non-LOS signal

Non-LOS DC gain

$$DC_{non.LOS} := \rho \cdot L_1 \cdot L_2$$

$$DC_{nondLOS} := -10\log\left(DC_{non.LOS}\right)$$

$$DC_{nondLOS} = 36.36$$

Required transmitted power for non-LOS link

$$P_{T.nonLOS} := \frac{P_{rv}}{\left(DC_{non.LOS}\right)}$$

$$P_{T.nonLOS} = 7.501 \times 10^{-3}$$

Required transmitted power for diffuse link

$$P_{T.diff} := \frac{P_{rv}}{\left(DC_{gainTot}\right)}$$

$$P_{T.diff} = 2.237 \times 10^{-4}$$

Simulation of DPPM VLC receiver sensitivity, operating at 1 Gbps data rate and 3 PCM bits. using photodiode (FDS025, Thorlabs) and preamplifier (Philips CGY2110CU) Model (1)

Number of like symbols in PCM

$$n := 10$$

offset

$$i := 0, 1 .. 30 \qquad v_i := v_{off} + \frac{i}{1000}$$

Quantum energy

$$\eta q := 1.6 \cdot 10^{-19}$$

This is the wavelength of operation $\lambda := 650 \cdot 10^{-9}$

$$photon\_energy := \frac{6.63 \cdot 10^{-34} \cdot 3 \cdot 10^{8}}{\lambda}$$

Resposivity

$$R_o := \frac{\eta q}{photon\_energy}$$

Preamp noise at input - double sided

$$S_o := 50 \cdot 10^{-24}$$

Bit rate

$$B := 1 \cdot 10^{9}$$

PCM bit time

$$T_b := \frac{1}{B}$$

Number of PCM Bits

$$M := 3$$

Slot Time for

$$T_s := \frac{M \cdot T_b}{2^M + gu}$$

Preamp

$$f_c := 0.5$$

$$\omega_c := 2 \cdot \pi \cdot f_c$$

$$H_{pre}(\omega) := \frac{1}{1 + j \cdot \frac{\omega}{\omega_c}}$$

Pulse shape

Area of the reflecting element

$$A_{ref1} := 0.085$$

photodiode area

$$A_{PD} := 0.018$$

irradiance angles $\phi_0 := 25$ $\phi_1 := 40$ $\phi_2 := 35$

incidence angles $\theta_0 := 15$ $\theta_1 := 25$ $\theta_2 := 20$

Half semi-angle $\varphi := 50$

Lambertian order $m := \frac{-\ln(2)}{\ln(\cos(\varphi \cdot deg))}$

average wall reflectivity $\rho := 0.8$

LOS distance $d_0 := 0.90$

NonLOS distance $d_1 := 0.750$ $d_2 := 0.75$

LOS channel DC gain $L_0 := \frac{A_{PD} \cdot (m + 1) \cdot \left(\cos\left(\phi_0 \cdot deg\right)\right)^m \cdot \cos\left(\theta_0 \cdot deg\right)}{2 \cdot \pi \cdot {d_0}^2}$

NonLOS channel DC gain $L_1 := \frac{A_{ref1} \cdot (m + 1) \cdot \left(\cos\left(\phi_1 \cdot deg\right)\right)^m \cdot \cos\left(\theta_1 \cdot deg\right)}{2 \cdot \pi \cdot {d_1}^2}$

$L_2 := \frac{A_{PD} \cdot \cos\left(\phi_2 \cdot deg\right) \cdot \cos\left(\theta_2 \cdot deg\right)}{\pi \cdot {d_2}^2}$

$cc := 3 \cdot 10^8$

Propagation delay for LOS signal $\Delta t_{los} := 10^9 \cdot \frac{d_0}{cc}$ $\Delta t_{los} = 3$

Propagation delay for non-LOS signal $\Delta t_{diff} := 10^9 \cdot \frac{\left(d_1 + d_2\right)}{cc}$ $\Delta t_{diff} = 5$ n

VLC impulse response

$h_{LOS}(t) := \int_0^{2 \cdot t} \text{Re}\ L_0 \cdot \exp\ i \cdot \omega \cdot \left(t - \Delta t_{los}\right)\ d\omega$

$h_{nonLOSf}(t) := \int_0^{2t} \text{Re}\ \rho \cdot L_1 \cdot L_2 \cdot \exp\ i \cdot \omega \cdot \left(t - \Delta t_{diff}\right)\ d\omega$

$$h(t) := \left[\int_0^{2t} \text{Re}\ \left[L_0 \cdot \exp\ i \cdot \omega \cdot \left(t - \Delta t_{los}\right) + \left(\rho \cdot L_1 \cdot L_2\right) \cdot \exp\ i \cdot \omega \cdot \left(t - \Delta t_{diff}\right)\right] \cdot \left(H_{pre}(\omega)\right)\ d\omega\right]$$

$t := 0, 0.1 .. 14$

Gaussian Transmitted Pulse

$\alpha_p := \frac{0.1874 \cdot T_b}{f_n}$

$f_n \equiv 0.7$

$$\alpha_{pn} := \frac{\alpha_p}{T_b}$$

$$Pulse(t) := \frac{1}{\sqrt{2\cdot\pi}\cdot\alpha_{pn}\cdot 1}\cdot\exp\left(\frac{-t^2}{2\cdot\alpha_{pn}{}^2}\right)$$

Matched Filter

$$Pulse_{matched}(t) := \left(2\cdot\int_0^t Pulse(\tau)\cdot Pulse(t-\tau)\,d\tau\right)$$

Received Pulse Shape

$$V_0(t) := \left(\frac{2}{T_s}\cdot\int_0^t h(\tau)\cdot Pulse_{matched}(t-\tau)\,d\tau\right)$$

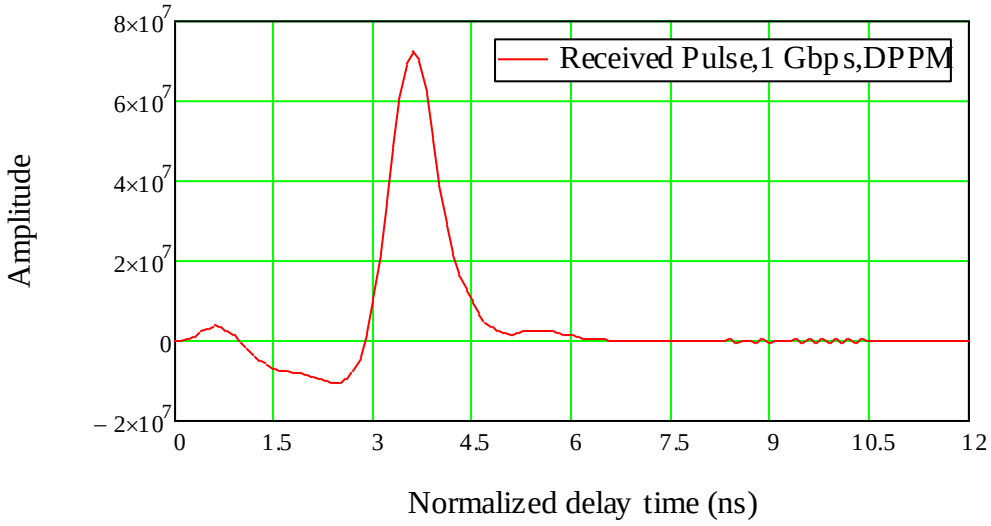

$$I_0(t) := V_0(t)$$

$$I_1(t) := \frac{d}{dt}I_0(t)$$

$$t := 3.5$$

Guess at the peak time

This is the peak time

$$t_{pk} := root\left(I_1(t)\cdot T_s{}^2, t\right)$$

$$t_{pk} = 3.605$$

This is the peak voltage

$$v_{pk} := I_0\left(t_{pk}\right) \qquad v_{pk} = 7.269\times 10^7$$

receiver noise

$$noise := \frac{2}{2\cdot\pi}\cdot\int_0^{\frac{1}{T_s}\cdot 10^3}\left[\left|\frac{1}{1+j\cdot\frac{T_s\cdot\omega}{\omega_c}}\cdot\exp\left[-\left(T_b\cdot\alpha_{pn}\right)^2\cdot\frac{\omega^2}{2}\right]\right|\right]^2 d\omega$$

Error sources

Erasure of pulse

$b \equiv 2 \cdot 10^5$

$$Q_{e_i} := \eta q \cdot \frac{v_{pk} - v_i \cdot v_{pk}}{\sqrt{S_o \cdot noise}}$$

input noise= $S_o \cdot noise$

$S_o \cdot noise = 4.913 \times 10^{-14}$

$$P_{er}(b,i) := \frac{1}{2} \cdot erfc\left(\frac{Q_{e_i} \cdot b}{\sqrt{2}}\right)$$

$$P_{erdigitaPPM}(b,i) := \frac{2^M}{2 \cdot \left(2^M - 1\right)} \cdot P_{er}(b,i)$$

False alarm

$$Q_{e_i} := \eta q \cdot \frac{v_i \cdot v_{pk}}{\sqrt{S_o \cdot noise}}$$

$$P_{ef}(b,i) := \frac{1}{2} \cdot erfc\left(\frac{Q_{e_i} \cdot b}{\sqrt{2}}\right)$$

$$P_{efdigitaPPM}(b,i) := \frac{2^M}{4} \cdot P_{ef}(b,i)$$

$$P_{eb}(b,i) := P_{erdigitaPPM}(b,i) + P_{efdigitaPPM}(b,i)$$

Set for 1 in 10^9 errors

$$pc(b,i) := \left(\log\left(P_{eb}(b,i)\right) + 9\right)$$

$P_{erdigitaPPM}(b,0) = 3.942 \times 10^{-8}$ $P_{efdigitaPPM}(b,0) = 1.733 \times 10^{-7}$

Find the root to give 1 in 10^9

guard intervals $gu \equiv 0$ $\rho := 0.8$ $v_{off} \equiv 0.498$

$$a_i := root(pc(b,i), b)$$

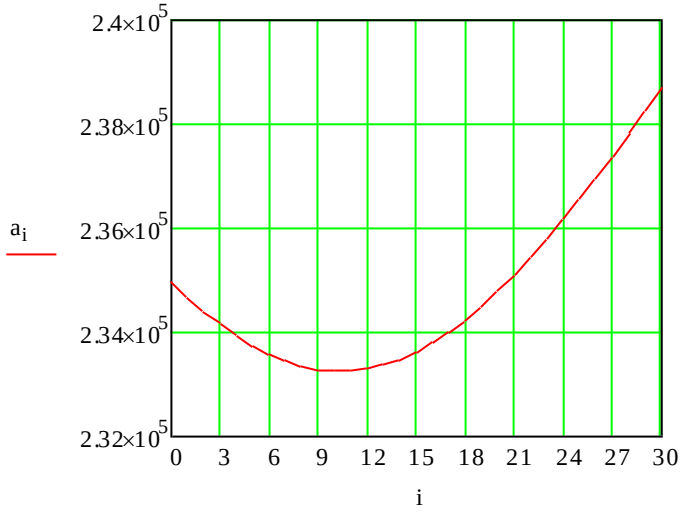

pc(b, i) =

2.328
2.313
2.298
2.285
2.273
2.262
2.252
2.243
2.235
2.228
2.223
2.219
2.217
2.216
2.216
...

Number of photons $minimum := min(a)$

$minimum = 2.333 \times 10^{5}$

$P_{T.nonLOS} = 0.103$

Average received optical power

$$P_{rv} := minimum photon\_energy \cdot \frac{B}{M + gu} \qquad P_{rv} = 2.379 \times 10^{-5}$$

$$dBm := 10 \cdot \log\left(minimum \frac{photon\_energy}{10^{-3}} \cdot \frac{B}{M + gu} \right) \qquad dBm = -16.236$$

Calculate the required transmitted power

Total channel DC gain $DC_{gainTot} := \left(L_0 + \rho \cdot L_1 \cdot L_2\right)$

Path loss for diffuse signal $DC_{dBmTot} := -10\log\left(DC_{gainTot}\right)$ $DC_{dBmTot} = 21.106$

Non-LOS DC gain $DC_{non.LOS} := \rho \cdot L_1 \cdot L_2$

Path loss for non-LOS signal

$DC_{nondLOS} := -10\log\left(DC_{non.LOS}\right)$ $DC_{nondLOS} = 36.36$

Required transmitted power for diffuse link $P_{T.diff} := \frac{P_{rv}}{\left(DC_{gainTot}\right)}$ $P_{T.diff} = 3.07 \times 10^{-3}$

Required transmitted power for non-LOS link $P_{T.nonLOS} := \frac{P_{rv}}{\left(DC_{non.LOS}\right)}$

Simulation of DiPPM VLC, receiver sensitivity, operating at 100 Mbps data rate and 3 PCM bits. using photodiode (SM05PD1A, Thorlabs) and preamplifier (Philips TZA 3043) Model (2)

Number of like symbols in PCM $n := 10$

$i := 0, 1 .. 30$ $v_i := v_{off} + \frac{i}{1000}$

Quantum energy $\eta q := 1.6 \cdot 10^{-19}$

This is the wavelength of operation $\lambda := 650 \cdot 10^{-9}$

$$photon\_energy := \frac{6.63 \cdot 10^{-34} \cdot 3 \cdot 10^{8}}{\lambda}$$

$$R_o := \frac{\eta q}{photon\_energy}$$

Preamp noise at input - $S_o := 16 \cdot 10^{-24}$

Bit rate $B := 100 \cdot 10^{6}$

PCM bit time $T_b := \frac{1}{B}$

Slot time $T_s := \frac{T_b}{2 + gu}$

Preamplifier $f_c := 0.5$ $\omega_c := 2 \cdot \pi \cdot f_c$

$f_0 := 10 \cdot 10^{6}$ $H_{pre}(\omega) := \frac{1}{1 + j \cdot \frac{\omega}{\omega_c}}$

Photodiode area $A_R := 0.0018$ m^2

Room area $A_{room} := 25$ m^2 $\rho := 0.8$

$FOV := 80$

Incidence angle $\theta_1 := 20$ Irradiance angle $\phi_1 := 25$

Lambertian order $mq := \frac{-\ln(2)}{\ln(\cos(50 \cdot deg))}$

LOS distance between LED & PD $d := 0.7$

LOS Channel Dc gain $H_{0.los} := \frac{A_R \cdot (mq + 1) \cdot \left(\cos\left(\phi_1 \cdot deg\right)\right)^{mq} \cdot \cos\left(\theta_1 \cdot deg\right)}{2 \cdot \pi \cdot d^2}$

non-LOS Channel Dc gain $H_{non.LOS} := \frac{A_R \cdot (\sin(FOV \cdot deg))^2 \cdot \rho}{A_{room} \cdot (1 - \rho)}$

Propagation delay for LOS signal $\Delta t_{los} := 2$

Propagation delay for non-LOS signal $\Delta t_{non.LOS} := 6.($

VLC chaneel impul;se response

$$h_{nonLosref}(t) := \int_0^{2t} Re\left[\frac{H_{non.LOS}}{1 + \frac{j \cdot \omega}{2 \cdot \pi \cdot f_0}} \cdot \exp\left[i \cdot \omega \cdot \left(t - \Delta t_{non.LOS}\right)\right]\right] d\omega$$

$t := 0, 0.1 .. 1($

$$h(t) := \left[\left[\int_0^{2t} Re\left[\left[H_{0.los} \cdot \exp\left[i \cdot \omega \cdot \left(t - \Delta t_{los}\right)\right] + \frac{H_{non.LOS}}{1 + \frac{j \cdot \omega}{2 \cdot \pi \cdot f_0}} \cdot \exp\left[i \cdot \omega \cdot \left(t - \Delta t_{non.LOS}\right)\right]\right] \cdot \left(H_{pre}(\omega)\right)\right] d\omega\right]\right]$$

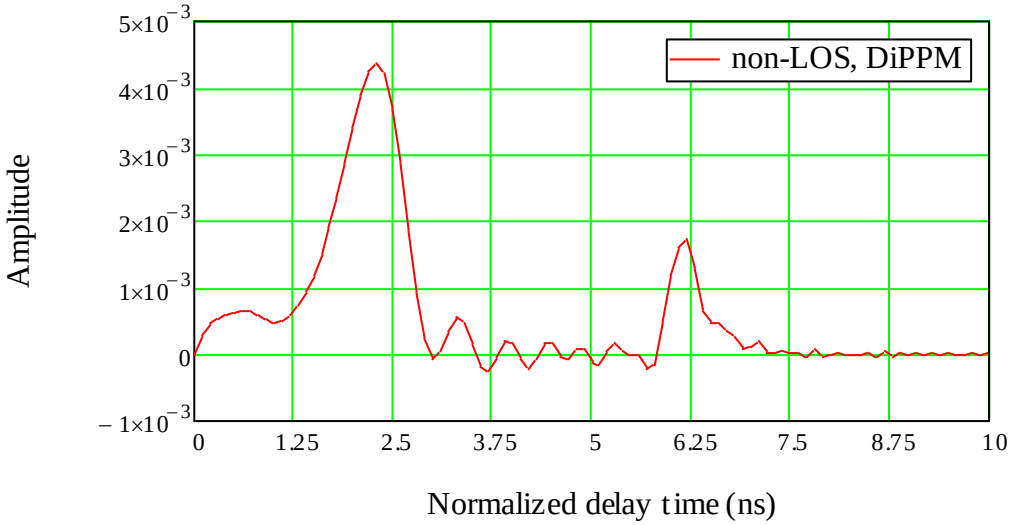

Transmitted Gaussian pulse

$f_n \equiv 0.7$

$\alpha_p := \frac{0.18741 T_b}{f_n}$

$\alpha_{pn} := \frac{\alpha_p}{T_b}$

$$Pulse(t) := \frac{1}{\sqrt{2\cdot\pi}\cdot\alpha_{pn}\cdot 1}\cdot\exp\left(\frac{-t^2}{2\cdot\alpha_{pn}^{\,2}}\right)$$

Matched filter

$$Pulse_{matched}(t) := \left(2\cdot\int_0^t Pulse(\tau)\cdot Pulse(t-\tau)\,d\tau\right)$$

Received Pulse

$$V_0(t) := \left(\frac{2}{T_s}\cdot\int_0^t h(\tau)\cdot Pulse_{matched}(t-\tau)\,d\tau\right)$$

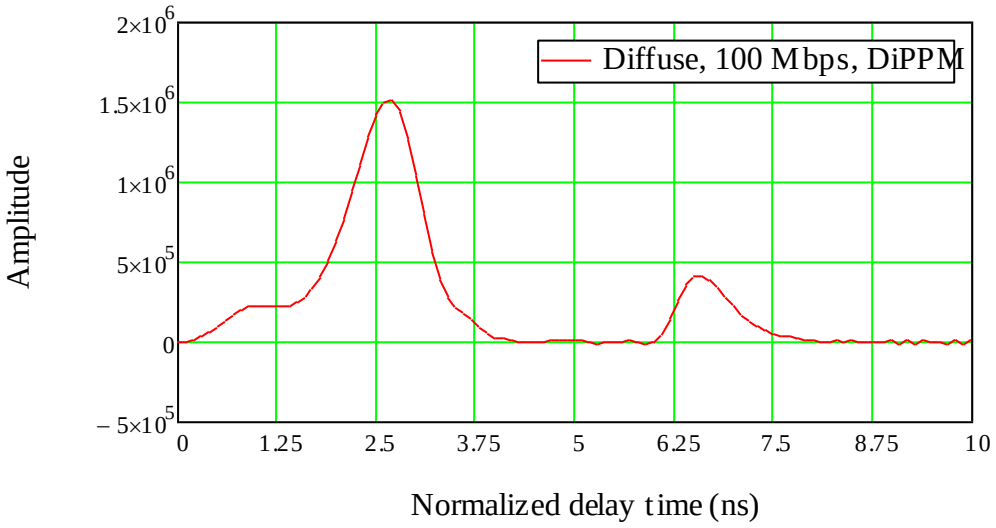

$$I_0(t) := V_0(t)$$

$$I_1(t) := \frac{d}{dt}I_0(t)$$

Guess at the peak time

$$t := 2.4$$

This is the peak time

$$t_{pk} := root\left(I_1(t)\cdot T_s^{\,2}, t\right) \qquad t_{pk} = 2.660$$

This is the peak voltage

$$v_{pk} := I_0(t_{pk}) \qquad v_{pk} = 1.518\times 10^6$$

receiver noise

$$noise := \frac{2}{2\cdot\pi}\cdot\int_0^{\frac{1}{T_s}\cdot 10^3}\left[\frac{1}{1+j\cdot\frac{T_s\cdot\omega}{\omega_c}}\cdot\exp\left[-\left(T_b\cdot\alpha_{pn}\right)^2\cdot\frac{\omega^2}{2}\right]\right]^2 d\omega$$

Erasure of pulse

$b \equiv 1\cdot 10^4$,

$$Q_{e_i} := \eta q\cdot\frac{v_{pk} - v_i\cdot v_{pk}}{\sqrt{S_o\cdot noise}}$$

Total noise $S_o\cdot noise =$ ∎

$$P_r(b,i) := \frac{1}{2}\cdot erfc\left(\frac{Q_{e_i}\cdot b}{\sqrt{2}}\right)$$

$$P_{er}(b,i) := 2\cdot\sum_{x=0}^{n-1}\left[\left(\frac{1}{2}\right)^{x+3}\cdot P_r(b,i)\cdot(x+1) + \left(\frac{1}{2}\right)^{n+2}\cdot P_r(b,i)\cdot(n+1)\right]$$

False alarm

False alarm when pulse appears in slot R can spread into S-slot of following symbol P_{efISI1} or into previous S-slot of same symbol P_{efISI2} , $v_{oISI1} := Vo(td - Ts)$and $v_{oISI1} := Vo(td - Ts)$

$$v_{oISI1\_Ts_i} := v_i\cdot I_0\left(\frac{T_s\cdot t_{pk} - T_s}{T_s}\right)$$

$$v_{oISI2\_Ts_i} := v_i\cdot I_0\left(\frac{T_s\cdot t_{pk} + T_s}{T_s}\right)$$

$$Q_{eISI1_i} := \eta q\cdot\frac{v_i\cdot v_{pk} - v_{oISI1\_Ts_i}}{\sqrt{S_o\cdot noise}}$$

$$P_{efISI1}(b,i) := \frac{1}{2}\cdot erfc\left(\frac{Q_{eISI1_i}\cdot b}{\sqrt{2}}\right)$$

$$Q_{eISI2_i} := \eta q\cdot\frac{v_i\cdot v_{pk} - v_{oISI2\_Ts_i}}{\sqrt{S_o\cdot noise}}$$

$$P_{efISI2}(b,i) := \frac{1}{2}\cdot erfc\left(\frac{Q_{eISI2_i}\cdot b}{\sqrt{2}}\right)$$

$$P_{efR}(b,i) := \left\lceil \sum_{x=0}^{n-1} \left\lceil \left(\frac{1}{2}\right)^{x+3} \cdot P_{efISI1}(b,i)\cdot(x) + \left(\frac{1}{2}\right)^{n+2} \cdot P_{efISI1}(b,i)\cdot(n) \right\rceil \right\rceil \ldots$$
$$+ \sum_{x=0}^{n-1} \left\lceil \left(\frac{1}{2}\right)^{x+3} \cdot P_{efISI2}(b,i)\cdot(x+1) + \left(\frac{1}{2}\right)^{n+2} \cdot P_{efISI2}(b,i)\cdot(n+1) \right\rceil$$

False alarm no ISI accurs between S and R and the error apears within the run of N-symbols where k is the symbol position

False alarm between R and S pulses - N to SET

$$Q_{NS}(b,i) := \eta q \cdot \frac{v_i \cdot v_{pk}}{\sqrt{S_o \cdot noise}} \qquad P_{NS}(b,i) := \frac{1}{2}\cdot \operatorname{erfc}\left(\frac{Q_{NS}(b,i)\cdot b}{\sqrt{2}}\right)$$

$$P_{eNS}(b,i) := \sum_{y=3}^{n-1} \sum_{k=2}^{y-1} \left\lceil \left(\frac{1}{2}\right)^{y+3} \cdot P_{NS}(b,i)\cdot(y+1-k) \right\rceil + \sum_{k=2}^{n-1} \left\lceil \left(\frac{1}{2}\right)^{n+2} \cdot P_{NS}(b,i)\cdot(n+1-k) \right\rceil$$

False alarm between S and R pulses - N to R

$$Q_{NR}(b,i) := \eta q \cdot \frac{v_i \cdot v_{pk}}{\sqrt{S_o \cdot noise}} \qquad P_{NR}(b,i) := \frac{1}{2}\cdot \operatorname{erfc}\left(\frac{Q_{NR}(b,i)\cdot b}{\sqrt{2}}\right)$$

$$P_{eNR}(b,i) := \sum_{x=3}^{n-1} \sum_{k=2}^{x-1} \left\lceil \left(\frac{1}{2}\right)^{x+3} \cdot P_{NR}(b,i)\cdot(x+1-k) \right\rceil + \sum_{k=2}^{n-1} \left\lceil \left(\frac{1}{2}\right)^{n+2} \cdot P_{NR}(b,i)\cdot(n+1-k) \right\rceil$$

$$P_{fN}(b,i) := P_{eNS}(b,i) + P_{eNR}(b,i)$$

$$P_{efN}(b,i) := \sum_{x=1}^{n-1} \left\lceil \left(\frac{1}{2}\right)^{x+3} \cdot \sum_{k=1}^{x} P_{fN}(b,i)\cdot(x+1-k) \right\rceil + \left(\frac{1}{2}\right)^{n+2} \cdot \sum_{k=1}^{n} P_{fN}(b,i)\cdot(n+1-k) \ \ldots$$
$$+ \sum_{x=2}^{n-1} \left\lceil \left(\frac{1}{2}\right)^{x+3} \cdot \sum_{k=2}^{x} P_{fN}(b,i)\cdot(x+1-k) \right\rceil + \left(\frac{1}{2}\right)^{n+2} \cdot \sum_{k=2}^{n} P_{fN}(b,i)\cdot(n+1-k)$$

Total Fals alarm

$$P_{ef}(b,i) := P_{efN}(b,i) + P_{efR}(b,i)$$

$$P_{eb}(b,i) := P_{er}(b,i) + P_{ef}(b,i)$$

Set for 1 in 10^9 errors $\qquad pc(b,i) := \left(\log\left(P_{eb}(b,i)\right) + 9\right)$

Find the root to give 1 in 10^9

$a_i := root(pc(b, i), b)$

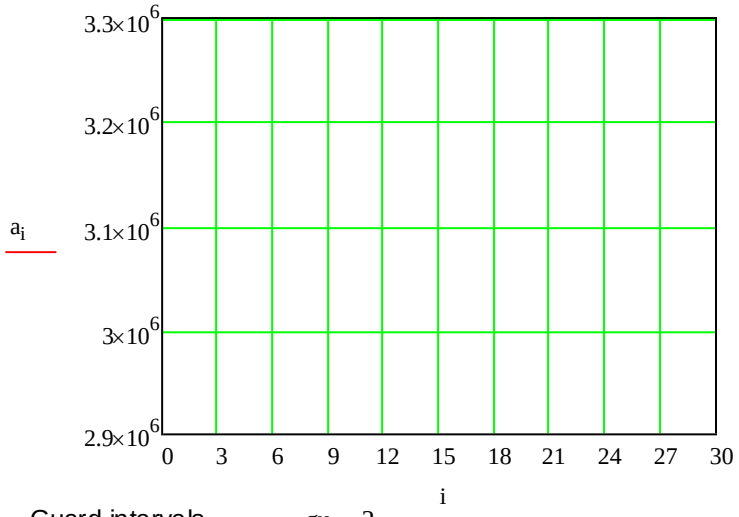

Guard intervals $gu \equiv 2$ $v_{off} \equiv 0.667$

Number of Photons $minimum := min(a)$ $minimum = 2.988 \times 10^{6}$

Average received power

$$P_r := \frac{minimum}{((gu + 2))} \cdot photon\_energy \cdot \left(\frac{1 + n}{8 \cdot n}\right) \cdot B \qquad P_r = 3.143 \times 10^{-6}$$

Receiver Sensitivity

$$dBm := 10 \cdot \log\left[\frac{minimum}{((gu + 2))} \cdot \frac{photon\_energy}{10^{-3}} \cdot \left(\frac{1 + n}{8 \cdot n}\right) \cdot B\right] \qquad dBm = -25.026$$

Minimum required transmitted power

Total optical path loss in dB $H_{0.tot} := H_{non.LOS} + H_{0.los}$ $H_{0.tot} = 1.489 \times 10^{-3}$

$L_{Tot1} := -10\log(H_{0.tot})$ $L_{Tot1} = 28.272$

Non-LOS optical path loss in dB $H_{non.LOS} = 2.793 \times 10^{-4}$

$L_{non.LOS} := -10\log(H_{non.LOS})$ $L_{non.LOS} = 35.539$

required transmitted powe for Diffuse link

$$P_{t.diff} := \frac{P_r}{H_{0.tot}} \qquad P_{t.diff} = 2.112 \times 10^{-3}$$

required transmitted powe for Non-LOS link is obtained only when received pulse of non-LOS is simulated

Simulation of DPPM VLC, receiver sensitivity, operating at 100 Mbps data rate and 3 PCM bits. using photodiode (SM05PD1A, Thorlabs) and preamplifier (Philips TZA 3043) Model (2)

Number of like symbols in PCM $n := 10$

$i := 0, 1 .. 30$ $v_i := v_{off} + \frac{i}{1000}$

Quantum energy $\eta q := 1.6 \cdot 10^{-19}$

This is the wavelength of operation $\lambda := 650 \cdot 10^{-9}$

$$photon\_energy := \frac{6.63 \cdot 10^{-34} \cdot 3 \cdot 10^{8}}{\lambda}$$

$$R_o := \frac{\eta q}{photon\_energy}$$

Preamp noise at input - double sided $S_o := 16 \cdot 10^{-24}$

Bit rate $B := 100 \cdot 10^{6}$

PCM bit time $T_b := \frac{1}{B}$

Number of PCM Bits $M := 3$

Slot Time for DPPM $T_s := \frac{M \cdot T_b}{2^M + gu}$

Preamplifier $f_c := 0.5$ $\omega_c := 2 \cdot \pi \cdot f_c$

$f_0 := 10 \cdot 10^{6}$ $H_{pre}(\omega) := \frac{1}{1 + j \cdot \frac{\omega}{\omega_c}}$

Photodiode area $A_R := 0.0018$ m^2

Room area $A_{room} := 25$ m^2 $\rho := 0.8$

$FOV := 80$

Incidence angle $\theta_1 := 20$ Irradiance angle $\phi_1 := 25$

Lambertian order $mq := \frac{-\ln(2)}{\ln(\cos(50 \cdot deg))}$

LOS distance between LED & PD $d := 0.7$

LOS Channel Dc gain $H_{0.los} := \frac{A_R \cdot (mq + 1) \cdot \left(\cos\left(\phi_1 \cdot deg\right)\right)^{mq} \cdot \cos\left(\theta_1 \cdot deg\right)}{2 \cdot \pi \cdot d^2}$

non-LOS Channel Dc gain $H_{non.LOS} := \frac{A_R \cdot (\sin(FOV \cdot deg))^2 \cdot \rho}{A_{room} \cdot (1 - \rho)}$

Propagation delay for LOS signal $\Delta t_{los} := 2$

Propagation delay for non-LOS signal $\Delta t_{non.LOS} := 6.($

VLC chaneel impul;se response

$$h_{nonLosref}(t) := \int_0^{2t} Re\left[\frac{H_{non.LOS}}{1 + \frac{j \cdot \omega}{2 \cdot \pi \cdot f_0}} \cdot \exp\left[i \cdot \omega \cdot \left(t - \Delta t_{non.LOS}\right)\right]\right] d\omega$$

$t := 0, 0.1 .. 1($

$$h(t) := \left[\left[\int_0^{2t} Re\left[\left[H_{0.los} \cdot \exp\left[i \cdot \omega \cdot \left(t - \Delta t_{los}\right)\right] + \frac{H_{non.LOS}}{1 + \frac{j \cdot \omega}{2 \cdot \pi \cdot f_0}} \cdot \exp\left[i \cdot \omega \cdot \left(t - \Delta t_{non.LOS}\right)\right]\right] \cdot \left(H_{pre}(\omega)\right)\right] d\omega\right]\right]$$

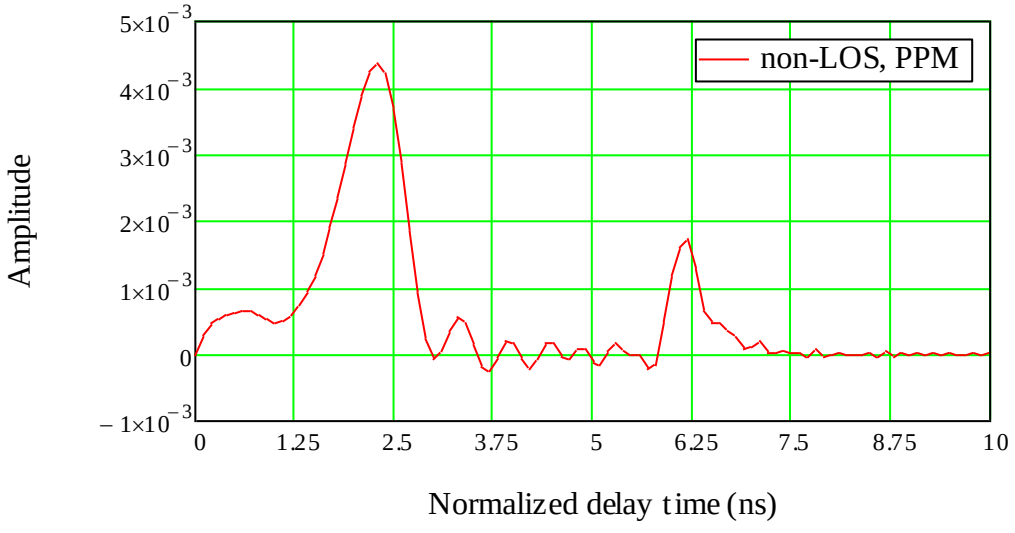

Transmitted Gaussian pulse

$f_n \equiv 0.7$

$$\alpha_p := \frac{0.18741 T_b}{f_n}$$

$$\alpha_{pn} := \frac{\alpha_p}{T_b}$$

$$Pulse(t) := \frac{1}{\sqrt{2\cdot\pi}\cdot\alpha_{pn}\cdot 1}\cdot\exp\left(\frac{-t^2}{2\cdot\alpha_{pn}^{\,2}}\right)$$

Matched filter

$$Pulse_{matched}(t) := \left(2\cdot\int_0^t Pulse(\tau)\cdot Pulse(t-\tau)\,d\tau\right)$$

Received Pulse

$$V_0(t) := \left(\frac{2}{T_s}\cdot\int_0^t h(\tau)\cdot Pulse_{matched}(t-\tau)\,d\tau\right)$$

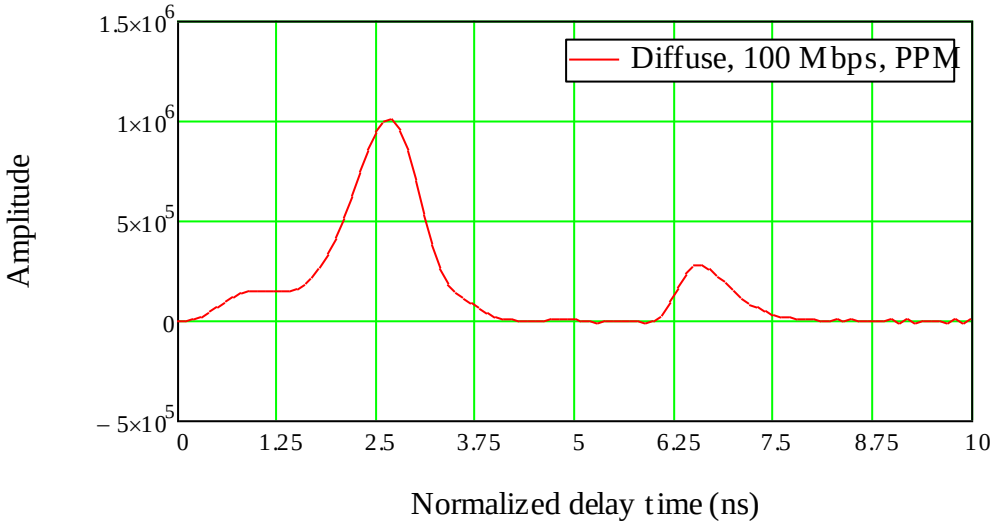

$$I_0(t) := V_0(t)$$

Guess at the peak time

This is the peak time $t_{pk} := root\left(I_1(t)\cdot T_s^{\,2}, t\right)$

This is the peak voltage $v_{pk} := I_0(t_{pk})$

receiver noise

$$noise := \frac{2}{2\cdot\pi}\cdot\int_0^{\frac{1}{T_s}\cdot 10^3}\left[\frac{1}{1+j\cdot\frac{T_s\cdot\omega}{\omega_c}}\cdot\exp\left[-\left(T_b\cdot\alpha_{pn}\right)^2\cdot\frac{\omega^2}{2}\right]\right]^2 d\omega$$

Error sources

Erasure of pulse

$$Q_{e_i} := \eta q\cdot\frac{v_{pk}-v_i\cdot v_{pk}}{\sqrt{S_o\cdot noise}}$$

$t_{pk} := t_{pk}\cdot T_s$ $\quad b \equiv 1\cdot 10^4$

total noise $S_o\cdot noise = 1.553\times 10^{-15}$

$$P_{er}(b,i) := \frac{1}{2}\cdot erfc\left(\frac{Q_{e_i}\cdot b}{\sqrt{2}}\right)$$

$$P_{erdigitaPPM}(b,i) := \frac{2^M}{2\cdot\left(2^M-1\right)}\cdot P_{er}(b,i)$$

False alarm

$$Q_{e_i} := \eta q\cdot\frac{v_i\cdot v_{pk}}{\sqrt{S_o\cdot noise}}$$

$$P_{ef}(b,i) := \frac{1}{2}\cdot erfc\left(\frac{Q_{e_i}\cdot b}{\sqrt{2}}\right)$$

$$P_{efdigitaPPM}(b,i) := \frac{2^M}{4}\cdot P_{ef}(b,i)$$

$$P_{eb}(b,i) := P_{erdigitaPPM}(b,i) + P_{efdigitaPPM}(b,i)$$

$pc(b,i) := \left(\log\left(P_{eb}(b,i)\right)+9\right)$ Set for 1 in 10^9 errors

$P_{erdigitaPPM}(b,0) = 0.281$ $\quad P_{efdigitaPPM}(b,0) = 0.984$

Find the root to give 1 in 10^9

$a_i := root(pc(b,i),b)$

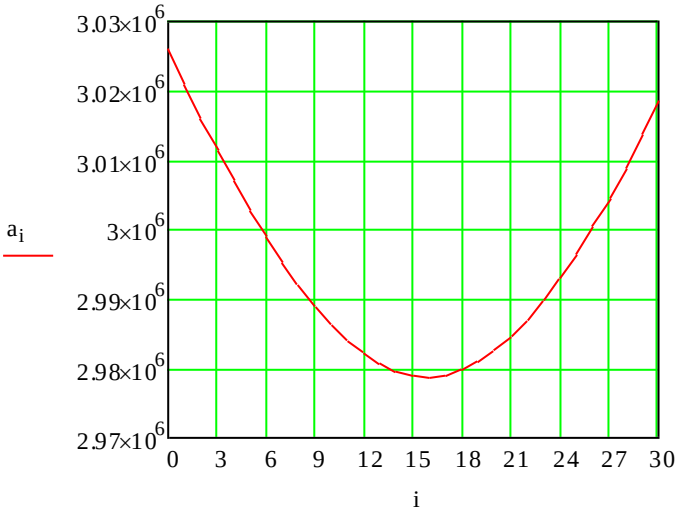

Guard intervals $gu \equiv 0$ $v_{off} \equiv 0.492$

Number of Photons $minimum := min(a)$ $minimum = 2.979 \times 10^{6}$

Average received power

$$P_r := minimum\frac{photon\_energy}{1} \cdot \frac{B}{M + gu} \qquad P_r = 3.038 \times 10^{-5}$$

Receiver Sensitivity

$$dBm := 10\log\left(minimum\frac{photon\_energy}{10^{-3}} \cdot \frac{B}{M + gu}\right) \qquad dBm = -15.174$$

Minimum required transmitted power

Total optical path loss in dB $H_{0.tot} := H_{non.LOS} + H_{0.los}$ $H_{0.tot} = 1.489 \times 10^{-3}$

$L_{Tot1} := -10\log(H_{0.tot})$ $L_{Tot1} = 28.272$

Non-LOS optical path loss in dB $H_{non.LOS} = 2.793 \times 10^{-4}$

$L_{non.LOS} := -10\log(H_{non.LOS})$ $L_{non.LOS} = 35.539$

Required transmitted power for Diffuse link

$$P_{t.diff} := \frac{P_r}{H_{0.tot}} \qquad P_{t.diff} = 0.02 \quad W$$

Required transmitted power for Non-LOS link is obtained only when received pulse of non-LOS is simulated

Appendix-B1

Calculation of DiPPM VLC receiver sensitivity, without ISI, operating at 1 Gbps data rate and 3 PCM bits. using photodiode (FDS025, Thorlabs) and preamplifier (Philips CGY2110CU) Model (1)

System Parameters

PCM data rate $B := 1 \cdot 10^{9}$

Number of like symbols in PCM $n := 10$

Number of PCM bits $N_{bit} := 3$

I_2 Noise bandwidth factor for Gaussian input pulse $I_2 := 0.376$ $\beta := 0.1$

Boltzmann's constant $K_B := 1.38 \cdot 10^{-23}$

Absolute temperature (kelivn) $T_k := 300$

Electron charge $q := 1.602 \cdot 10^{-19}$

Quantum efficiency $\eta := 94$

Planck's constant (JS) $h := 6.624 \cdot 10^{-34}$

Philips CGY2110CU

Preamlifier Parameters

input source capacitance A^2/Hz $N_0 := 50 \cdot 10^{-24}$

Gain dB $Gain := 25$

Data Rate 10 GHz

Photodiode Parameters

Peak Wavelength (nm) $\lambda := 650 \cdot 10^{-9}$

Responsivity (A/W) $R_0 := 0.4$

Dark Current (A) $I_D := 35 \cdot 10^{-12}$

System Performance Utilizing DIPPM Scheme

$$T_b := \frac{1}{B}$$

Slot time for DiPPM $T_s := \frac{T_b}{2}$

Bit rate

$B_1 := 2 \cdot B$

noise spectral density

$N_0 = 50.000 \times 10^{-24}$

The mean-square equivalent input noise current

$I_{eq.in.noise} := N_0 \cdot B_1 \cdot I_2$

The total equivalent input noise current

$I_{tot.noise} := I_{eq.in.noise} + 2 \cdot q \cdot I_D \cdot B_1 \cdot I_2$

$I_{tot.noise} = 37.600 \times 10^{-15}$ A^2

Sensitivity Determination

Signal-to-noise parameter Q

$Q := 6$ for error rate of 10^9

mean optical power required page 196

$P := \frac{Q}{R_0} \cdot \left(\sqrt{I_{tot.noise}} + q \cdot B_1 \cdot I_2 \right)$

then $P = 2.910 \times 10^{-6}$

The output current of Photodiode

$I := Q \cdot \sqrt{N_0 \cdot B_1 \cdot I_2}$

$I = 1.163 \times 10^{-6}$

then

The received power is given by

$P_r := \frac{I}{R_0}$

$P_r = 2.909 \times 10^{-6}$ Watt

then the sensitivity of the receiver using DiPPM coding schem in dBm

$P_{dBm} := 10 \log(1000 \cdot P)$

$P_{dBm} = -25.360 \times 10^0$

The number of the received photons is given by

$NP := P_r \cdot \lambda \cdot \frac{T_s}{h \cdot 3 \cdot 10^8}$

then $NP = 4.757 \times 10^3$

Average transmitted power

PD area m^2 $A_{PD} := 0.018$ $\rho := 0.8$ $cc := 3 \cdot 10^8$

Area of reflecting element $A_{ref1} := 0.085$

1/2(Viewing angle) $\phi_{1/2} := 50$

Incidence angles $\theta_0 := 15 \quad \theta_1 := 25$

$\theta_2 := 20$

Irradiance angles $\phi_0 := 25 \quad \phi_1 := 40$

$\phi_2 := 35$

Lambertian order $m := \frac{-\ln(2)}{\ln\left(\cos\left(\phi_{1/2}\cdot deg\right)\right)}$ LOS distance $d_0 := 0.90$

non_LOS distance $d_2 := 0.750 \quad d_1 := 0.75$

LOS channel DC gain $L_{LOS} := \frac{A_{PD}\cdot(m+1)\cdot\left(\cos\left(\phi_0\cdot deg\right)\right)^m\cdot\cos\left(\theta_0\cdot deg\right)}{2\cdot\pi\cdot {d_0}^2}$

$L_{LOS} = 7.520\times 10^{-3}$

non_LOS channel DC gain $L_1 := \frac{A_{ref1}\cdot(m+1)\cdot\left(\cos\left(\phi_1\cdot deg\right)\right)^m\cdot\cos\left(\theta_1\cdot deg\right)}{2\cdot\pi\cdot {d_1}^2}$

$L_2 := \frac{A_{PD}\cdot\cos\left(\phi_2\cdot deg\right)\cdot\cos\left(\theta_2\cdot deg\right)}{\pi\cdot {d_2}^2}$

$L_{nonLOS} := \rho\cdot L_1\cdot L_2$

$G_{Diff} := L_{LOS} + \left(L_{nonLOS}\right)$ $G_{Diff} = 7.751\times 10^{-3}$

$P_r = 2.909\times 10^{-6}$

then the required transmitted power for Diffuse Link $P_{Diff} := \frac{P_r}{G_{Diff}}$ $P_{Diff} = 375.256\times 10^{-6}$

optical path loss in dB $L_{nonLOS.dB} := -10\log\left(L_{nonLOS}\right)$ $L_{nonLOS.dB} = 36.360\times 10^{0}$

optical path diffuse link loss in dB $L_{diff} := -10\log\left(G_{Diff}\right)$ $L_{diff} = 21.106\times 10^{0}$

then the required transmitted power for non-LOS Link $P_{nonLOS} := \frac{P_r}{L_{nonLOS}}$ $P_{nonLOS} = 12.581\times 10^{-3}$

Calculation of DiPPM VLC receiver sensitivity, with ISI, operating at 1 Gbps data rate and 3 PCM bits. using photodiode (FDS025, Thorlabs) and preamplifier (Philips CGY2110CU) Model (1)

System Parameters

PCM data rate $B := 1 \cdot 10^{9}$

Number of like symbols in PCM $n := 10$

Number of PCM bits $N_{bit} := 3$

I_2 Noise bandwidth factor for Gaussian input pulse $I_2 := 0.564$ $\beta := 1$

Boltzmann's constant $K_B := 1.38 \cdot 10^{-23}$

Absolute temperature (kelivn) $T_k := 300$

Electron charge $q := 1.602 \cdot 10^{-19}$

Quantum efficiency $\eta := 94$

Planck's constant (JS) $h := 6.624 \cdot 10^{-34}$

Philips CGY2110CU

Preamlifier Parameters

input source capacitance A^2/Hz $N_0 := 50 \cdot 10^{-24}$

Gain dB $Gain := 25$

Data Rate 10 GHz

Photodiode Parameters

Peak Wavelength (nm) $\lambda := 650 \cdot 10^{-9}$

Responsivity (A/W) $R_0 := 0.4$

Dark Current (A) $I_D := 35 \cdot 10^{-12}$

System Performance Utilizing DIPPM Scheme

$$T_b := \frac{1}{B}$$

Slot time for DiPPM $T_s := \frac{T_b}{2}$

Bit rate $B_1 := 2 \cdot B$

noise spectral density $N_0 = 50.000 \times 10^{-24}$

The mean-square equivalent input noise current $I_{eq.in.noise} := N_0 \cdot B_1 \cdot I_2$

The total equivalent input noise current $I_{tot.noise} := I_{eq.in.noise} + 2 \cdot q \cdot I_D \cdot B_1 \cdot I_2$

$I_{tot.noise} = 56.400 \times 10^{-15}$ A^2

Sensitivity Determination

Signal-to-noise parameter Q $Q := 6$ for error rate of 10^9

mean optical power required page 196 $P := \frac{Q}{R_0} \cdot \left(\sqrt{I_{tot.noise}} + q \cdot B_1 \cdot I_2 \right)$

then $P = 3.565 \times 10^{-6}$

The output current of Photodiode $I := Q \cdot \sqrt{N_0 \cdot B_1 \cdot I_2}$

$I = 1.425 \times 10^{-6}$

then

The received power is given by $P_r := \frac{I}{R_0}$

$P_r = 3.562 \times 10^{-6}$ Watt

then the sensitivity of the receiver using DiPPM coding schem in dBm $P_{dBm} := 10 \log(1000 \cdot P)$

$P_{dBm} = -24.479 \times 10^0$

The number of the received photons is given by $NP := P_r \cdot \lambda \cdot \frac{T_s}{h \cdot 3 \cdot 10^8}$

then $NP = 5.826 \times 10^3$

Average transmitted power

PD area m^2 $A_{PD} := 0.018$ $\rho := 0.8$ $cc := 3 \cdot 10^8$

Area of reflecting element $A_{ref1} := 0.085$

1/2(Viewing angle) $\phi_{1/2} := 50$

Incidence angles $\theta_0 := 15 \quad \theta_1 := 25$

$\theta_2 := 20$

Irradiance angles $\phi_0 := 25 \quad \phi_1 := 40$

$\phi_2 := 35$

Lambertian order $m := \frac{-\ln(2)}{\ln\left(\cos\left(\phi_{1/2}\cdot deg\right)\right)}$ LOS distance $d_0 := 0.90$

non_LOS distance $d_2 := 0.750 \quad d_1 := 0.75$

LOS channel DC gain $L_{LOS} := \frac{A_{PD}\cdot(m+1)\cdot\left(\cos\left(\phi_0\cdot deg\right)\right)^m\cdot\cos\left(\theta_0\cdot deg\right)}{2\cdot\pi\cdot {d_0}^2}$

$L_{LOS} = 7.520\times 10^{-3}$

non_LOS channel DC gain $L_1 := \frac{A_{ref1}\cdot(m+1)\cdot\left(\cos\left(\phi_1\cdot deg\right)\right)^m\cdot\cos\left(\theta_1\cdot deg\right)}{2\cdot\pi\cdot {d_1}^2}$

$L_2 := \frac{A_{PD}\cdot\cos\left(\phi_2\cdot deg\right)\cdot\cos\left(\theta_2\cdot deg\right)}{\pi\cdot {d_2}^2}$

$L_{nonLOS} := \rho\cdot L_1\cdot L_2$

$G_{Diff} := L_{LOS} + \left(L_{nonLOS}\right)$ $G_{Diff} = 7.751\times 10^{-3}$

$P_r = 3.562\times 10^{-6}$

then the required transmitted power for Diffuse Link $P_{Diff} := \frac{P_r}{G_{Diff}}$ $P_{Diff} = 459.592\times 10^{-6}$

optical path loss in dB $L_{nonLOS.dB} := -10\log\left(L_{nonLOS}\right)$ $L_{nonLOS.dB} = 36.360\times 10^{0}$

optical path diffuse link loss in dB $L_{diff} := -10\log\left(G_{Diff}\right)$ $L_{diff} = 21.106\times 10^{0}$

then the required transmitted power for non-LOS Link $P_{nonLOS} := \frac{P_r}{L_{nonLOS}}$ $P_{nonLOS} = 15.409\times 10^{-3}$

Calculation of DPPM VLC receiver sensitivity, with ISI, operating at 1 Gbps data rate and 3 PCM bits. using photodiode (FDS025, Thorlabs) and preamplifier (Philips CGY2110CU) Model (1)

System Parameters

PCM data rate $B := 1 \cdot 10^{9}$

Number of like symbols in PCM $n := 10$

Number of PCM bits $N_{bit} := 3$

I_2 Noise bandwidth factor for Gaussian input pulse $I_2 := 0.564$ $\beta := 0.1$

Boltzmann's constant $K_B := 1.38 \cdot 10^{-23}$

Absolute temperature (kelivn) $T_k := 300$

Electron charge $q := 1.602 \cdot 10^{-19}$

Quantum efficiency $\eta := 94$

Planck's constant (JS) $h := 6.624 \cdot 10^{-34}$

Preamlifier Parameters Philips CGY2110CU

input source capacitance A^2/Hz $N_0 := 50 \cdot 10^{-24}$

Gain dB $Gain := 25$

Bandwidth 10 GHz

Photodiode Parameters

Peak Wavelength (nm) $\lambda := 650 \cdot 10^{-9}$

Responsivity (A/W) $R_0 := 0.4$

Dark Current (A) $I_D := 35 \cdot 10^{-12}$

System Performance Utilizing DIPPM Scheme

$$T_b := \frac{1}{B}$$

Slot time for DiPPM

$$T_s := \frac{3 \cdot T_b}{2^3}$$

Bit rate $B_1 := \frac{2^3 \cdot B}{3}$ $B_1 = 2.667 \times 10^9$

noise spectral density $N_0 = 50.000 \times 10^{-24}$

The mean-square equivalent input noise current $I_{eq.in.noise} := N_0 \cdot B_1 \cdot I_2$

The total quevalent input noise curret $I_{tot.noise} := I_{eq.in.noise} + 2 \cdot q \cdot I_D \cdot B_1 \cdot I_2$

$I_{tot.noise} = 75.200 \times 10^{-15}$ A^2

Sensitivity Determination

Signal-to-noise parameter Q $Q := 6$ for error rate of 10^9

mean optical power required $P_r := \frac{Q}{R_0} \cdot \left(\sqrt{I_{tot.noise}} + q \cdot B_1 \cdot I_2 \right)$

then $P_r = 4.117 \times 10^{-6}$

The output current of Photodiode $I := Q \cdot \sqrt{N_0 \cdot B_1 \cdot I_2}$

$I = 1.645 \times 10^{-6}$

then

The received power is given by $P_o := \frac{I}{R_0}$ $P_o = 4.113 \times 10^{-6}$

then the sensitivity of the receiver using DiPPM coding schem in dBm $P_{dBm} := 10 \log\left(1000 \cdot P_r\right)$

$P_{dBm} = -23.854 \times 10^0$

The number of the received photons is given by $NP := P_r \cdot \lambda \cdot \frac{T_s}{h \cdot 3 \cdot 10^8}$ $NP = 5.050 \times 10^3$

Average transmitted power

PD area m^2 $A_{PD} := 0.018$ $\rho := 0.8$ $cc := 3 \cdot 10^8$

Area of reflecting element $A_{ref1} := 0.085$

1/2(Viewing angle) $\phi_{1/2} := 50$

Incidence angles $\theta_0 := 15 \quad \theta_1 := 25$

$\theta_2 := 20$

Irradiance angles $\phi_0 := 25 \quad \phi_1 := 40$

$\phi_2 := 35$

Lambertian order $m := \frac{-\ln(2)}{\ln\left(\cos\left(\phi_{1/2}\cdot deg\right)\right)}$ LOS distance $d_0 := 0.90$

non_LOS distance $d_2 := 0.750 \quad d_1 := 0.75$

LOS channel DC gain $L_{LOS} := \frac{A_{PD}\cdot(m+1)\cdot\left(\cos\left(\phi_0\cdot deg\right)\right)^m\cdot\cos\left(\theta_0\cdot deg\right)}{2\cdot\pi\cdot {d_0}^2}$

$L_{LOS} = 7.520\times 10^{-3}$

non_LOS channel DC gain $L_1 := \frac{A_{ref1}\cdot(m+1)\cdot\left(\cos\left(\phi_1\cdot deg\right)\right)^m\cdot\cos\left(\theta_1\cdot deg\right)}{2\cdot\pi\cdot {d_1}^2}$

$L_2 := \frac{A_{PD}\cdot\cos\left(\phi_2\cdot deg\right)\cdot\cos\left(\theta_2\cdot deg\right)}{\pi\cdot {d_2}^2}$

$L_{nonLOS} := \rho\cdot L_1\cdot L_2$

$G_{Diff} := L_{LOS} + \left(L_{nonLOS}\right)$ $G_{Diff} = 7.751\times 10^{-3}$

$P_r = 4.117\times 10^{-6}$

then the required transmitted power for Diffuse Link $P_{Diff} := \frac{P_r}{G_{Diff}}$ $P_{Diff} = 531.158\times 10^{-6}$

optical path loss in dB $L_{nonLOS.dB} := -10\log\left(L_{nonLOS}\right)$ $L_{nonLOS.dB} = 36.360\times 10^{0}$

optical path diffuse link loss in dB $L_{diff} := -10\log\left(G_{Diff}\right)$ $L_{diff} = 21.106\times 10^{0}$

then the required transmitted power for non-LOS Link $P_{nonLOS} := \frac{P_r}{L_{nonLOS}}$ $P_{nonLOS} = 17.808\times 10^{-3}$

Calculation of DPPM VLC receiver sensitivity, without ISI, operating at 1 Gbps data rate and 3 PCM bits. using photodiode (FDS025, Thorlabs) and preamplifier (Philips CGY2110CU) Model (1)

System Parameters

PCM data rate $B := 1 \cdot 10^{9}$

Number of like symbols in PCM $n := 10$

Number of PCM bits $N_{bit} := 3$

I_2 Noise bandwidth factor for Gaussian input pulse $I_2 := 0.376$ $\beta := 0.1$

Boltzmann's constant $K_B := 1.38 \cdot 10^{-23}$

Absolute temperature (kelivn) $T_k := 300$

Electron charge $q := 1.602 \cdot 10^{-19}$

Quantum efficiency $\eta := 94$

Planck's constant (JS) $h := 6.624 \cdot 10^{-34}$

Preamlifier Parameters Philips CGY2110CU

input source capacitance A^2/Hz $N_0 := 50 \cdot 10^{-24}$

Gain dB $Gain := 25$

Bandwidth 10 GHz

Photodiode Parameters

Peak Wavelength (nm) $\lambda := 650 \cdot 10^{-9}$

Responsivity (A/W) $R_0 := 0.4$

Dark Current (A) $I_D := 35 \cdot 10^{-12}$

System Performance Utilizing DIPPM Scheme

Slot time for DiPPM $T_b := \frac{1}{B}$

$T_s := \frac{3 \cdot T_b}{2^3}$

Bit rate $B_1 := \frac{2^3 \cdot B}{3}$ $B_1 = 2.667 \times 10^9$

noise spectral density $N_0 = 50.000 \times 10^{-24}$

The mean-square equivalent input noise current $I_{eq.in.noise} := N_0 \cdot B_1 \cdot I_2$

The total quevalent input noise curret $I_{tot.noise} := I_{eq.in.noise} + 2 \cdot q \cdot I_D \cdot B_1 \cdot I_2$

$I_{tot.noise} = 50.133 \times 10^{-15}$ A^2

Sensitivity Determination

Signal-to-noise parameter Q $Q := 6$ for error rate of 10^9

mean optical power required $P_r := \frac{Q}{R_0} \cdot \left(\sqrt{I_{tot.noise}} + q \cdot B_1 \cdot I_2 \right)$

then $P_r = 3.361 \times 10^{-6}$

The output current of Photodiode $I := Q \cdot \sqrt{N_0 \cdot B_1 \cdot I_2}$

$I = 1.343 \times 10^{-6}$

then

The received power is given by $P_o := \frac{I}{R_0}$ $P_o = 3.359 \times 10^{-6}$

then the sensitivity of the receiver using DiPPM coding schem in dBm $P_{dBm} := 10 \log\left(1000 \cdot P_r\right)$

$P_{dBm} = -24.735 \times 10^0$

The number of the received photons is given by $NP := P_r \cdot \lambda \cdot \frac{T_s}{h \cdot 3 \cdot 10^8}$ $NP = 4.123 \times 10^3$

Average transmitted power

PD area m^2 $A_{PD} := 0.018$ $\rho := 0.8$ $cc := 3 \cdot 10^8$

Area of reflecting element $A_{ref1} := 0.085$

1/2(Viewing angle) $\phi_{1/2} := 50$

Incidence angles $\theta_0 := 15$ $\theta_1 := 25$

$\theta_2 := 20$

Irradiance angles $\phi_0 := 25$ $\phi_1 := 40$

$\phi_2 := 35$

Lambertian order $m := \frac{-\ln(2)}{\ln\left(\cos\left(\phi_{1/2}\cdot deg\right)\right)}$ LOS distance $d_0 := 0.90$

non_LOS distance $d_2 := 0.750$ $d_1 := 0.75$

LOS channel DC gain $L_{LOS} := \frac{A_{PD}\cdot(m+1)\cdot\left(\cos\left(\phi_0\cdot deg\right)\right)^m\cdot\cos\left(\theta_0\cdot deg\right)}{2\cdot\pi\cdot {d_0}^2}$

$L_{LOS} = 7.520\times 10^{-3}$

non_LOS channel DC gain $L_1 := \frac{A_{ref1}\cdot(m+1)\cdot\left(\cos\left(\phi_1\cdot deg\right)\right)^m\cdot\cos\left(\theta_1\cdot deg\right)}{2\cdot\pi\cdot {d_1}^2}$

$L_2 := \frac{A_{PD}\cdot\cos\left(\phi_2\cdot deg\right)\cdot\cos\left(\theta_2\cdot deg\right)}{\pi\cdot {d_2}^2}$

$L_{nonLOS} := \rho\cdot L_1\cdot L_2$

$G_{Diff} := L_{LOS} + \left(L_{nonLOS}\right)$ $G_{Diff} = 7.751\times 10^{-3}$

$P_r = 3.361\times 10^{-6}$

then the required transmitted power for Diffuse Link $P_{Diff} := \frac{P_r}{G_{Diff}}$ $P_{Diff} = 433.619\times 10^{-6}$

optical path loss in dB $L_{nonLOS.dB} := -10\log\left(L_{nonLOS}\right)$ $L_{nonLOS.dB} = 36.360\times 10^{0}$

optical path diffuse link loss in dB $L_{diff} := -10\log\left(G_{Diff}\right)$ $L_{diff} = 21.106\times 10^{0}$

then the required transmitted power for non-LOS Link $P_{nonLOS} := \frac{P_r}{L_{nonLOS}}$ $P_{nonLOS} = 14.538\times 10^{-3}$

Calculation of DiPPM VLC receiver sensistivity without ISI, for DiPPM 100 Mbps data and 3 PCM bits. using photodiode (SM05PD1A, Thorlabs) and preamplifier (TZA 3043, Philips)

System Parameters

PCM data rate $B := 100 \cdot 10^{6}$

Number of like symbols in PCM $n := 10$

Number of PCM bits $N_{bit} := 3$

I_2 Gaussian input pulse (for diffuse pulse) $I_2 := 0.376$ $\beta := 0.1$

Boltzmann's constant $K_B := 1.38 \cdot 10^{-23}$

Absolute temperature (kelivn) $T_k := 300$

Electron charge $q := 1.602 \cdot 10^{-19}$

Quantum efficiency $\eta := 94$

Planck's constant (JS) $h := 6.624 \cdot 10^{-34}$

Preamlifier Parameters

Equivalent input noise density (A^2/Hz) $N_0 := 16 \cdot 10^{-24}$

Gain dB $Gain := 30$

Photodiode Parameters

Peak Wavelength (nm) $\lambda := 650 \cdot 10^{-9}$

Responsivity (A/W) $R_0 := 0.45$

Dark Current (A) $I_D := 0.3 \cdot 10^{-9}$

System Performance Utilizing DIPPM Scheme

$$T_b := \frac{1}{B}$$

Slot time for DiPPM $$T_s := \frac{T_b}{2}$$

Bit rate $B_1 := 2 \cdot B$

input noise density $N_0 = 1.600 \times 10^{-23}$

The mean-square equivalent input noise current $I_{eq.in.noise} := N_0 \cdot B_1 \cdot I_2$

The total equivalent input noise current $I_{tot.noise} := I_{eq.in.noise} + 2 \cdot q \cdot I_{A^2} \cdot B_1 \cdot I_2$

$I_{tot.noise} = 1.203 \times 10^{-15}$

Sensitivity Determination

Signal-to-noise parameter Q $Q := 6$ for 1 error rate of 10^{9}

mean optical power required page 196 $P_r := \frac{Q}{R_0} \cdot \left(\sqrt{I_{tot.noise}} + q \cdot B_1 \cdot I_2 \right)$

then

$P_r = 4.627 \times 10^{-7}$

The output current of Photodiode $I := Q \cdot \sqrt{N_0 \cdot B_1 \cdot I_2}$

then $I = 2.081 \times 10^{-7}$

The received power is given by $P_o := \frac{I}{R_0}$

$P_o = 4.625 \times 10^{-7}$

then the sensitivity of the receiver using DiPPM coding schem in dBm $P_{dBm} := 10 \log\left(1000 \cdot P_r\right)$

$P_{dBm} = -33.347$

The number of the received photons is given by $NP := P_r \cdot \lambda \cdot \frac{T_s}{h \cdot 3 \cdot 10^{8}}$

then

$NP = 7.567 \times 10^{3}$

$A_R := 0.0018 \quad m^2$ $\rho := 0.8$ $A_{room} := 25 \quad m^2$

$FOV := 80$ $\phi_1 := 25$ $\theta_1 := 20$ $d := .70$

$mq := \frac{-\ln(2)}{\ln(\cos(50 \cdot deg))}$

Channel H(0) gain for LOS $H_{0.los} := \frac{A_R \cdot (mq + 1) \cdot \left(\cos\left(\phi_1 \cdot deg\right)\right)^{mq} \cdot \cos\left(\theta_1 \cdot deg\right)}{2 \cdot \pi \cdot d^2}$

$H_{0.los} = 1.209 \times 10^{-3}$

Channel H(0) gain for non-LOS $H_{0..nonLOS} := \frac{A_R \cdot (\sin(FOV \cdot deg))^2 \cdot \rho}{A_{room} \cdot (1 - \rho)}$

$H_{0..nonLOS} = 2.793 \times 10^{-4}$

Total gain diffuse link $H_{0.diff} := H_{0..nonLOS} + H_{0.los}$

$H_{0.diff} = 1.489 \times 10^{-3}$

optical path loss in dB $L_{diff} := -10 \log\left(H_{0.diff}\right)$

$L_{diff} = 28.272$

$L_{nonLOS} := -10 \log\left(H_{0..nonLOS}\right)$

$L_{nonLOS} = 35.539$

then the required transmitted power for diffuse link $P_t := \frac{P_r}{H_{0.diff}}$

$P_t = 3.108 \times 10^{-4}$

then the required transmitted power for diffuse link $P_{t.nonLOS} := \frac{P_r}{H_{0..nonLOS}}$

$P_{t.nonLOS} = 1.656 \times 10^{-3}$

Calculation of DiPPM VLC receiver sensistivity with ISI, for DiPPM 100 Mbps data and 3 PCM bits. using photodiode (SM05PD1A, Thorlabs) and preamplifier (TZA 3043, Philips)

System Parameters

PCM data rate $B := 100 \cdot 10^{6}$

Number of like symbols in PCM $n := 10$

Number of PCM bits $N_{bit} := 3$

I_2 Gaussian input pulse (for diffuse pulse) $I_2 := 0.564$ $\beta := 0.1$

Boltzmann's constant $K_B := 1.38 \cdot 10^{-23}$

Absolute temperature (kelivn) $T_k := 300$

Electron charge $q := 1.602 \cdot 10^{-19}$

Quantum efficiency $\eta := 94$

Planck's constant (JS) $h := 6.624 \cdot 10^{-34}$

Preamlifier Parameters

Equivalent input noise density (A^2/Hz) $N_0 := 16 \cdot 10^{-24}$

Gain dB $Gain := 30$

Photodiode Parameters

Peak Wavelength (nm) $\lambda := 650 \cdot 10^{-9}$

Responsivity (A/W) $R_0 := 0.45$

Dark Current (A) $I_D := 0.3 \cdot 10^{-9}$

System Performance Utilizing DIPPM Scheme

$$T_b := \frac{1}{B}$$

Slot time for DiPPM $$T_s := \frac{T_b}{2}$$

Bit rate $B_1 := 2 \cdot B$

input noise density $N_0 = 1.600 \times 10^{-23}$

The mean-square equivalent input noise current $I_{eq.in.noise} := N_0 \cdot B_1 \cdot I_2$

The total equivalent input noise current $I_{tot.noise} := I_{eq.in.noise} + 2 \cdot q \cdot I_{} \cdot B_1 \cdot I_2$

A^2

$I_{tot.noise} = 1.805 \times 10^{-15}$

Sensitivity Determination

Signal-to-noise parameter Q $Q := 6$ for 1 error rate of 10^{9}

mean optical power required page 196 $P_r := \frac{Q}{R_0} \cdot \left(\sqrt{I_{tot.noise}} + q \cdot B_1 \cdot I_2 \right)$

then

$P_r = 5.667 \times 10^{-7}$

The output current of Photodiode $I := Q \cdot \sqrt{N_0 \cdot B_1 \cdot I_2}$

then $I = 2.549 \times 10^{-7}$

The received power is given by $P_o := \frac{I}{R_0}$

$P_o = 5.664 \times 10^{-7}$

then the sensitivity of the receiver using DiPPM coding schem in dBm $P_{dBm} := 10 \log\left(1000 \cdot P_r\right)$

$P_{dBm} = -32.467$

The number of the received photons is given by $NP := P_r \cdot \lambda \cdot \frac{T_s}{h \cdot 3 \cdot 10^8}$

then

$NP = 9.268 \times 10^{3}$

$A_R := 0.0018 \quad m^2$ $\rho := 0.8$ $A_{room} := 25 \quad m^2$

$FOV := 80$ $\phi_1 := 25$ $\theta_1 := 20$ $d := .70$

$mq := \frac{-\ln(2)}{\ln(\cos(50 \cdot deg))}$

Channel H(0) gain for LOS $H_{0.los} := \frac{A_R \cdot (mq + 1) \cdot \left(\cos\left(\phi_1 \cdot deg\right)\right)^{mq} \cdot \cos\left(\theta_1 \cdot deg\right)}{2 \cdot \pi \cdot d^2}$

$H_{0.los} = 1.209 \times 10^{-3}$

Channel H(0) gain for non-LOS $H_{0..nonLOS} := \frac{A_R \cdot (\sin(FOV \cdot deg))^2 \cdot \rho}{A_{room} \cdot (1 - \rho)}$

$H_{0..nonLOS} = 2.793 \times 10^{-4}$

Total gain diffuse link $H_{0.diff} := H_{0..nonLOS} + H_{0.los}$

$H_{0.diff} = 1.489 \times 10^{-3}$

optical path loss in dB $L_{diff} := -10 \log\left(H_{0.diff}\right)$

$L_{diff} = 28.272$

$L_{nonLOS} := -10 \log\left(H_{0..nonLOS}\right)$

$L_{nonLOS} = 35.539$

then the required transmitted power for diffuse link $P_t := \frac{P_r}{H_{0.diff}}$

$P_t = 3.807 \times 10^{-4}$

then the required transmitted power for diffuse link $P_{t.nonLOS} := \frac{P_r}{H_{0..nonLOS}}$

$P_{t.nonLOS} = 2.029 \times 10^{-3}$

Calculation of DPPM VLC receiver sensistivity without ISI, for DPPM 100 Mbps data and 3 PCM bits. using photodiode (SM05PD1A, Thorlabs) and preamplifier (TZA 3043, Philips)

System Parameters

PCM data rate $B := 100 \cdot 10^{6}$

Number of like symbols in PCM $n := 10$

Number of PCM bits $N_{bit} := 3$

I_2 Gaussian input pulse (for diffuse pulse) $I_2 := 0.376 \qquad \beta := 0.1$

Boltzmann's constant $K_B := 1.38 \cdot 10^{-23}$

Absolute temperature (kelivn) $T_k := 300$

Electron charge $q := 1.602 \cdot 10^{-19}$

Quantum efficiency $\eta := 94$

Planck's constant (JS) $h := 6.624 \cdot 10^{-34}$

Preamlifier Parameters

Equivalent input noise density (A^2/Hz) $N_0 := 16 \cdot 10^{-24}$

Gain dB $Gain := 25$

Photodiode Parameters

Peak Wavelength (nm) $\lambda := 650 \cdot 10^{-9}$

Responsivity (A/W) $R_0 := 0.45$

Dark Current (A) $I_D := 0.3 \cdot 10^{-9}$

System Performance Utilizing DIPPM Scheme

$$T_b := \frac{1}{B}$$

Slot time for DiPPM $$T_s := \frac{3 \cdot T_b}{2^3}$$

Bit rate

$$B_1 := \frac{2^3 \cdot B}{3}$$

input noise density

$$N_0 = 16.000 \times 10^{-24}$$

The mean-square equivalent input noise current

$$I_{eq.in.noise} := N_0 \cdot B_1 \cdot I_2$$

The total equivalent input noise current

$$I_{tot.noise} := I_{eq.in.noise} + 2 \cdot q \cdot I_D \cdot B_1 \cdot I_2$$

$$I_{tot.noise} = 1.604 \times 10^{-15} \quad A^2$$

Sensitivity Determination

Signal-to-noise parameter Q

$$Q := 6$$ for 1 error rate of 10^9

mean optical power required page 196

$$P_r := \frac{Q}{R_0} \cdot \left(\sqrt{I_{tot.noise}} + q \cdot B_1 \cdot I_2 \right)$$

then

$$P_r = 534.260 \times 10^{-9}$$

The output current of Photodiode

$$I := Q \cdot \sqrt{N_0 \cdot B_1 \cdot I_2}$$

$$I = 240.320 \times 10^{-9}$$

then

The received power is given by

$$P_o := \frac{I}{R_0}$$

$$P_o = 534.044 \times 10^{-9}$$

then the sensitivity of the receiver using DiPPM coding schem in dBm

$$P_{dBm} := 10 \log\left(1000 \cdot P_r\right)$$

$$P_{dBm} = -32.722 \times 10^0$$

The number of the received photons is given by

$$NP := P_r \cdot \lambda \cdot \frac{T_s}{h \cdot 3 \cdot 10^8}$$

then

$$NP = 6.553 \times 10^3$$

$A_R := 0.0018 \quad m^2$ $\rho := 0.8$ $A_{room} := 25 \quad m^2$

$FOV := 80$ $\phi_1 := 25$ $\theta_1 := 20$ $d := .70$

$$mq := \frac{-\ln(2)}{\ln(\cos(50 \cdot deg))}$$

Channel H(0) gain for LOS $H_{0.los} := \frac{A_R \cdot (mq + 1) \cdot \left(\cos\left(\phi_1 \cdot deg\right)\right)^{mq} \cdot \cos\left(\theta_1 \cdot deg\right)}{2 \cdot \pi \cdot d^2}$

$H_{0.los} = 1.209 \times 10^{-3}$

Channel H(0) gain for non-LOS $H_{0..nonLOS} := \frac{A_R \cdot (\sin(FOV \cdot deg))^2 \cdot \rho}{A_{room} \cdot (1 - \rho)}$

$H_{0..nonLOS} = 279.316 \times 10^{-6}$

Total gain diffuse link $H_{0.diff} := H_{0..nonLOS} + H_{0.los}$

$H_{0.diff} = 1.489 \times 10^{-3}$

optical path loss in dB $L_{diff} := -10 \log\left(H_{0.diff}\right)$

$L_{diff} = 28.272 \times 10^{0}$

$L_{nonLOS} := -10 \log\left(H_{0..nonLOS}\right)$

$L_{nonLOS} = 35.539 \times 10^{0}$

then the required transmitted power for diffuse link $P_t := \frac{P_r}{H_{0.diff}}$

$P_t = 358.894 \times 10^{-6}$

then the required transmitted power for diffuse link $P_{t.nonLOS} := \frac{P_r}{H_{0..nonLOS}}$

$P_{t.nonLOS} = 1.913 \times 10^{-3}$

Calculation of DPPM VLC receiver sensistivity with ISI, for DPPM 100 Mbps data and 3 PCM bits. using photodiode (SM05PD1A, Thorlabs) and preamplifier (TZA 3043, Philips)

System Parameters

PCM data rate $B := 100 \cdot 10^{6}$

Number of like symbols in PCM $n := 10$

Number of PCM bits $N_{bit} := 3$

I_2 Gaussian input pulse (for diffuse pulse) $I_2 := 0.564$ $\beta := 1$

Boltzmann's constant $K_B := 1.38 \cdot 10^{-23}$

Absolute temperature (kelivn) $T_k := 300$

Electron charge $q := 1.602 \cdot 10^{-19}$

Quantum efficiency $\eta := 94$

Planck's constant (JS) $h := 6.624 \cdot 10^{-34}$

Preamlifier Parameters

Equivalent input noise density (A^2/Hz) $N_0 := 16 \cdot 10^{-24}$

Gain dB $Gain := 25$

Photodiode Parameters

Peak Wavelength (nm) $\lambda := 650 \cdot 10^{-9}$

Responsivity (A/W) $R_0 := 0.45$

Dark Current (A) $I_D := 0.3 \cdot 10^{-9}$

System Performance Utilizing DIPPM Scheme

$$T_b := \frac{1}{B}$$

Slot time for DiPPM

$$T_s := \frac{3 \cdot T_b}{2^3}$$

Bit rate $B_1 := \frac{2^3 \cdot B}{3}$

input noise density $N_0 = 16.000 \times 10^{-24}$

The mean-square equivalent input noise current $I_{eq.in.noise} := N_0 \cdot B_1 \cdot I_2$

The total equivalent input noise current $I_{tot.noise} := I_{eq.in.noise} + 2 \cdot q \cdot I_D \cdot B_1 \cdot I_2$

$I_{tot.noise} = 2.406 \times 10^{-15}$ A^2

Sensitivity Determination

Signal-to-noise parameter Q $Q := 6$ for 1 error rate of 10^9

mean optical power required page 196 $P_r := \frac{Q}{R_0} \cdot \left(\sqrt{I_{tot.noise}} + q \cdot B_1 \cdot I_2 \right)$

then $P_r = 654.391 \times 10^{-9}$

The output current of Photodiode $I := Q \cdot \sqrt{N_0 \cdot B_1 \cdot I_2}$

$I = 294.330 \times 10^{-9}$

then

The received power is given by $P_o := \frac{I}{R_0}$

$P_o = 654.068 \times 10^{-9}$

then the sensitivity of the receiver using DiPPM coding schem in dBm $P_{dBm} := 10 \log\left(1000 \cdot P_r\right)$

$P_{dBm} = -31.842 \times 10^0$

The number of the received photons is given by $NP := P_r \cdot \lambda \cdot \frac{T_s}{h \cdot 3 \cdot 10^8}$

then

$NP = 8.027 \times 10^3$

$A_R := 0.0018$ m^2 $\rho := 0.8$ $A_{room} := 25$ m^2

$FOV := 80$ $\phi_1 := 25$ $\theta_1 := 20$ $d := .70$

$mq := \frac{-\ln(2)}{\ln(\cos(50 \cdot deg))}$

Channel H(0) gain for LOS $H_{0.los} := \frac{A_R \cdot (mq + 1) \cdot \left(\cos\left(\phi_1 \cdot deg\right)\right)^{mq} \cdot \cos\left(\theta_1 \cdot deg\right)}{2 \cdot \pi \cdot d^2}$

$H_{0.los} = 1.209 \times 10^{-3}$

Channel H(0) gain for non-LOS $H_{0..nonLOS} := \frac{A_R \cdot (\sin(FOV \cdot deg))^2 \cdot \rho}{A_{room} \cdot (1 - \rho)}$

$H_{0..nonLOS} = 279.316 \times 10^{-6}$

Total gain diffuse link $H_{0.diff} := H_{0..nonLOS} + H_{0.los}$

$H_{0.diff} = 1.489 \times 10^{-3}$

optical path loss in dB $L_{diff} := -10 \log\left(H_{0.diff}\right)$

$L_{diff} = 28.272 \times 10^{0}$

$L_{nonLOS} := -10 \log\left(H_{0..nonLOS}\right)$

$L_{nonLOS} = 35.539 \times 10^{0}$

then the required transmitted power for diffuse link $P_t := \frac{P_r}{H_{0.diff}}$

$P_t = 439.593 \times 10^{-6}$

then the required transmitted power for diffuse link $P_{t.nonLOS} := \frac{P_r}{H_{0..nonLOS}}$

$P_{t.nonLOS} = 2.343 \times 10^{-3}$

Appendix-C1

(VHDL DiPPM)

VHDL-DiPPM-coder

```
Library IEEE;
use IEEE.STD_LOGIC_1164.all;
entity DiPPMcoders is
port(
CLK : in BIT;
PCM : in BIT;
DiPPM:out bit;
D1:out bit;
D2:out bit;
D3:out bit;
D4:out bit);
end DiPPMcoders;
architecture beh of DiPPMcoders is
signal DiPPMss:bit;
signal DiPPMr:bit;
signal DiPPMrr:bit;
signal DiPPMrrr:bit;
Signal R:bit;
Signal S:bit;
begin
process
begin
wait until clk='1' and clk'event;
DiPPMss<=PCM;
```

```
end process;
S<= '1' when PCM='1' and DiPPMss='0' else '0';
DiPPMr<='1' when PCM='0'else '0';
process
begin
wait until clk='0' and clk'event;
DiPPMrr<=DiPPMr;
end process;
process
begin
wait until clk='1' and clk'event;
DiPPMrrr<=DiPPMrr;
end process;
R<='1' when DiPPMrrr='0' and DiPPMrr='1' else '0';
DiPPM<= '1' when S='1' and R='0'else
'1' when S='0' and R='1'else '0';
D1<= DiPPMss;
D2<= DiPPMr;
D3<= DiPPMrr;
D4<= DiPPMrrr;
end beh;
```

VHDL DiPPM decoder

```
library ieee;
use ieee.std_logic_1164.all;
use ieee.std_logic_arith.all;
use ieee.std_logic_unsigned.all;
entity DiPPMdecoder is
```

```
port(                          CLK : in std_logic;  -- Clock pin
DiPPM: in bit;                          -- DiPPM input pin
PCM_out:out bit);                       -- PCM output pin
end DiPPMdecoder;
architecture beh of DiPPMdecoder is
SIGNAL SR : bit := '0';      -- S'R' latch
SIGNAL PCM_out_reg : bit;    -- PCM_out register
begin
process
begin
WAIT UNTIL RISING_EDGE (CLK);
SR <= SR XOR DiPPM;  -- Set/Reset
IF SR = '0' AND DiPPM = '1' THEN
PCM_out_reg <='1';   -- Set PCM_out
ELSIF SR = '1' AND DiPPM = '1' THEN
PCM_out_reg <='0';          -- Reset PCM_out
END IF;
end process;
PCM_out <= PCM_out_reg;             -- Output decoded PCM
end beh;
```

Appendix-C2

(VHDL DPPM)

VHDL DPPM sipo3bitlatch

```
library IEEE;
use IEEE.std_logic_1164.all;
use IEEE.STD_LOGIC_UNSIGNED.all;
ENTITY TXsipo3bitlatch IS
PORT   (clk  : IN STD_LOGIC;
res  : IN STD_LOGIC;
sin  : IN STD_LOGIC;
pout : OUT STD_LOGIC_VECTOR(2 downto 0));
END TXsipo3bitlatch;
ARCHITECTURE behaviour OF TXsipo3bitlatch IS
SIGNAL   control              : STD_LOGIC_VECTOR(2 downto 0):="001";
SIGNAL    sipo                        : STD_LOGIC_VECTOR(2 downto 0):="000";       --(Internal Signals)
BEGIN
PROCESS
BEGIN
WAIT UNTIL RISING_EDGE (clk);
IF (res = '1') THEN                                                    --(Reset State)
control   <= "001";
sipo <= "000";
ELSIF (res = '0') THEN                              --(Normal Behaviour)
sipo <= sin & sipo(2 downto 1);
IF control(2)= '1' THEN
pout <= sipo(2 downto 0);
END IF;
control(2 downto 0) <= (control(0))& (control(2 downto 1));
```

```
END IF;

END PROCESS;

END behaviour;
```

VHDL DPPM erom

```
library ieee;

use ieee.std_logic_1164.all;

entity erom is

port(  IP  : in std_logic_vector(2 downto 0);

OP          : out std_logic_vector(7 downto 0));

end erom;

architecture behv of erom is

begin

process (IP)

begin

case IP is

when "000"    => OP <= "00000001";

when "001"    => OP <= "00000010";

when "010"    => OP <= "00000100";

when "011"    => OP <= "00001000";

when "100"    => OP <= "00010000";

when "101"    => OP <= "00100000";

when "110"    => OP <= "01000000";

when "111"    => OP <= "10000000";

when others         => OP <= "XXXXXXXX";

end case;

end process;

end behv;
```

VHDL DPPM piso8bitlatch

```
library IEEE;
use IEEE.STD_LOGIC_1164.ALL;
use IEEE.STD_LOGIC_UNSIGNED.ALL;
entity piso8bitlatch is
PORT(Sout : OUT  std_logic;
PIn : IN  std_logic_vector(7 downto 0);
res : IN  std_logic;
clk : IN  std_logic);
end piso8bitlatch;
architecture Behavioral of piso8bitlatch is
signal piso : std_logic_vector(7 downto 0):="00000000";
signal Load : std_logic_vector(7 downto 0):="00000001";
begin
process
begin
WAIT UNTIL RISING_EDGE (clk);
if res = '1' then
piso <= "00000000";
Load <= "00000001";
elsif res = '0' then
if( Load (7) ='0' ) then
piso       <= piso(6 downto 0)& '0';                                                                    else
piso <= PIn;
end if;
end if;
Sout <= piso(7);
Load (7 downto 0) <= (Load(0))&(Load(7 downto 1));
```

```
end process;

end Behavioral;
```

VHDL DPPM sipo8bitlatch

```
library IEEE;

use IEEE.std_logic_1164.all;

use IEEE.STD_LOGIC_UNSIGNED.all;

ENTITY sipo8bitlatch IS

PORT   (clk  : IN STD_LOGIC;

res  : IN STD_LOGIC;

sin  : IN STD_LOGIC;

pout : OUT STD_LOGIC_VECTOR(7 downto 0));

END sipo8bitlatch;

ARCHITECTURE behaviour OF sipo8bitlatch IS

SIGNAL   control              : STD_LOGIC_VECTOR(7 downto 0);

SIGNAL    sipo                : STD_LOGIC_VECTOR(7 downto 0);     --(Internal Signals)

BEGIN

PROCESS

BEGIN

WAIT UNTIL RISING_EDGE (clk);

IF (res = '1') THEN                                          --(Reset State)

control   <= "00000100";

ELSIF (res = '0') THEN                                                --(Normal Behaviour)

sipo <= sin & sipo(7 downto 1);

IF control(7)= '1' THEN                                               --(Assessor and Corrector)

pout <= sipo(7 downto 0);

END IF;

control(7 downto 0) <= (control(0))& (control(7 downto 1));

END IF;
```

```
END PROCESS;

END behaviour;
```

VHDL DPPM drom

```
library ieee;                          -- Defines std_logic types

use ieee.std_logic_1164.all;

entity drom is

PORT ( IP   : in std_logic_vector(7 downto 0);  -- Defines ports

OP          : out std_logic_vector(2 downto 0));

END drom;

architecture behv of drom is

begin

process (IP)  begin

case IP is          -- Encode with input data

when "10000000" => OP <= "000";

when "01000000" => OP <= "100";

when "00100000" => OP <= "010";

when "00010000" => OP <= "110";

when "00001000" => OP <= "001";

when "00000100" => OP <= "101";

when "00000010" => OP <= "011";

when "00000001" => OP <= "111";

when others => OP <= "XXX";            -- Illegal condition

end case;

end process;

end behv;
```

VHDL DPPM piso3bitlatch

```
library IEEE;

use IEEE.STD_LOGIC_1164.ALL;
```

```
use IEEE.STD_LOGIC_UNSIGNED.ALL;

entity piso3bitlatch is

PORT(Sout : OUT  std_logic;

PIn : IN  std_logic_vector(2 downto 0);

res : IN  std_logic;

clk : IN  std_logic);

end piso3bitlatch;

architecture Behavioral of piso3bitlatch is

signal piso : std_logic_vector(2 downto 0):="000";

signal Load : std_logic_vector(2 downto 0):="001";

begin

process

begin

WAIT UNTIL RISING_EDGE (clk);

if res = '1' then

piso <= "000";

Load <= "001";

elsif res = '0' then

if( Load (2) ='0' ) then

piso       <= piso(1 downto 0)& '0';

else

piso <= PIn;

end if;

end if;

Sout <= piso(2);

Load (2 downto 0) <= (Load(0))&(Load(2 downto 1));

end process;

end Behavioral;
```

References

Alam, S. (2006). Comparison of Selected Digital ModulationSchemes (OOK, PPM and DPIM) for WirelessOptical Communica

tions. *4thStudent Conference on Research and Development (SCOReD 2006), 1*.

Ali, A. Y., Zhang, Z., & Zong, B. (2014). *Pulse position and shape modulation for visible light communication system.* Paper presented at the Electromagnetics in Advanced Applications (ICEAA), 2014 International Conference on.

ALTERA. (2013). Cyclone IV GX FPGA Development Board.

Audeh, M. D., & Kahn, J. M. (1994). *Performance evaluation of L-pulse-position modulation on non-directed indoor infrared channels.* Paper presented at the Communications, 1994. ICC'94, SUPERCOMM/ICC'94, Conference Record,'Serving Humanity Through Communications.'IEEE International Conference on.

Audeh, M. D., & Kahn, J. M. (1995). Performance evaluation of baseband OOK for wireless indoor infrared LAN's operating at 100 Mb/s. *Communications, IEEE Transactions on, 43*(6), 2085-2094.

Barry, J. R., Kahn, J. M., Krause, W. J., Lee, E. A., & Messerschmitt, D. G. (1993). Simulation of multipath impulse response for indoor wireless optical channels. *Selected Areas in Communications, IEEE Journal on, 11*(3), 367-379.

Benjadid, S. M. S. (2012). Implementation of Digital Pulse-Position Modulation. UK: UNIVERSITY OF HUDDERSFIELD.

Borogovac, T., Borogovac, T., Rahaim, M., Rahaim, M., Carruthers, J. B., & Carruthers, J. B. (2010). *Spotlighting for visible light communications and illumination*.

Brundage, H. (2010). *Designing a wireless underwater optical communication system.* Massachusetts Institute of Technology.

Buhafa, A. M., Al-Nedawe, B., Sibley, M. J. N., & Mather, P. (2013). MATLAB Simulation for DiPPM over Diffuse Optical Wireless Communications: University of Huddersfield.

Buhafa, A. M., Al-Nedawe, B. M., Sibley, M. J., & Mather, P. J. (2014). *VLC system performance using Dicode Pulse Position Modulation over an indoor diffuse link.* Paper presented at the Telecommunications Forum Telfor (TELFOR), 2014 22nd.

Calvert, N., Sibley, M. J., & Unwin, R. T. (1988). Experimental optical fibre digital pulse-position modulation system. *Electronics letters, 24*(2), 129-131.

Carruthers, J. B., & Carroll, S. (2005). Statistical impulse response models for indoor optical wireless channels. *International Journal of Communication Systems, 18*(3), 267-284.

Carruthers, J. B., & Kahn, J. M. (1997). Modeling of nondirected wireless infrared channels. *Communications, IEEE Transactions on, 45*(10), 1260-1268.

Charitopoulos, R. (2009). *Implementation & Performance Investigation of Dicode PPM over Dispersive Optical Channels.* University of Huddersfield.

Charitopoulos, R., & Sibley, M. (2007). *Dicode pulse position modulation coder simulation.* Paper presented at the School of Computing and Engineering Researchers' Conference, University of Huddersfield.

Charitopoulos, R., & Sibley, M. J. (2010). Slot and frame synchronisation in dicode pulse-position modulation. *IET Optoelectronics, 4*(4), 174-182.

Charitopoulos, R., & Sibley, M. J. (2011). Experimental verification of the power spectral density of dicode pulse-position modulation with practical impairments. *IET Optoelectronics, 5*(6), 233-240.

Cryan, R., & Sibley, M. J. (2006). *Minimising intersymbol interference in optical-fibre dicode PPM systems.* Paper presented at the Optoelectronics, IEE Proceedings-.

Cryan, R., & Unwin, R. (1993). Optimal and suboptimal detection of optical fibre digital PPM. *IEE Proceedings J (Optoelectronics), 140*(6), 367-375.

Cryan, R., Unwin, R. T., Garrett, I., Sibley, M. J., & Calvert, N. (1990). *Optical fibre digital pulse-position-modulation assuming a Gaussian received pulse shape.* Paper presented at the Optoelectronics, IEE Proceedings J.

Cui, K., Chen, G., Xu, Z., & Roberts, R. D. (2010). *Line-of-sight visible light communication system design and demonstration.* Paper presented at the Communication Systems Networks and Digital Signal Processing (CSNDSP), 2010 7th International Symposium on.

Din, I. (2014). Energy-Efficient Brightness Control and Data Transmission for Visible Light Communication. *IEEE photonics technology letters, 26*(8), 781-784. doi: 10.1109/LPT.2014.2306195

EPSRC's. (2013). Ultra-parallel visible light communications (UP-VLC) project.

Gagliardi, R. M., & Karp, S. (1976). Optical communications. *New York, Wiley-Interscience, 1976. 445 p., 1*.

Garrett, I. (1983). *Digital pulse-position modulation over slightly dispersive optical fibre channels.* Paper presented at the Int. Symp. Information Theory, St. Jovite.

Garrett, I. (1983). Pulse-position modulation for transmission over optical fibers with direct or heterodyne detection. *Communications, IEEE Transactions on, 31*(4), 518-527.

Gfeller, F. R., & Bapst, U. (1979). Wireless in-house data communication via diffuse infrared radiation. *Proceedings of the IEEE, 67*(11), 1474-1486.

Ghassemlooy, Z., & Hayes, A. (2003a). Indoor optical wireless communications systems–Part I: Review. *School of Engineering, Northumbria University*.

Ghassemlooy, Z., & Hayes, A. (2003b). Indoor optical wireless communications systems–Part I: Review. *Newcastle upon Tyne, UK: School of Engineering, Northumbria University*.

Ghassemlooy, Z., & Rajbhandari, S. (2007). *Performance of diffused indoor optical wireless links employing neural and adaptive linear equalizers.* Paper presented at the Information, Communications & Signal Processing, 2007 6th International Conference on.

Ghosna, F. J. (2010). *Pulse Position Modulation Coding Schemes for Optical Inter-satellite Links in Free Space.* University of Huddersfield.

Goodwin, F. E. (1970). A review of operational laser communication systems. *Proceedings of the IEEE, 58*(10), 1746-1752.

Grubor, J., Jamett, O., Walewski, J., Randel, S., & Langer, K.-D. (2007). High-speed wireless indoor communication via visible light. *ITG-Fachbericht-Breitbandversorgung in Deutschland-Vielfalt für alle?*

Hirt, W., Hassner, M., & Heise, N. (2001). IrDA-VFIr (16 Mb/s): modulation code and system design. *Personal Communications, IEEE, 8*(1), 58-71.

Humphreys, C. J. (2008). Solid-state lighting. *MRS bulletin, 33*(04), 459-470.

Hunter, R. D. M., & Johnson, T. T. (1995). *Introduction to VHDL*: Springer Science & Business Media.

IEEE. (2011). IEEE Standard for Local and Metropolitan Area Networks - Part

15.7:.

Iwasaki, S., Wada, M., Endo, T., Fujii, T., & Tanimoto, M. (2007). *Basic experiments on paralle wireless optical communication for ITS.* Paper presented at the Intelligent Vehicles Symposium, 2007 IEEE.

JDSU. (2009). Optical Transceiver Testing Using the JDSU Multiple Application Platform (MAP-200). 2014, from http://www.jdsu.com/ProductLiterature/map200.an.fop.tm.ae.pdf

John R. Barry, J. M. K., William J. Krause, Edward A. Lee, and David G. Messerschmitt. (1993). Simulation of Multipath Impulse Response for Indoor Wireless Optical Channels. *IEEE JOURNAL ON SELECTED AREAS IN COMMUNICATIONS, 11*, 3.

Jungnickel, V., Pohl, V., Nonnig, S., & Von Helmolt, C. (2002). A physical model of the wireless infrared communication channel. *Selected Areas in Communications, IEEE Journal on, 20*(3), 631-640.

Kahn, D.-s. S. J. M. (199). Differential Pulse-Position Modulation for Power-Efficient Optical Communication. *IEEE TRANSACTIONS ON COMMUNICATIONS, VOL. 47*(8).

Kahn, J., Barry, J., Krause, W., Audeh, M., Carruthers, J., Marsh, G., . . . Messerschmitt, D. (1992). *High-speed non-directional infrared communication for wireless local-area networks.* Paper presented at the Signals, Systems and Computers, 1992. 1992 Conference Record of The Twenty-Sixth Asilomar Conference on.

Kahn, J. M., & Barry, J. R. (1997). Wireless infrared communications. *Proceedings of the IEEE, 85*(2), 265-298.

Kaur, S., Liu, W., & Castor, D. (2009). VLC dimming proposal: IEEE 802.15-09-0641-00-0007, Sep. 2009 [Online]. Available: https://mentor. ieee. org/802.15/documents.

Kavehrad, M. (2010). Sustainable energy-efficient wireless applications using light. *Communications Magazine, IEEE, 48*(12), 66-73.

KIZILIRMAK, R. (2013). Impact of repeaters on the performance of indoor visible light communications. *Turk J Engin, 8*(1).

KIZILIRMAK, R. C. (2013). Impact of repeaters on the performance of indoor visible light communications. *Turk J Elec Engin, 8*(1).

Komine, T., Lee, J. H., Haruyama, S., & Nakagawa, M. (2009). Adaptive equalization system for visible light wireless communication utilizing multiple white LED lighting equipment. *Wireless Communications, IEEE Transactions on, 8*(6), 2892-2900.

Komine, T., & Nakagawa, M. (2004). Fundamental analysis for visible-light communication system using LED lights. *Consumer Electronics, IEEE Transactions on, 50*(1), 100-107.

Kotzin, M. D., & van den Heuvel, A. P. (1986). *A duplex infra-red system for in-building communications.* Paper presented at the Vehicular Technology Conference, 1986. 36th IEEE.

Kumar, N., Lourenco, N., Spiez, M., & Aguiar, R. L. (2008). Visible light communication systems conception and vidas. *IETE Technical Review, 25*(6), 359-367.

Kumar, N., & Lourenco, N. R. (2010). Led-based visible light communication system: a brief survey and investigation. *J. Eng. Appl. Sci, 5*(4), 296-307.

Lee, I. E., Sim, M. L., & Kung, F. W. L. (2008). *A dual-receiving visible-light communication system for intelligent transportation system.* Paper presented at the Circuits and Systems for Communications, 2008. ICCSC 2008. 4th IEEE International Conference on.

Lee, K., & Park, H. (2011a). *Channel model and modulation schemes for visible light communications.* Paper presented at the Circuits and Systems (MWSCAS), 2011 IEEE 54th International Midwest Symposium on.

Lee, K., & Park, H. (2011b). Modulations for visible light communications with dimming control. *Photonics Technology Letters, IEEE, 23*(16), 1136-1138.

Lee, R., Yun, K., Yoo, J.-H., Jung, S.-Y., & Kwon, J. K. (2013). *Performance analysis of M-ary PPM in dimmable visible light communications.* Paper presented at the Ubiquitous and Future Networks (ICUFN), 2013 Fifth International Conference on.

Li, X., Gani, A., Salleh, R., & Zakaria, O. (2009). *The future of mobile wireless communication networks.* Paper presented at the Communication Software and Networks, 2009. ICCSN'09. International Conference on.

Lo, S. C. (2004). Visible Light Communications. *IEEE Transactions on Consumer Electronics, 50*(1).

Lueftner, T., Kroepl, C., Huemer, M., Hausner, J., Hagelauer, R., & Weigel, R. (2003). Edge-position modulation for high-speed wireless infrared communications. *IEE Proceedings-Optoelectronics, 150*(5), 427-437.

Massarella, A. J., & Sibley, M. J. (1991). Experimental results on suboptimal filtering for optical digital pulse-position modulation. *Electronics letters, 27*(21), 1953-1954.

Menon, M., & Cryan, R. (2005). Optical wireless communications utilizing a dicode PPM PIN-BJT receiver. *Microwave and optical technology letters, 45*(4), 273-277.

Moreira, A., Valadas, R., & de Oliveira Duarte, A. (1996). *Performance of infrared transmission systems under ambient light interference.* Paper presented at the Optoelectronics, IEE Proceedings-.

Moreira, A. J., Valadas, R. T., & de Oliveira Duarte, A. (1995). *Characterisation and modelling of artificial light interference in optical wireless communication systems.* Paper presented at the Personal, Indoor and Mobile Radio Communications, 1995. PIMRC'95. Wireless: Merging onto the Information Superhighway., Sixth IEEE International Symposium on.

Noh, J., & Ju, M. (2012). *Visible light communications with color and dimming control by employing VPPM coding.* Paper presented at the 2012 Fourth International Conference on Ubiquitous and Future Networks (ICUFN).

Noshad, M., & Brandt-Pearce, M. (2014). Application of expurgated PPM to indoor visible light communications—Part I: Single-user systems. *Journal of Lightwave Technology, 32*(5), 875-882.

O'Brien, D., Le Minh, H., Zeng, L., Faulkner, G., Lee, K., Jung, D., . . . Won, E. T. (2008). *Indoor visible light communications: challenges and prospects.* Paper presented at the Optical Engineering+ Applications.

Park, H., & Kim, J. (2014). A Coding Scheme for Visible Light Communication with Wide Dimming Range.

Personick, S. D. (1973). Receiver design for digital fiber optic communication systems, I. *Bell system technical journal, 52*(6), 843-874.

Pohl, V., Jungnickel, V., & Von Helmolt, C. (2000). Integrating-sphere diffuser for wireless infrared communication. *IEE Proceedings-Optoelectronics, 147*(4), 281-285.

Poulin, R. L., Pauluzzi, D. R., & Walker, M. R. (1992). *A multi-channel infrared telephony demonstration system for public access applications.* Paper presented at the Wireless Communications, 1992. Conference Proceedings., 1992 IEEE International Conference on Selected Topics in.

Proakis, J. G. (2001). *Intersymbol Interference in Digital Communication Systems*: Wiley Online Library.

Rani, J., Chauhan, P., & Tripathi, R. (2012). Li-Fi (Light Fidelity)-The future technology In Wireless communication. *Int. J. of Applied Engineering Research, 7*(11).

Saadi, M., Wattisuttikulkij, L., Zhao, Y., & Sangwongngam, P. (2013). Visible light communication: opportunities, challenges and channel models. *International Journal of Electronics & Informatics, 2*(1), 1-11.

Sangwongngam, P. (2015). Visible light communication VLC. 2015, from http://www.thaitelecomkm.org/OQC/index.php/en/visible-light-communication-system

semiconductor, f. (2008). Quad 2-Input NAND Gate. 2015, from www.fairchildsemi.com

Shalaby, H. M. H. (1993). Performance of uncoded overlapping PPM under communication constraints. *Communications, 1993. ICC '93 Geneva. Technical Program, Conference Record, IEEE International Conference, 1*.

Sibley, M. (2005). Performance analysis of a dicode PPM system, operating over plastic optical fibre, using maximum likelihood sequence detection. *IEE Proceedings-Optoelectronics, 152*(6), 337-343.

Sibley, M. J. (1994). *Optical communications* (Vol. 2): Palgrave Macmillan.

Sibley, M. J. (2003a). Analysis of dicode pulse position modulation using a PINFET receiver and a slightly/highly dispersive optical channel. *IEE Proceedings-Optoelectronics, 150*(3), 205-209.

Sibley, M. J. (2003b). Dicode pulse-position modulation: a novel coding scheme for optical-fibre communications. *IEE Proceedings-Optoelectronics, 150*(2), 125-131.

Sibley, M. J. (2004). Suboptimal filtering in a zero-guard, dicode PPM system operating over dispersive optical channels. *IEE Proceedings-Optoelectronics, 151*(4), 237-243.

Sibley, M. J., & Massarella, A. J. (1993). *Detection of digital pulse position modulation over highly/slightly dispersive optical channels.* Paper presented at the Berlin-DL tentative.

Sibley, M. J. N. (1995). *Optical communications: components and systems*. Basingstoke: Macmillan.

Siddique, A. B., & Tahir, M. (2011). *Joint brightness control and data transmission for visible light communication systems based on white LEDs.* Paper presented at the Consumer Communications and Networking Conference (CCNC), 2011 IEEE.

Sterckx, K., & Saengudomlert, P. (2011). *Visible light communication via dimmable LED lamps using pulses of equal shape.* Paper presented at the Networks and Optical Communications (NOC), 2011 16th European Conference on.

Sugiyama, H., Haruyama, S., & Nakagawa, M. (2007). *Brightness control methods for illumination and visible-light communication systems.* Paper presented at the Wireless and Mobile Communications, 2007. ICWMC'07. Third International Conference on.

Technology., S. o. I. S. a. (2013). speed on Internet using light waves.

VLCC. (2008). Visible Light Communications Consortium.

Wada, M., Yendo, T., Fujii, T., & Tanimoto, M. (2005). *Road-to-vehicle communication using LED traffic light.* Paper presented at the Intelligent Vehicles Symposium, 2005. Proceedings. IEEE.

Wang, J.-B., Hu, Q.-S., Wang, J., Huang, Y.-H., & Wang, J.-Y. (2013). *Channel capacity for dimmable visible light communications.* Paper presented at the Global Communications Conference (GLOBECOM), 2013 IEEE.

WANG, J.-y., ZOU, N.-y., Dong, W., Kentaro, I., Zensei, I., & NAMIHIRA, Y. (2012). Experimental study on visible light communication based on LED. *The Journal of China Universities of Posts and Telecommunications, 19*, 197-200.

Yang, A., Li, X., & Jiang, T. (2012). Enhancement of LED indoor communications using OPPM-PWM modulation and grouped bit-flipping decoding. *Optics express, 20*(9), 10170-10179.

Zhang, X., Cui, K., Yao, M., Zhang, H., & Xu, Z. (2012). *Experimental characterization of indoor visible light communication channels.* Paper presented at the Communication Systems, Networks & Digital Signal Processing (CSNDSP), 2012 8th International Symposium on.